PA12/PBT reactive blending with hydropolysiloxane by carbonyl hydrosilylation reaction : towards new polymer materials

Jingping Li

Université Claude Bernard Lyon 1

UNIVERSITÉ DE LYON

N° d'ordre NNT : 2016LYSE1306

THESE DE L'UNIVERSITE DE LYON
Délivrée par
UNIVERSITE CLAUDE BERNARD LYON1

ECOLE DOCTORALE MATERIAUX DE LYON

DIPLOME DE DOCTORAT

Soutenue le 15 Décembre 2016
SPECIALITE : MATERIAUX INNOVANTS

Par

Jingping LI

PA12/PBT reactive blending with hydropolysiloxane by carbonyl hydrosilylation reaction: towards new polymer materials

Directeur de thèse : **Pr. Philippe CASSAGNAU**
Co-directeur de thèse : **Dr. Véronique BOUNOR-LEGARE**

Jury :

M. CASSAGNAU Philippe	Université de Lyon1	Directeur de thèse
Mme. BOUNOR-LEGARE Véronique	Université de Lyon1	Co-directrice de thèse
Mme. ESPUCHE Eliane	Université de Lyon 1	Examinatrice
M.BOUQUEY Michel	Université de Strasbourg	Rapporteur
M. CHAPEL Jean-Paul	Centre de Recherche Paul Pascal, Bordeaux	Rapporteur
M. PRADEL Jean-Laurent	Addiplast	Examinateur

UNIVERSITE CLAUDE BERNARD - LYON 1

Président de l'Université	**M. François-Noël GILLY**
Vice-président du Conseil d'Administration	M. le Professeur Hamda BEN HADID
Vice-président du Conseil des Etudes et de la Vie Universitaire	M. le Professeur Philippe LALLE
Vice-président du Conseil Scientifique	M. le Professeur Germain GILLET
Directeur Général des Services	M. Alain HELLEU

COMPOSANTES SANTE

Faculté de Médecine Lyon Est – Claude Bernard	Directeur : M. le Professeur J. ETIENNE
Faculté de Médecine et de Maïeutique Lyon Sud – Charles Mérieux	Directeur : Mme la Professeure C. BURILLON
Faculté d'Odontologie	Directeur : M. le Professeur D. BOURGEOIS
Institut des Sciences Pharmaceutiques et Biologiques	Directeur : Mme la Professeure C. VINCIGUERRA
Institut des Sciences et Techniques de la Réadaptation	Directeur : M. le Professeur Y. MATILLON
Département de formation et Centre de Recherche en Biologie Humaine	Directeur : Mme. la Professeure A-M. SCHOTT

COMPOSANTES ET DEPARTEMENTS DE SCIENCES ET TECHNOLOGIE

Faculté des Sciences et Technologies	Directeur : M. F. DE MARCHI
Département Biologie	Directeur : M. le Professeur F. FLEURY
Département Chimie Biochimie	Directeur : Mme Caroline FELIX
Département GEP	Directeur : M. Hassan HAMMOURI
Département Informatique	Directeur : M. le Professeur S. AKKOUCHE
Département Mathématiques	Directeur : M. le Professeur Georges TOMANOV
Département Mécanique	Directeur : M. le Professeur H. BEN HADID
Département Physique	Directeur : M. Jean-Claude PLENET
UFR Sciences et Techniques des Activités Physiques et Sportives	Directeur : M. Y.VANPOULLE
Observatoire des Sciences de l'Univers de Lyon	Directeur : M. B. GUIDERDONI
Polytech Lyon	Directeur : M. P. FOURNIER
Ecole Supérieure de Chimie Physique Electronique	Directeur : M. G. PIGNAULT
Institut Universitaire de Technologie de Lyon 1	Directeur : M. le Professeur C. VITON
Ecole Supérieure du Professorat et de l'Education	Directeur : M. le Professeur A. MOUGNIOTTE
Institut de Science Financière et d'Assurances	Directeur : M. N. LEBOISNE

Acknowledgments

In 2013, I got doctoral scholarship from China Scholarship Council, arrived in lab IMP@ Lyon 1 on October and started my Ph.D study. My supervisors are Prof. Philippe CASSAGNAU and Dr. Véronique BOUNOR LEGARE. Until now, I still think I am so lucky to be your student. During the past three years, no matter when I met problem and no matter when I need help, you are always the first one and the only one I want to ask for help. Now, I will leave France, I would like to express my heartfelt gratitude to you, my dear supervisors, for your intellectual guidance and for your warm and constant encouragement during the process of my study in our lab. I will never forget our nice trip to Chengdu and Shanghai in November 2015 and hope we can meet again in China one day. Merci à vous.

Secondly, I would like to express my heartfelt gratitude to Professor Eliane ESPUCHE, the president of my defense and who led me into the work of gas permeability. I am also greatly indebted to M.BOUQUEY Michel, M. CHAPEL Jean-Paul and M.PRADEL Jean-Laurent, my juries, you are so professional and nice during the defense and give me quite useful suggestions about my future work.

I also want to thank Fernande and Christine, two nice ladies, who gave me great help to carry out experiment and relative analysis of NMR, you let me know the magic world of it.

My cordial and sincere thanks go to all the colleagues in the lab, such as dear Flavien, Adrien, Pierre, Ali and Agnès, who helped me a lot to carry out experiment. Thanks dear Sylvie for helping me really a lot and dear Margarita, Alice, Marie-Gamille, Fabien, Antoine, Imed, Marwa…to be honest, without you, life would be quite boring and lonely for me.

I am also very grateful to my Chinese friends, Danjun, Quanyi, Xiaolu, Qing, Wenjun, Lili, Bin, Yue, Xichen, Boliang, Jiang, Min, who have given me a lot of help and courage during my stay in Lyon and throughout the process of writing this thesis.

Last but not the least; big thanks go to my parents, grandparents and all my family members who shared with me my worries, frustrations, and hopefully my ultimate happiness in eventually finishing this thesis. 谢谢爸爸妈妈！

Abstract

Polydimethylsiloxane (PDMS) containing thermoplastics have attracted much attention due to their potential in wide range of applications. They combine some of the unique and excellent properties of PDMS like flexibility, hydrophobicity, gas permeability, biocompatibility and UV stability. There are two main routes to achieve such materials, one is to synthesize PDMS based copolymers and another one is to blend PDMS with commercial thermoplastics directly. When blending PDMS with thermoplastics, the problem of compatibility cannot be ignored. More specifically, due to the low surface energy and relatively low viscosity of PDMS compared with most thermoplastics polymers, dispersion of polysiloxane is difficult and generally results in two separated phases. This results in weak mechanical properties. Therefore, the main challenge in PDMS and thermoplastic blending is to find an efficient and convenient way such as *in situ* reactive blending to realize the compatibilization between the two or more phases.

Recently, the laboratory has shown that the hydrosilylation reaction between hydrosilane (SiH) and carbonyl group catalyzed by triruthenium dodecacarbonyl [$Ru_3(CO)_{12}$] is efficient under molten conditions. The reaction corresponds to the addition of SiH to unsaturated carbonyl group. This was efficient when it was carried out with an ethylene-vinyl acetate copolymers at temperature around 120°C. But the extension to high polymers processing temperatures is not reported. Therefore, we intend to apply such carbonyl hydrosilylation to hydride PDMS/polyamide compounds and even polymethylhydrosiloxane (PMHS)/PBT ones which are processed at higher temperature to find a potential and efficient method for PDMS/thermoplastics reactive compatibilization.

Firstly, we investigated the mechanism of $Ru_3(CO)_{12}$ catalyzed hydrosilylation reaction of *N*-methylpropionamide, a model compound of polyamide 12 (PA12), and hydride terminated PDMS. It was found that the yield of *N*-silylated compounds can reach 70 mol% after 2 hours reaction at 100 °C, which was confirmed by several NMR techniques (^{1}H, ^{13}C and ^{29}Si). The *N*-silylated compounds mainly include *N*-siloxane-*N*-methylpropionamide and *N*-siloxane-*N*-methylpropionamine which can work as compatibilizers in reactive blending.

Secondly, this hydrosilylation reaction was extended to the reactive blending of PA12 with hydride terminated PDMS under molten processing conditions. It is clear that in the presence of $Ru_3(CO)_{12}$ (1wt%), the reaction was carried out quickly (in 1 minute at 170 °C) since the mixing torque began to increase rapidly after the introduction of catalyst in the PDMS mixture, this phenomenon was not observed in the absence of catalyst. Compared to the unreacted polymers blend, the dispersion of PDMS in the reactive blend was obviously improved as the size of the PDMS domains decreased from 3-4 μm to around 0.8 μm diameters. Besides, in such reactive conditions and in presence of $Ru_3(CO)_{12}$, PDMS-SiH oxidation reaction was partially observed. This phenomenon leads to a second PDMS gel based phase with a characteristic size around 20-30 nm diameter. We also investigated the influence of the physico-chemical parameters on the blend microstructure. Properties such as thermal stability, crystalline behavior, surface energy and gas permeability and separation were studied. We confirmed that for PA12/PDMS blends, the introduction of PDMS can significantly improve the hydrophobicity of PA12.

Thirdly, we applied the $Ru_3(CO)_{12}$ catalyzed hydrosilylation to PBT and PMHS. We also confirmed the possibility and efficiency of such reaction through model study. However, PBT needs to be processed at higher temperature (220 °C). The final material not only includes the crosslinking network formed between PBT and PMHS, but also contains a part of PMHS self-crosslinking leading to a PMHS gel-like phase. As a result, the final material is made of a PBT/PMHS network with gel-like PMHS phase. Therefore, it should be noted that for the application of carbonyl hydrosilylation to thermoplastics processed at high temperatures, the side reaction of hydride polysiloxane self-crosslinking is likely to occur.

Finally, the perspectives of the thesis are described. These results show a potential application of ruthenium catalyzed hydrosilylation to reactive compatibilization between hydropolysiloxane and polyamide or polyester. We can also adjust the microstructure of the final blend through physico-chemical parameters and finally achieve the target materials.

Keywords: *PA12, PDMS, hydrosilylation, reactive compatibilization, gas permeability, surface free energy*

Résumé

Les thermoplastiques contenant du polydiméthoxysilane (PDMS) présentent un grand intérêt dans la formulation des matériaux polymères en raison de leur spécificité et de leur potentialité de développement dans un large spectre d'applications. Ils combinent ainsi des propriétés uniques et excellentes du PDMS, comme la flexibilité, l'hydrophobicité, la perméation aux gaz, la biocompatibilité et la stabilité aux rayons ultraviolets. Deux méthodes principales existent pour créer de tels matériaux ; l'une consiste à synthétiser des copolymères à base de PDMS et l'autre à mélanger directement le PDMS avec des thermoplastiques commerciaux.

Lors du mélange d'un PDMS avec des polymères thermoplastiques, le problème de la compatibilité ne peut être ignoré. Plus précisément, la dispersion de polysiloxane est difficile à cause de sa faible énergie de surface et relativement faible viscosité en comparaison avec la plupart des polymères, ce qui conduit généralement à une séparation de phase. Par conséquent, le défi principal des mélanges PDMS/thermoplastique est de trouver un moyen efficace et adapté, comme le mélange réactif avec la génération *in situ* d'un copolymères, pour compatibiliser les deux phases et contrôler ainsi leurs morphologies.

Récemment, le laboratoire a montré qu'une réaction d'hydrosilylation les fonctions hydrosilane (SiH) portés par un PDMS-SiH et les groupes carbonyle d'un copolymère d'éthylène et d'acétate de vinyle catalysée par le triruthénium dodécacarbonyle [$Ru_3(CO)_{12}$] était efficace pour la compotibilisation de mélanges de polymères. Cette réaction n'est en fait efficace que lorsqu'elle est réalisée dans des conditions douces en particulier à des températures inféieures à 120°C. Dans le cadre de ce travail de doctorat, nous nous sommes intéressés au potentiel de ces réactions d'hydrosilylation pour des systèmes PDMS-hydride/polyamides et polyméthylhydrosilane/polybutylène téréphthalate (PMHS/PBT) nécessitant des températures de mise en œuvre aux environs de 200°C.

Dans un premier temps, nous avons étudié le mécanisme de la réaction d'hydrosilylation catalysée par le le triruthénium dodécacarbonyle dans le cas du N-méthylpropionamide, composé modèle du polyamide 12 (PA12), avec un PDMS terminé hydride. Il a été montré

que la création de composés N-silylilés peut atteindre jusqu'à 70 mol% après 2 heures de réaction à 100°C, ce qui a été confirmé par RMN multinucléaire (^{1}H, ^{13}C et ^{29}Si). Les composés N-silylés incluent principalement le *N*-siloxane-*N*-méthylpropionamide et le *N*-siloxane-*N*-méthylpropionamine qui peuvent jouer par la suite le rôle de compatibilisant lors du mélange réactif.

Dans un deuxième temps, cette réaction d'hydrosilylation a été étendue au mélange réactif de PA12 avec du PDMS terminé hydride en conditions de mélange fondu. Le catalyseur rend la réaction possible et très rapide : ceci est clairement mis en évidence par l'augmentation rapide du couple de mélange (en 1 minute à 170 °C) lors de l'ajout de 1m% de $Ru_3(CO)_{12}$ dans le PDMS fondu, phénomène non observé en l'absence du catalyseur. La microstructure du système réactif est clairement améliorée puisque la taille des domaines de PDMS diminue de 3-4 microns à environ 0,8 micron de diamètre. En outre, dans de telles conditions réactives et en présence du catalyseur de ruthénium, une réaction concomitante d'oxydation du PDMS-SiH est partiellement observée. Ce phénomène conduit à une seconde population de PDMS sous forme de gel, dont la taille caractéristique avoisine 20 à 30 nanomètres de diamètre. Nous avons également étudié l'influence des paramètres physico-chimiques sur la microstructure des mélanges. Ceci inclut par exemple les propriétés de stabilité thermique, de comportement cristallin, d'énergie de surface et de perméabilité et séparation des gaz. Nous avons pu confirmer que dans le cas de mélange PA12/PMDS, l'introduction de PDMS peut améliorer de façon significative l'hydrophobicité du PA12 (mettre une valeur d'angle de contact).

Dans un troisième temps, nous nous sommes intéressés à l'application de la réaction d'hydrosilylation catalysée par le ruthénium aux composites PBT/polyméthylhydrosiloxane (PMHS). A plus haute température, nous avons également confirmé la possibilité et l'efficacité de cette réaction sur un système modèle. Cependant, à cause des températures plus élevées nécessaires à la mise en forme du PBT (220 °C), non seulement une réaction de réticulation entre le PBT et le PMHS apparaît mais également une auto-réticulation du PMHS. Il en résulte un matériau final composé d'un réseau de PBT/PMHS avec des phases de PMHS gélifié. Par conséquent, il faut noter que l'application de l'hydrosilylation carbonyle aux thermoplastiques mis en forme à plus hautes températures doit prendre en compte la réaction

secondaire de réticulation du polysiloxane. Ceci nécessite donc un choix judicieux des caractéristiques physico-chimiques des PMDS (masse molaire, concentration de SiH etc..).

Enfin, les perspectives de la thèse sont décrites. Ces résultats montrent une application potentielle de l'hydrosilylation catalysée par le ruthénium à la compatibilisation réactive entre le polysiloxane hydride et les polyamides ou polyesters. Nous pouvons également ajuster la microstructure du mélange final par les paramètres physico-chimiques et obtenir finalement un matériau présentant des propriétés innovantes. Enfin cette approche originale permet d'envisager des nouveaux mélanges à base de PDMS et de thermoplastiques porteur de groupement carbonyle sans modification préalable des polymères pour y introduire une fonction réactive complémentaire comme cela est classiquement abordé.

Mots clés : *PA12, PMDS, hydrosilylation, compatibilisation réactive, perméabilité aux gaz, énergie libre de surface*

Table of contents

Chapter I: Literature review and general concept

I.1 Introduction

There has been an increasing interest in using polysiloxanes as section of various functional materials, due to unusual combination of properties of these polymers. The repeating unit of a polysiloxane consists of alternating silicon-oxygen atoms, in which two monovalent organic radicals (*i.e.* $-CH_3$,$-CH_2CH_3$,$-OCH_3$) are attached to each of the silicon atoms as shown below:

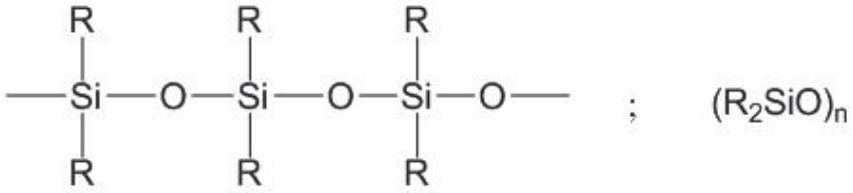

Figure I.1: Molecular structure of siloxane [1].

The polysiloxane chain has exceptionally high flexibility, which is related to very low barriers of rotation around the Si-O bond and of linearization of the Si-O-Si angle. Thus, the polysiloxane chain has a very high deformation ability easily adopting various shapes. It adapts itself readily to its surrounding and the functional groups attached to polysiloxanes are available for the interaction with neighboring molecules. Taking into account that substituents appear only at every second atom in the chain, the Si-O bond is relatively long (1.63Å) and the Si-O-Si angle usually large (145^o), the polysiloxane flexibility is not much restricted by substituents unless they are very bulky. In addition, the nature of the polysiloxane backbone is inorganic, which gives this polymer a high thermal stability and also, in some sense, an amphiphilic character. Its inorganic skeleton is formed of strongly polar Si-O bonds, but it bears nonpolar organic groups. Due to this feature, the polysiloxane tends to go to the interface, adopting a deformation in which its polar skeleton sticks to more hydrophilic surface, while organic groups are directed towards more hydrophobic surface. In this way it decreases the interfacial surface tension [2]. Therefore, polysiloxane has special properties caused by its molecular structure and polysiloxane like silicon or gums are used in a variety of commercial applications including: tubing, prosthetic devices, gaskets, wire insulation, construction sealants, adhesives, encapsulates, insulating foams, antifoams, greases, heat transfer fluids, fire stops, moisture repellents, surfactants, release agents, lubricants, anticaking agents, dashpot liquids, diffusion pump fluids, *etc*. Many of these products are

based on polydimethylsiloxane (PDMS) itself, however, for some applications, only the properties of PDMS fall short of those desired, like its weak mechanical properties. Therefore, the modification of PDMS such as PDMS containing copolymers or blend seems more attractive recently [1].

I.2 Preparation of PDMS containing materials

I.2.1 PDMS containing copolymers

I.2.1.1 Introduction

A very important way to improve the properties of a polymer is by the controlled synthesis of a block (AB or ABA) or a segmented [$(AB)_n$] copolymer. This approach has been well recognized and widely used in polymer chemistry [3-5]. In particular, the synthesis of PDMS based copolymer can not only achieve a new material containing both of their properties but also overcome the immiscible problem between PDMS and most organic macromolecules. A wide variety of block or segmented copolymers containing PDMS as the soft segment and various thermoplastics as the hard segment have been synthesized and characterized. For such synthesis, preparation of various, reactive organofunctional siloxane oligomers and their use in the copolymerization reactions together with numerous conventional "organic" monomers or oligomers have made it possible.

I.2.1.2 Functional PDMS

To functional siloxane oligomers, the main factors determining their reactivity are the type and nature of the terminal functional groups. Due to the fundamental differences in their structures, chemical reactivities and overall properties, it is possible to divide functionally terminated siloxane oligomers into two groups. The first group consists of oligomers with (Si-X) terminal units and the other one with (Si-R-X) units, where (X) and (R) represent the reactive functional group and a short hydrocarbon moiety respectively. However, as reported, most of the studies focused on the organofunctionally terminated (Si-X) siloxane oligomers. The general structure of the (Si-X) terminated siloxane oligomers and a list of important reactive functional end groups (X) are given in Table I.1. A very interesting feature of (Si-X) groups is their much higher reactivities towards nucleophilic reagents when compared with

analogous (C-X) functionalities. This may be attributed to the pronounced difference between the electro-negativities of silicon (1.8) and carbon (2.5) atoms [6], which determine the nature (polarity) of the bonds formed.

A large number of organofunctional end-groups may be introduced into PDMS. Hydrosilylation is used in most cases to attach the organic group to silicon. As shown in Figure I.2, different possibilities may be considered in terms of the step chosen for hydrosilylation.

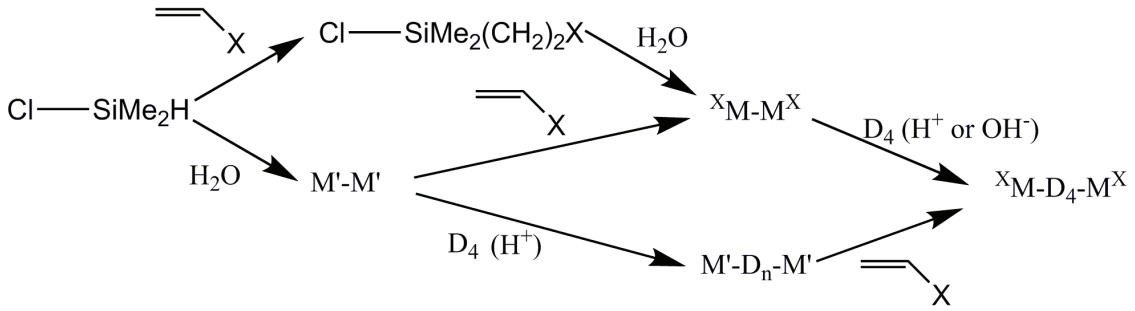

Figure I.2: Routes for the synthesis of α, ω-bis(organofunctional) PDMS (according to the usual terminology in silicone chemistry D= -$SiMe_2O$- and M'= $HSiMe_2O_{1/2}$-) [7].

This route consists in the preparation of a 1, 3-difunctional disiloxane (X-$SiMe_2OSiMe_2$-X or $M^X{}_2$) either by hydrosilylation of chlorodimethylsilane followed by hydrolysis or by hydrosilylation of M'_2. The disiloxane $M^X{}_2$ is then used as an 'end-blocker' in the equilibration of D_4 [7]. The choice of a cationic or an anionic polymerization depends on the nature of the functional groups. For example, in the case of aminoalkyl groups, anionic polymerization initiated by tetraalkylammonium hydroxide or silanolate will be chosen [8]. Alternatively, an α, ω-bis(hydrosilyl)-PDMS may be obtained by cationic equilibration of D_4 in the presence of M'_2 and hydrosilylation is carried out. A lot of examples of difunctional polysiloxanes were obtained by one of the synthetic routes as shown in Figure I.2. Whatever the step in which hydrosilylation is realized, it may be useful to protect functional groups such as OH or NH_2 to avoid side reactions and loss of functionality but some authors have performed hydrosilylation with non-protected alcoholic compounds [9]. It is notable that an increasing number of difunctional polysiloxanes are now commercially available (hydroxy, amino, phenol, carboxylic, *etc*.).

Table I.1: General structure of the (Si-X) terminated siloxane oligomers and important functional end groups [6].

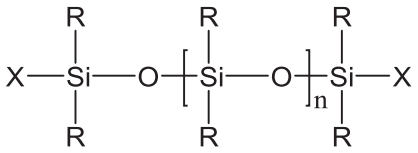

(X) : -Cl -OH $-OCH_3$ $-OC_2H_5$

-H $-NH_2$ $-N(CH_3)_2$ $-CH=CH_2$

(n) : Number of repeating units

(R) : An organic group, usually ($-CH_3$)

In general, such functional terminated PDMS are divided in two groups according to the number of functional group (one or two terminal groups). Among them α, ω-difunctional polysiloxanes with functional groups such as chloro-, hydroxy-, alkoxy-, primary or tertiary aminosilanes and hydrosilanes react very easily with nucleophiles. Hydroxy end groups may be obtained by controlled hydrolysis of the chloro end-groups. α, ω-dichloro- and α,ω-dialkoxy polysiloxanes are obtained by hydrolysis of dichloro- or dialkoxysilanes respectively using a slight deficit of water to control the molar mass of the product. Dimethylamino end-groups are usually obtained by exchange with chloro- terminated siloxanes [10]. The molar mass of the oligomer may be increased by anionic equilibration of D_4. α, ω-Bis(hydrosilyl)polysiloxanes are particularly important because a wide class of organofunctional PDMS may be obtained from them by hydrosilylation. They can be prepared by hydrolysis of dichlorodimethylsilane with chlorodimethylsilane acting as an 'end-blocker'. It is also possible to use the cationic equilibration of octamethylcyclotetrasiloxane (D_4) in the presence of 1, 1, 3, 3-hexamethyldisiloxane (M'_2). Molar mass is controlled by the ratio $[D_4]/[M'_2]$, but the linear polymer is not easy to be separated from cyclic oligomers (about 13%

in the case of PDMS) [7].

I.2.1.3 Methods of PDMS containing copolymers preparation

PDMS containing linear or graft copolymer is always obtained by reacting α, ω-difunctional PDMS chain with a difunctional compound. Recently, the synthetic techniques leading to the formation of PDMS containing copolymers is classified according to the type and the nature of the copolymerization reaction like: 1) living anionic polymerization, 2) step-growth (condensation) polymerization, 3) polymerization by hydrosilylation and 4) other methods. A lot of literature reported the mentioned method for PDMS containing copolymer synthesis. For example, styrene-dimethylsiloxane triblock copolymers have been synthesized by the anionic polymerization of styrene and siloxane monomer (D_3 or D_4), in toluene/THF solutions using lithium or sodium biphenyl as the initiator [11]. The effects like initiator concentration, type of counterion, polymerization temperature and nature of the siloxane monomer (D_3 or D_4) on the molar mass distribution (MWD) have been investigated. However, the most versatile technique used for the synthesis of novel PDMS containing copolymer is step-growth (condensation) polymerization. This is mainly due to the availability of a wide variety of well-defined, organofunctionally terminated reactive siloxane oligomers as we have discussed previously. These oligomers constitute a very important bridge between organosiloxane chemistry and organic polymer chemistry. As a result, siloxane containing copolymers with a wide range of properties can be synthesized such as siloxane-urea, siloxane-amide, siloxane-ester *etc*. This method is generally divided into two different procedures polymer-monomer condensation or polymer-polymer condensation. In addition, copolymers combined by Si-O-C or Si-C linkers can be defined by the functional end-groups. Specifically, although similar methods are often used in either case, copolymers belonging to the first category were synthesized earlier because they are obtained from very reactive functional groups directly attached to the terminal silicon atom (silanol, chlorosilane, silylamine, alkoxysilane, *etc*.). Multiblock copolymers with Si-C links depend on the synthesis of organofunctional polysiloxanes of controlled functionality which are generally much less reactive (due the highest electronegativity of carbon compared to silicon) [7].

Polymer-Monomer Condensation: An example of copolymers with Si-O-C links is the PDMS-polycarbonate multiblock copolymer synthesized by Vaughn *et* al. [12] in 1969. In this

pioneering work α, ω- dichlorooligosiloxane was reacted with an excess of bisphenol-A (BPA), and the reaction medium was treated with phosgene. The number of blocks of each type can be quite large (up to 40) and the molar masses of the copolymers are relatively high (Mn = 96,000 $g.mol^{-1}$) [13].

Examples of such copolymers are collected in Table I.2. Various α,ω-difunctional PDMS (Figure I.3) have been incorporated in a large variety of random block copolymers including PDMS-polyester [9, 14], PDMS-polycarbonate [15], PDMS-polyurethane [16], PDMS-polyurea [17]. A two-step procedure is often preferred. The PDMS end-groups first react with an excess of one reactant and the second reactant is added in a second step to adjust the stoichiometric balance.

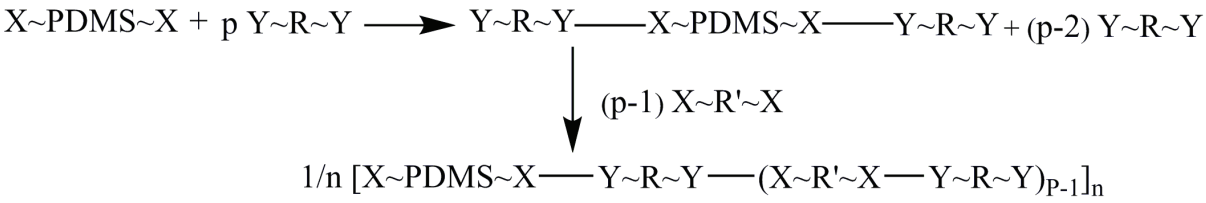

Figure I.3: Scheme of polymer-monomer condensation to obtain PDMS containing copolymers [7].

Table I.2: Synthesis of siloxane-organic random block copolymers obtained by polymer-monomer condensation (PDMS = polydimethylsiloxane; PC =polycarbonate; PE = polyester; PA = polyamide, PI = polyisoprene, PU = polyurethane) [7].

X~PDMS~X	X~X + Y~Y	Random Multiblock Copolymer
Cl-PDMS-Cl	BPA + $COCl_2$	(PDMS-PC)n
HOCO~~PDMS~~COOH	BPA + $COCl_2$	(PDMS-PC)n
H_2N~~PDMS~~ NH_2	BPA + ClCO-Ar-CO-Cl	(PDMS-PE)n
H_2N~~PDMS~~ NH_2	diol + dimethyl ester	(PDMS-PE)n
H_2N~~PDMS~~ NH_2	diamine + ClCO-R-COCl	(PDMS-PA)n
H_2N~~PDMS~~ NH_2	Diamine + diisocyanate	(PDMS-polyurea)n
H_2N~~PDMS~~ NH_2	diamine + dianhydride	(PDMS-PI)n
anhydride~PDMS~anhydride	diamine + dianhydride	(PDMS-PI)n
HO~~PDMS~~OH	diol + diisocyanate	(PDMS-PU)n

Generally, multiblock copolymers containing polyesters have been prepared by this way. For instance, α, ω-bis(aminoalkyl)-PDMS was end-capped with ester groups by reaction with an excess of a cycloaliphatic diester. 1, 4-Butanediol was then added with $Ti(OPr)_4$ as transesterification catalyst. PDMS-aromatic polyester copolymers based on dimethyl terephthalate and l, 4-butanediol were also prepared [18]. A small proportion of a hydrophilic α, ω-diol polysiloxane-g-poly(ethylene oxide) has been also incorporated randomly in poly(ethylene terephthalate) (PET) to improve fiber and film wettability [19].

Polymer-Polymer Condensation: Polycondensation of α, ω-difunctional PDMS with α, ω-difunctional organic polymer constitutes a large class of reactions yielding multiblock copolymers (Table I.3). The nature of the reactive end groups is only limited by the imagination of researchers. Examples of such copolymers are the reaction of an α, ω-dichloro-PDMS with an α, ω-dihydroxy aliphatic polyester [10] or unsaturated polyester (UPE) [20], or the reaction of an α, ω-bis(dimethylamino)-PDMS with an α, ω-dihydroxypolysulfone [21], an α, ω-dihydroxypolycarbonate [22], an α, ω-dihydroxypolyarylester [23], an α, ω-dihydroxypoly(α-methyl styrene) [22] or an α, ω-dihydroxypoly(2,6-diphenyl-1,4-phenylene oxide) [24]. In the rare cases where osmometry has been performed, the degree of chain extension appears to be rather low (n = 1.5-3 for aliphatic polyester PDMS [10] and n = 4-5 for UPE-PDMS [20]).

Table I.3: Synthesis of regularly alternating siloxane-organic block copolymers obtained by polycondensation [Pyr = pyrimidine (coupling by transimidisation); UPE = unsaturated polyester; PE = polyester; PαMS = poly(α-methylstyrene); PEEK = poly(ether ether ketone); PEEKt = poly(ether ether ketimine; PB = polybutadiene; PSU = polysulfone)] [7].

X~PDMS~X	Y~P~Y	Alternating Multiblock Copolymer
Cl-PDMS-Cl	HO-UPE-OH	(PDMS-UPE)n
Cl-PDMS-Cl	HO-PE-OH	(PDMS-PE)n
Me_2N-PDMS- NMe_2	HO-Ph-PSU-Ph-OH	(PDMS-PSU)n
Me_2N-PDMS- NMe_2	HO-PC-OH	(PDMS-PC)n
Me_2N-PDMS- NMe_2	HO-PE-OH	(PDMS-PE)n
Me_2N-PDMS- NMe_2	HO-PαMS-OH	(PDMS- PαMS)n
Me_2N-PDMS- NMe_2	HO-PPO-OH	(PDMS- PPO)n
HOCO-PDMS-COOH	OCN-PA-NCO	(PDMS-PA)n
H_2N-PDMS-NH_2	ClCO-PA-COCl	(PDMS-PA)n
H_2N-PDMS-NH_2	OCN-PU-NCO	(PDMS-PU)n
H_2N-PDMS-NH_2	OCN-polyurea-NCO	(PDMS-polyurea)n
H_2N-PDMS-NH_2	Pyr-polyimide-Pyr	(PDMS-polyimide)n
CH_2OCH-PDMS-$CHOCH_2$	HOCO-UPE-COOH	(PDMS-UPE)n
CH_2OCH-PDMS-$CHOCH_2$	HOCO-PB-COOH	(PDMS-PB)n
CH_2OCH-PDMS-$CHOCH_2$	HO-Ar-PSU-Ar-OH	(PDMS-PSU)n
Anhydride-PDMS-anhydride	H_2N-PEEKt-NH_2	(PDMS-PEEK)n
OHC-Ph-PDMS-Ph-CHO	H_2N-PA-NH_2	(PDMS-PA)n
H-PDMS-H	HO-PE-OH	(PDMS-PE)n
H-PDMS-H	Cl-Ar-PSU-Ar-Cl	(PDMS-PSU)n

It should be noted that, firstly, these copolymers linked by Si-O-C bonds are often claimed to be sensitive to hydrolysis, though examples of excellent hydrolytic stability have been reported. For instance, a polysulfone-PDMS multiblock copolymer with Si-O-C links retained 80% of its reduced viscosity after 14 days in boiling water and degradation in 10%

HCl was found to be significant. Secondly, comparing with polymer-monomer condensation, the molar masses, the polydispersity and the distribution of the blocks are better controlled ('perfectly' alternating multiblock copolymers) for the polymer-polymer condensation route, in principle. These materials are more suitable for the study of structure-properties relationships.

Other method for obtaining PDMS containing copolymers like polymerization by hydrosilylation reaction is also reported in some literatures, because PDMS with Si-H terminal bonds are easily prepared and commercially available. Early development of hydrosilylation reaction is conducted between silane (Si-H) terminated siloxane oligomer and olefinic terminated poly(alkylene oxide) oligomers. Consequently the resulting system contains (Si-C) linkages between different segments. The development of this method is very slow, the most well-known application is the one of Ringsdorf *and* Finkelmann [25, 26] who synthesized various novel thermoplastic liquid crystalline copolymers where siloxanes had been utilized as flexible spacers and improved the processability of these materials. For this method, there are two main difficulties. One is in controlling side-reactions that might strongly limit the molar masses [27]. As reported, multiblock PDMS-polystyrene and PDMS-poly(α-methylstyrene) copolymers were obtained from polystyrene and poly(α-methylstyrene) end-capped with vinylsilane functions (obtained by anionic polymerization using a bifunctional initiator and end-capping with chlorodimethylvinylsilane) [28]. Vinyl silane end-groups are known to be highly reactive and to give less side reactions than other ethylenic groups. However, the degree of polymerization is quite low in this case due to side-reactions which vary from one system to another. Another difficulty is to obtain high conversions. However for hydrosilylation reaction, a common solvent is not so easy to find, even at low concentration. As a result, by hydrosilylation reaction, the molar mass of copolymer is usually very low. Although sometimes a high molar mass is not always a goal, like when the copolymer is designed to be incorporated into a network, the low molar mass is also a weak point for wider application.

I.2.1.4 Conclusion

PDMS containing copolymers combine their unique properties together through synthesis, such as surface activity, high oxygen permeability, physiological inertness

(biocompatibility), hydrophobicity, atomic oxygen resistance and extremely low temperature flexibility. Organofunctional siloxane oligomers and siloxane containing copolymers offer a wide range of specialty applications in many diverse fields. However, there are still some weak points of this method. First of all, a critical problem for many of these polymerization reactions involving siloxanes and other organic monomers is the proper choice of the reaction solvent(s). This is especially important in producing high molar mass copolymers with useful mechanical properties. It is well known that polydimethylsiloxanes are extremely non-polar and have very low solubility parameters. Therefore they are not soluble in polar solvents such as DMF, DMAC or NMP which are conventionally employed in the synthesis of polyurethanes or polyurethanes ureas for example. So it is very difficult to find a common solvent that will homogeneously solvate the reaction mixture during the various stages of the polymerization. This usually leads to the formation of low molar mass copolymers with uncontrollable structures. As a result, the mechanical properties of the copolymers obtained are fairly poor. Secondly, the lack of reliable commercial sources for the supply of well-defined starting materials, especially the telechelic organofunctionally terminated disiloxanes "end-blockers" and related reactive oligomers. Although there are various small suppliers of these materials, since the volumes are very small the prices are artificially high. Quality and purity of the materials are also sometimes not very dependable. Finally, a new material synthesis will always need complex steps which also limited the industrialization and further application. As a conclusion, although the research on PDMS containing copolymers is growing fast, until now it is still far from being wildly applied. In order to solve the problem, we need a more efficient and convenient method to combine the unique properties of PDMS with other organic materials.

I.2.2 PDMS containing organic materials through blending

I.2.2.1 Introduction

Generally, polymer blends are classified into either homogeneous (miscible at a molecular level) or heterogeneous (immiscible) blends [29]. Miscible or immiscible property is defined by the compatibility. Specifically, the interface between the polymer phases in a polymer system is characterized by the interfacial tension which, when approaching zero,

causes the blend to become miscible. In other words, if there are strong interactions between the phases then the polymer blend will be miscible in nature. Large interfacial tensions lead to phase separation, with the phase-separated particles perhaps undergoing coalescence resulting in an increased of the particle size and, in turn, decreased of the mechanical properties [30, 31]. Most of the reports in the literature deal with novel methods for compatibilization of polymer blends, mainly focused on the modification of the interface and studying the effect of such modifications on the phase morphology and the mechanical properties. Compatibility of polymer blends can be achieved by reducing the interfacial tension or increasing the interfacial adhesion through the addition of interfacial active agents, for instance block or graft copolymers. Another way is to create *in situ* copolymers in the melt. The copolymer, either added or created *in situ* by the melt coupling reaction at the interface, is believed to play a dual role in promoting mixing of blend components. One is to reduce the interfacial tension by accumulating at the interface, as shown in Figure I.4, and consequently to promote droplet break-up depending on the change of capillary number when melt mixing in a shear field. The other one is to provide the steric hindrance between dispersed phase particles and thus suppress droplet coalescence.

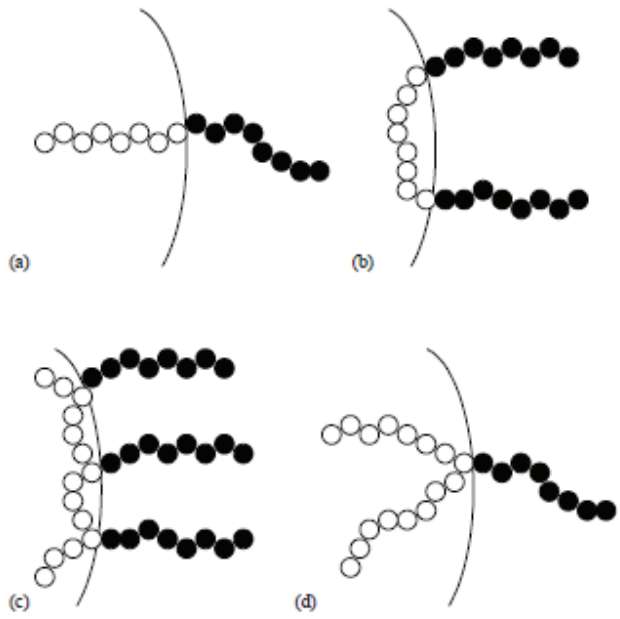

Figure I.4: Schematic picture of the supposed conformation of some compatibilizer molecules such as (a) diblock, (b) triblock, (c) multigraft, (d) singlegraft copolymers at the interface of a heterogeneous polymer blend [32].

For PDMS containing blends, due to the low surface energy and relatively low viscosity

of PDMS phase compared to most thermoplastics, the dispersion is generally difficult and results in phase segregation of PDMS in most polymer-blend systems. In order to increase the interfacial adhesion and avoid debonding between PDMS domains and thermoplastic matrix, blend compatibilization is the most important step need to be carried out.

I.2.2.2 PDMS containing blends compatibilized by pre-made copolymers

There are two routes to realize blend compatibilization of PDMS/thermoplastic blend mainly based on the rule of copolymer compatibilizer introduction. The first one is to add pre-made [33-35] block, graft, or random copolymer composed of polymer blocks, which are miscible with the blend components. This is the conventionally used method. An added block copolymer, in which one constitutive block is miscible with one blend component and the second block is miscible with the other blend component. These copolymers are expected to form a bridge-like layer by accumulating at the interface, thus lowering the interfacial tension that improves the dispersion of dispersed phase and stabilizes the morphology against coalescence. Usually, the effect of compatibilization on blends is studied in terms of obtaining fine and stable morphology. For instance, Prakashan *et* al. [36] realized the blend compatibilization of polypropylene (PP)/poly(dimethylsiloxane) (PDMS) by using a maleic anhydride grafted polypropylene (PP-g-MAH) and found that the addition of PP-g-MAH reduced the size of dispersed PDMS domains, and narrowed the domain size distribution, which is attributed to an effect of interfacial adhesion. Besides, the micromechanical deformations are enhanced with the improvement of blend morphology. However, there are some limits in using pre-made block or graft copolymers as compatibilizers in polymer blends. Most of the block copolymers are in the micro-phase separated state at mixing temperatures and they have high viscosities. This makes them difficult to disperse near the interface. In addition, added premade block copolymers reside in micelles rather than move to the interface between the immiscible homopolymers [37]. Block copolymers start to form micelles before they saturate the interface. Macosko *et* al.[38] have shown that low molar mass diblocks are able to get disperse quickly to the interface, reduce interfacial tension, and prevent dynamic coalescence. But there are still some shortcomings as they are not entangled enough in the homopolymers to prevent them from being pushed out of the interface by an approaching particle at long times. On the other hand, high molar mass diblocks are not effective because

their critical micelle concentration is too low to act as an efficient emulsifier. So, even if diffusion is aided by the mixing flow field, these long diblocks get stuck in micelles. [38] Despite these demerits, the synthesis of block or graft copolymer is often very expensive and complex. This method is often difficult to achieve in commercially processed blends, even though the conditions favoring good interfacial adhesion. Therefore, this method of using a costly copolymer may be an inefficient strategy.

I.2.2.3 PDMS containing blends obtained by reactive compatibilization

In order to prevent these shortcomings, interests had been turned towards to *in situ* compatibilization, in which copolymers are formed at the interface during processing. This strategy is commonly termed as reactive compatibilization and the processing method is known as reactive blending or reactive processing. Reactive blending is a robust and low-cost way for material preparation. Reactive compatibilization had been used in several PDMS-containing cases like Zhou *and* Osby [39] who demonstrated the formation of polycarbonate (PC)/PDMS compatibilized blends through the use of hydroxyl-terminated PDMS (PDMS-OH) reacting with PC by twin-screw extrusion at 280 °C (Figure I.5). The new formed PC-PDMS copolymer provides a compatibilization effect for the stable sub-micron blend morphology in an otherwise immiscible PC/PDMS (95/5 wt%) blend system. Silicone material was found to be well dispersed in the polycarbonate major phase forming small spherical domains with the domain size of about 0.2-0.9 μm.

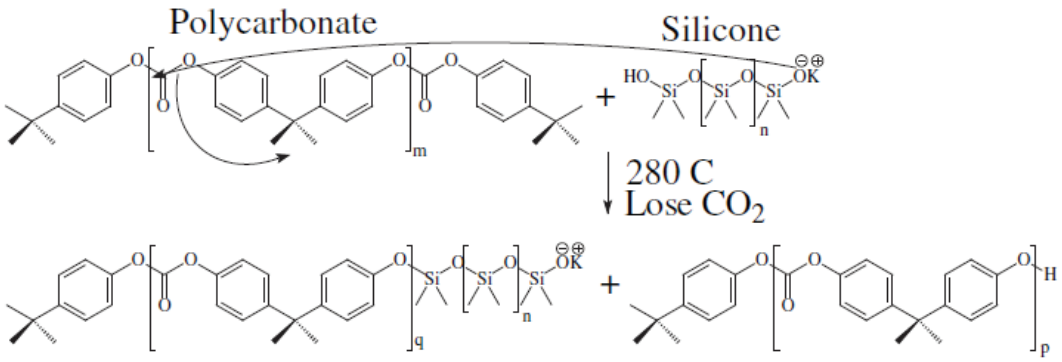

Figure I.5: A proposed reaction scheme between PDMS-OH and PC during melt extrusion [39].

In addition, Maric *et* al. [40] used reactive compatibilization to control and stabilize 20-30wt% PDMS dispersion in polyamide 6 (PA6). Specifically, two kinds of anhydride (An) functional PDMS (one is An-difunctional and the other one contains 4 random An along

PDMS chain) were used to react with amine (NH_2) end-groups of PA6. They found reactive blending of PA6 and difunctional PDMS-$(An)_2$ did not decrease PDMS particle size compared with non-reactive blend (~ 10 μm). However, particle size decreased significantly to about 0.5 μm when PA6 was blended with PDMS containing 4 random An.

The reactive compatibilization is effective to control morphology and to design high performance materials. However, for reactive blending, each blend component should bare an appropriate functional group either at the side chain or at the chain end. The compatibilization is accomplished through the melt coupling reaction between the functional groups of blend components. Depending on the molecular architecture of the blend components, block or graft copolymers are formed at the interface, assuming that the coupling reaction occurs between the functional groups which are located at the interface. However, the amount of copolymer (and the rate formation) plays a vital role for the compatibilization of immiscible blends, thus improving adhesion between polymer-polymer interfaces [41, 42]. Other methods such as the addition of a reactive polymer to the blend as a third component [43, 44] or using low molar mass compounds for instance peroxides and coupling agents as interfacial modifiers, which can react at the interface causing the formation of block copolymers [45, 46] were also reported.

It should also be noted that for reactive compatibilization, the kinetics plays a vital role. It will decide the amount and the structure of the *in-situ* formed compatibilizer. For instance, [41] polystyrene (PS) and poly(methyl methacrylate) (PMMA) containing complementary functional groups were used to determine the homogeneous coupling reaction rates, including acid/amine, hydroxyl/anhydride or acid, amine/epoxy, acid/epoxy, acid/oxazoline, aliphatic amine/anhydride and aromatic amine/anhydride. Among them, the aliphatic amine/cyclic anhydride reaction was found to be significantly the fastest. Finally, this very high reactivity may be responsible for the ability to form high levels of block copolymers during mixing. Moreover, the improvements in interfacial properties are most significant in systems of relatively high reactivity. In blends, high reactivity generally also leads to large reductions in dispersed particle size and better mechanical properties.

I.2.3 Conclusion

Generally, there are several methods for combing PDMS with thermoplastics to achieve a new kind of material with both properties, such as synthesis PDMS-containing copolymers or blend PDMS and thermoplastic directly. The latter one is more efficient for wide application, but need to improve the blend compatibilization first. Blend compatibilization is mainly depending on the introduction of amphiphilic copolymer either by adding pre-made one (physical compatibilization) or formed at the interface by reaction during process (reactive compatibilization). Recently, the application of reactive compatibilization is limited since there are not enough efficient reactions between functional PDMS and thermoplastics studied and reported. However, this method is one of the most efficient and potential one for obtaining PDMS containing organic material blends. So the most important step for reactive blending is to find useful and applicable reactions between PDMS and organic materials.

I.3 Carbonyl group hydrosilylation reaction

We originally focused on reactive blending between PDMS and polyester or polyamide based on hydrosilylation reaction. This approach aimed to carry out reaction between SiH and ester or amide groups, in the presence of catalyst, in order to create copolymers at the interface and finally realized the blend compatibilization (chapter II, III and IV). Such application of hydrosilylation reaction in polymer processing condition (high temperature, high viscosity) has not been reported except our proper studies. Besides, it should be pointed out that hydrosilylation needs a judicious choice of catalyst to promote the reaction and ensure its efficiency.

I.3.1 Introduction

Hydrosilylation [47] is a term that describes addition reaction of organic and inorganic hydrosilane to multiple bonds such as carbon-carbon, carbon-nitrogen, carbon-oxygen, nitrogen-oxygen, nitrogen-nitrogen, etc. They occur according to the following scheme:

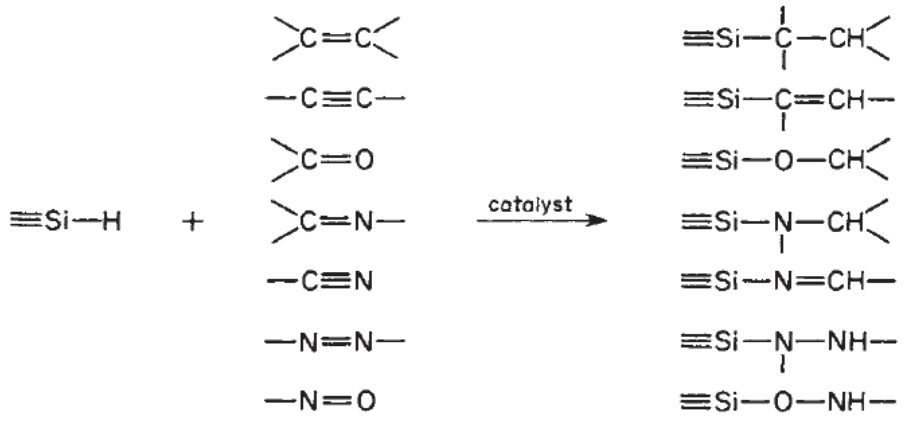

Figure I.6: Schemes of hydrosilylation reaction between different reactional groups [47] .

The addition of the Si-H bond to unsaturated compounds proceeds either in the presence of free-radical initiators (homolytic addition) or with various catalysts. These catalysts may be nucleophilic, such as tertiary amines; Lewis acids, such as metal salts; supported metals; metals reduced *in situ*; Ziegler catalysts and transition metal complex which form a very important class of catalyst for this reaction. In our work, the hydrosilylation reaction of ester or amide is mainly based on the addition between SiH and carbonyl group. The catalyst used for such kind of hydrosilylation is generally a transition metal complex especially the metal complexes of group VIII, since they can be employed in homogeneous systems or attached to inorganic and polymer substrates.

I.3.2 Rhodium complex catalyst

Rhodium complexes represent one of the most important two catalyst families being used for carbonyl hydrosilylation. This kind of catalyst was first developed for the asymmetric version of hydrosilylation reaction combined with chiral ligands [48, 49]. In addition they are mainly used for the reduction of carbonyl bond [50]. Wilkinson catalyst ($RhCl[PPh_3]_3$) is the original type of them. The mechanism of hydrosilylation in the presence of rhodium complex is shown in Figure I.7, this cyclic mechanism is started by the oxidative addition of silane to rhodium complex [50] and formed Rh-Si bond. Then, the addition is followed by coordination and insertion of carbonyl group forming an alkylmetal hydride and reductive elimination of the product to complete the catalytic cycle [50]. The associated ligands of rhodium complex using for reduction of carbonyl group are mainly diamine

pyridine ligands [51], phosphine ligands [52] or mixed ligands based on phosphorus and nitrogen [53].

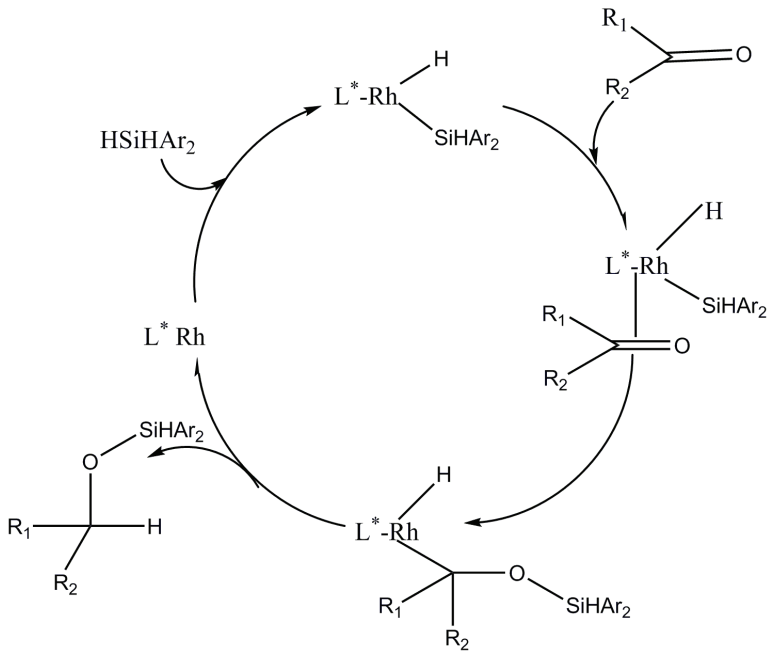

Figure I.7: Catalytic cycle of carbonyl bond hydrosilylation with rhodium complex catalyst [50].

There are a lot of work carried out about the efficiency of $RhCl[PPh_3]_3$ for carbonyl group hydrosilylation reaction. As reported, Ojima *et* al. [54] investigated the efficiency of Wilkinson catalyst for hydrosilylation reaction of carbonyl compounds having an electron donor group in α position. Hydrosilylation of simple or α, β-unsaturated carbonyl compounds with monohydrogen silanes have yields more than 95 mol% under mild conditions (reaction temperature at 60 °C, reaction time of 30 min). For example, hydrosilylation reaction of equimolar triethylsilane/cyclohexanone mixture in the presence of 0.5 mol% $RhCl[PPh_3]_3$ has a yield around 98 mol% after 5 min reaction at room temperature.

Other kinds of rhodium complex catalysts were also developed and used for hydrosilylation reaction, such as dirhodium trtrakis(perfluorobutyrate) $[Rh_2(pfb)_4]$ being used for α, β-unsaturated carbonyl compounds [55]. To be more exact, they used 0.01 mol% $Rh_2(pfb)_4$ for 2-cyclohexene-1-one hydrosilylation at 40 °C in chloroform and obtained a yield of 96 mol% after 1 h reaction. Besides, rhodium complexes used for hydrosilylation of amides were also reported [56]. In general, amide can be reduced to amine by hydrosilane in the presence of rhodium complex. For example, Kuwano *et* al. used 0.1 mol% $RhH(CO)(PPh_3)_3$ to catalyze reaction between Ph_2SiH_2 and *N*,*N*-dibenzylacetamide at room

temperature. After 1 h the reaction was almost completed and yielded 94 mol% of dibenzylethylamine. They also proved other rhodium complexes without a hydride ligand, like $RhCl_3 \cdot 3H_2O$, $RhCl(PPh_3)_3$ and $[Rh(COD)_2]BF_4$-$2PPh_3$, could also promote the reduction of tertiary amide to amine with a high yield. The mechanism for the reduction of amides with a hydrosilane was also investigated as shown in Figure I.8, the catalytic cycle may start from oxidative addition of hydrosilane to Rh(I) complex (3), forming hydrido(silyl)rhodium (III) (4), whose Rh-Si bond undergoes insertion of an amide carbonyl group. It might be presumed that rapid hydride transfer to the resultant Rh(III) complex (5) from 4 leads to selective reductive cleavage of the C-O bond of 5 with the formation of alkylrhodium complex 6. The catalytic cycle ends up with reductive elimination from complex 6 [56].

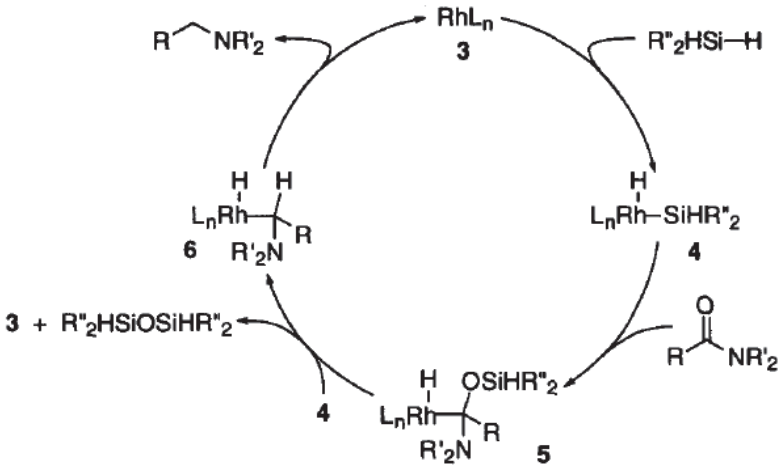

Figure I.8: Catalytic cycle of amide carbonyl bond hydrosilylation with rhodium complex catalyst [56].

I.3.3 Ruthenium catalyst

Ruthenium complexes represent another important catalyst family used for carbonyl hydrosilylation. For instance, Eaborn *et* al. [57] reported hydrosilylation reaction worked between triethylsilane and aldehyde or ketone in the presence of ruthenium complex as $RuCl_2(PPh_3)$ and $RuClH(PPh_3)$. However, they proved that such addition reaction were less efficient than the one using rhodium complex since the yield of aliphatic ketones or aldehyde hydrosilylation after 1-3 h reaction at 90 °C was around 70 mol% is quite lower than rhodium-catalyzed one with a yield over 90 mol% as mentioned before. It means that chlorohydridotris (triphenylphosphane) ruthenium complex is less effective than Wilkinson catalyst. However, in 2008, Köytepe *et* al. [58] found a method to synthesize

polyimide-supported ruthenium catalyst. In contrary, comparing with similar rhodium complex catalyst, it is more effective especially when used at higher reaction temperature. To be more precise, it is prepared by functionalizing a heat- and acid-resistant polyimide resin with a homogeneous metal catalyst of ruthenium (II) complex. Such heterogeneous polyimide-supported transition metal complex catalyst provides superior catalytic activity, stability and selectivity in the hydrosilylation of acetophenone. Further, the catalyst has strong resistance against acid and heat. Besides, the catalyst of the invention may provide the following advantage which is critical in industrial use: it can be easily separated from the reaction product, which eases recycling of the catalyst [58].

Igarashi *et* al. [59] reported that hydrosilylation reaction of ester and trimethylsilane being catalyzed by ruthenium complex can be achieved. For example (Figure I.9), different mixtures of ester, Et_3SiH and $Ru_3(CO)_{12}$ in toluene was heated at 100 °C for 16 h under argon atmosphere leading to hydrosilylation reaction yields ranged from 45 to 95 mol%. The yield is closely dependent on the nature of ester: methyl, isopropyl, and phenyl esters afforded satisfactory results (57-94 mol%) but sterically hindered esters such as tert-butyl ester has a much lower yield (45 mol%). The authors compared two kinds of catalyst, the $Ru_3(CO)_{12}$ and $[RuCl_2(CO)_3]_{12}$, and found similar activities when $[RuCl_2(CO)_3]_{12}$ is used in the presence of diethylamine and ethyl iodide as co-catalysts (57-98 mol%). Besides, the obtained products are stable enough toward air and moisture, and are easily handled without special care. Instead of triethylsilane, other kinds of hydrosilane such as tert-butyldimethylsilane and phenyldimethylsilane can also be applicable in the present reaction.

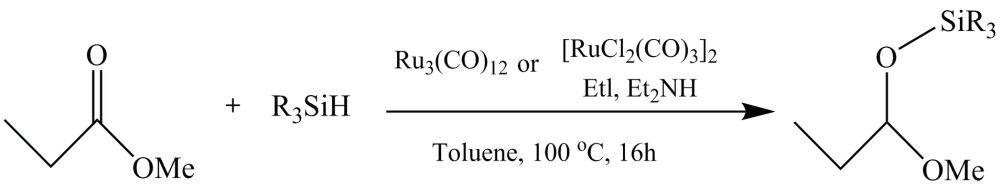

Figure I.9: Hydrosilylation of methylpropionate by hydrosilanes [59] .

In addition, Matsubara *et* al. [60] found catalyst (μ^3, η^2, η^3, η^5-acenaphthylene)$Ru_3(CO)_7$ as an efficient catalyst for carboxylic acids, esters and amides reaction with trialkylsilanes. For ester such as styrene-acrylic acid methyl ester, after 30 min at 20 °C in 1,4 dioxane with $HSiMe_2Et$ and catalyzed by $Ru_3(CO)_7$, the yield can reach 97 mol%. Under similar reaction

condition $Ru_3(CO)_7$ complex shows better catalytic activity than $Ru_3(CO)_{12}$. For carboxylic acids and amides, the results of such hydrosilylation reaction are different as they can lead to corresponding silylated ethers and amines as a dehydrogenative silylation exist. Similar phenomenon was also found by Hanada *et* al. [61]. Specifically, they found that the (μ^3, η^2, η^3, η^5 -acenaphthylene)$Ru_3(CO)_7$ can catalyze reduction of secondary amides with hydrosilanes, yielding a mixture of secondary amines, tertiary amines, and silylated enamines. They investigated the reaction mechanism in detail and described that such reduction was initiated by the addition of hydrosilane to amide carbonyl group. Thus, the adduct product will be dehydrogenated and an amine formed (Figure I.10). It should be noted that the factors determining the rate and the selectivity of the mentioned reactions are the structure of the silanes, the catalyst used, and the reaction temperature.

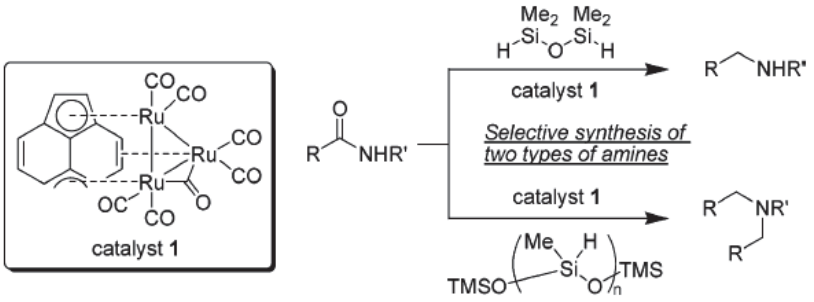

Figure I.10: Reduction of amides by hydrosilanes [61].

Therefore, both rhodium and ruthenium complexes show effectively catalytic ability of carbonyl from ester or amide, especially for amide to be reduced and finally leading to form amine or silyl amine. Apart from these two main catalyst families, there are still other kinds of metal complexes being developed for hydrosilylation and reduction of carbonyl group.

I.3.4 Other kinds of hydrosilylation catalysts

There are many metal catalyst families which are used for carbonyl hydrosilylation with different catalytic activities. For instance, titanium based complex is one of the hydrosilylation catalysts with high selectivity. Buchwald *et* al. [62-65] investigated the efficiency of titanium complex like Cp_2TiX (X=Cl or OAr) and $Ti(OiPr)_4$ for the reduction of esters or lactones by hydrosilylation reaction in the presence of polymethylhydrosiloxane (PMHS). Such reactions are effective at room temperature (25 °C). The yield of ester hydrosilylation with 5 mol% Cp_2TiCl_2 can reach among 70-90 mol% [64]. The

hydrosilylation reaction of lactones being catalyzed by $Cp_2Ti(OR)_2$/TBAF mixture or Cp_2TiF_2 in THF/NaOH solvent can achieve a yield higher than 90 mol% [62]. Besides, they found that PMHS as hydrosilane is suitable for many esters without pre-activating the catalyst.

Yang *and* Tilley [66] reported that iron(II) silylamide catalyst $[Fe\{N(SiMe_3)_2\}_2]$ is also efficient for carbonyl compounds hydrosilylation at mild temperature (23°C). Specifically, acetophenone or benzaldehyde can be rapidly reduced to $PhSiH(OCHRPh)_2$ as the dominant product within 3h in the presence of 2.7 mol% catalyst (yield is 90%, Figure I..11). In addition, secondary silanes are also suitable substrates for hydrosilylation catalyzed by $[Fe\{N(SiMe_3)_2\}_2]$. With Ph_2SiH_2 as the reductant, aldehydes and ketones underwent facile catalytic hydrosilylation at 23°C to cleanly afford the corresponding silyl ethers $Ph_2SiHOCHRR$.

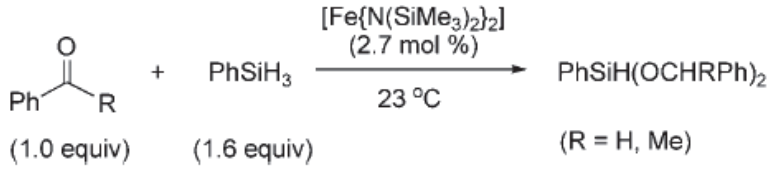

Figure I.11: Carbonyl hydrosilylation catalyzed by iron complex [66].

Complexes of Cu(I) associated with phosphine ligands ($CuH[PPh_3]$) are also reported useful for carbonyl compounds hydrosilylation. Brunner *et* al. [67] found such application in reduction of ketones. Lipshutz *et* al. [68] also investigated $CuH[PPh_3]$ catalyzed hydrosilylation being used for aldehydes and ketones reduction. With the use of 3 mol% of such catalyst and $PhMe_2SiH$, the yield of aldehyde reduction in toluene can be more than 90 mol% after 2 h. Riant *et* al. [69] used 1 mol% of CuF_2 complex associating with diphosphine as catalyst for acetophenone reduction and obtained around 80 mol% yield. Such Cu-catalyzed reactions were carried out in toluene at room temperature.

There are still a few reports about the use of aluminum complex working as catalyst for hydrosilylation of esters. For example, $Al(H_2PO_4)$ is efficient for *β*-ketonester in presence of alcohol. The yield can reach 80-95 mol% after 30 min reaction at 80 °C [70]. Other unusual metal-based complex such as MoO_2Cl_2 complex can also be used for hydrosilylation. The

catalytic mechanism is different as it is carried out with radical O^o passage. Usually, for hydrosilylation reaction of aromatics in acetonitrile catalyzed by MoO_2Cl_2, the yield can grow rapidly to almost 100 mol% in 15 min [71].

I.3.5 Conclusion

We introduced numbers of metal complexes which are potential carbonyl hydrosilylation catalysts according to the literatures. Generally, these reactions were carried out in mild conditions at reaction temperature below 90 °C, atmospheric pressure, and in solution. Reaction time and temperature vary depending on the type of catalyst. In addition, the majority of reported carbonyl hydrosilylation reaction is about low molar mass compounds.

Until now, the hydrosilylation reaction of carbonyl groups coming from polymer remains in the exploratory stage. Our colleagues Bonnet *et* al. [72, 73] had done the initial attempt to apply ruthenium catalyzed carbonyl hydrosilylation to ethylene-vinyl acetate (EVA) chemical modification with hydride terminated PDMS (PDMS-SiH) or polymethylhydrosiloxane (PMHS) in the presence of $Ru_3(CO)_{12}$. It focused on the addition of hydrogenosilane groups (SiH) from polysiloxane to the carbonyl groups of EVA. The influence of the nature of the polysiloxane on blend properties was investigated by rheology and scanning electron microscopy. Mixing of a low viscosity polysiloxane with a high viscosity EVA matrix produced a two-phase morphology. The occurrence of the hydrosilylation reaction at the EVA/polysiloxane interface promoted a homogenization of the blend depending on the molar ratio SiH/vinyl acetate groups, [SiH]/[VA], and the viscosity ratio of the blend. Two distinct behaviors were observed. The formation of a crosslinking network under shear was obtained for a low viscosity ratio between polysiloxane and EVA ($\lambda_{polysiloxane/EVA} = 4.0 \times 10^{-6}$) with a high concentration of SiH groups ([SiH]/[VA] = 0.5), while the formation of a compatibilized blend was observed for high molar mass polysiloxanes (Mn > 15,000 $g.mol^{-1}$) with a low concentration of SiH([SiH]/[VA] < 4.0×10^{-3}). Generally, a new and original method based on carbonyl hydrosilylation was developed to prepare EVA/polysiloxane polymer blends.

Except the work done by Bonnet, there is no more report about such application of

carbonyl hydrosilylation to polymer reactive compatibilization, especially for polyamide. Therefore, the addition of SiH groups to carbonyl groups of PA12, PBT and other carbonyl groups containing polymers is a challenge and provide a new method of polymer chemical modification. In our work, we will use the experimental conditions described by Igarashi *et* al. [59] about the hydrosilylation reaction of esters and by Bonnet *et* al. [72] about hydrosilylation of copolymer EVA catalyzed by $Ru_3(CO)_{12}$.

Application of this innovative polymer chemical modification will be described in details such as in PA12/polysiloxane (chapter II and III) and PBT/polysiloxane (chapter IV) blends.

I. 4 Potential applications of organic materials containing PDMS

I.4.1 Introduction

As introduced in the first part of this chapter, PDMS has special molecular structure and composition, inorganic skeleton (alternating silicon-oxygen atoms) and organic side groups, leading it to obtain some useful and particular properties [1] such as good resistance to UV radiation, excellent release properties and surface activity, high selective permeability, hydrophobicity, biocompatibility, *etc.* Therefore, the addition of PDMS to commercial polymers to modify such properties through either synthesis PDMS containing copolymers or polymer blends was widely reported. These applications range from surfactants to photoresists, protective coating to contact lenses, gas separation membranes to biomaterials [74]. However, it is important to note that, since most of the progress in the preparation of novel and well-defined PDMS containing organic material has been carried out well in recent decades. So here we want to discuss about not only their present use but also some potential application which are still in their development stages.

I.4.2 Hydrophobicity of PDMS containing materials

Some of the most interesting and unique features of PDMS containing organic materials are associated with their surface properties. PDMS is a well-known material with low surface energy. Because of its intrinsic deformability and hydrophobic property, PDMS can readily be used into superhydrophobic surfaces using various methods. For example, Jin *et* al. [75]

used a laser etching method to prepare a rough surface of PDMS elastomer containing micro-, submicro- and nanocomposite structures. Such a surface exhibited a superhydrophobicity property with water contact angle higher than 160° and sliding angle lower than 5°. Similarly, Khorasani *et* al. [76] treated PDMS using a CO_2-pulsed laser as an excitation source. The water contact angle for the treated PDMS was as high as 175° (Figure I.12a) which was believed to be due to both the chain ordering and porosity on the PDMS surface. Sun *et* al. [77] reported a nanocasting method to make superhydrophobic PDMS surface recently. They first made a negative PDMS template using lotus leaf as an original template and then used the negative template to make a positive PDMS template-a replica of the original lotus leaf. The positive PDMS template (Figure I.12b) had the same surface structures and superhydrophobicity as the lotus leaf. Given the difference in composition and consequent surface energy between the lotus leaf (paraffinic wax crystals, $-CH_2-$, 30-32 mN/m) and the PDMS replica ($-CH_3$, 20 mN/m), the similarity of the hydrophobicity obtained is surprising.

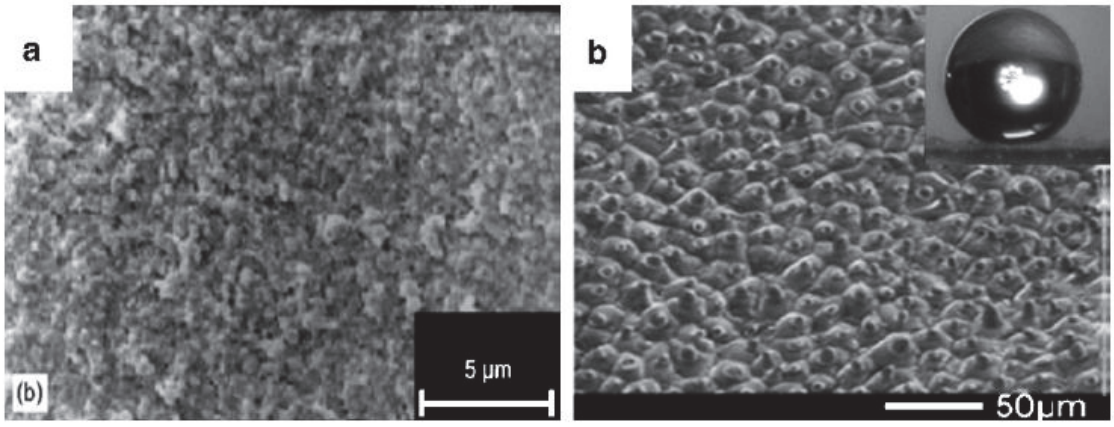

Figure I.12: SEM images of superhydrophobic surfaces made by roughening silicone-based materials: (a) PDMS surface treated by CO_2-pulsed laser [76] (reproduced by permission of Elsevier); (b) lotus leaf-like PDMS surface by nanocasting [77].

Since the excellent performance of PDMS in superhydrophobic application, therefore surface modification of commercial polymers through the combination with PDMS is widely concerned. For instance, Ma *et* al. [78] made a superhydrophobic membrane in the form of a nonwoven fiber mat by electrospinning a PS-PDMS block copolymer blended with PS homopolymer. The superhydrophobicity with water contact angle of 163° (Figure I.13) was attributed to the combination of enrichment of PDMS component on fiber surface and the surface roughness due to small fiber diameters (150 nm to 400 nm). The flexibility,

breathability and free-standing feature of the membrane are of particular interest in areas such as textile and biomedical applications. Recently, Zhao *et* al. [79] prepared a superhydrophobic surface by casting a micellar PS-PDMS solution in humid air based on the cooperation of vapor-induced phase separation and surface enrichment of PDMS block.

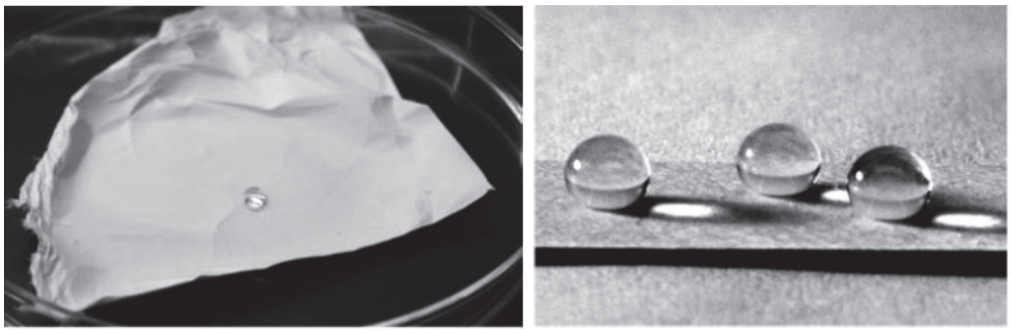

(a) (b)

Figure I.13: (a) Free-standing mat composed of the PS-PDMS/PS electrospun fibers with a water droplet on it; (b) several 20 ml water droplets on the mat, showing the superhydrophobicity [78].

Other examples like Verma *et* al. [80] who prepared polyester based, PDMS modified waterborne anticorrosive hydrophobic coating through mixing polyester resin, hydroxyl terminated polydimethylsiloxane, hexa(methoxymethyl)melamine (crosslinker) and para-toluene sulphonic acid (catalyst) with a suitable composition. This coating can be used on copper. The water contact angle increased significantly confirming the enhancement in the hydrophobicity of the coating after modification with PDMS as shown in Figure I.14.

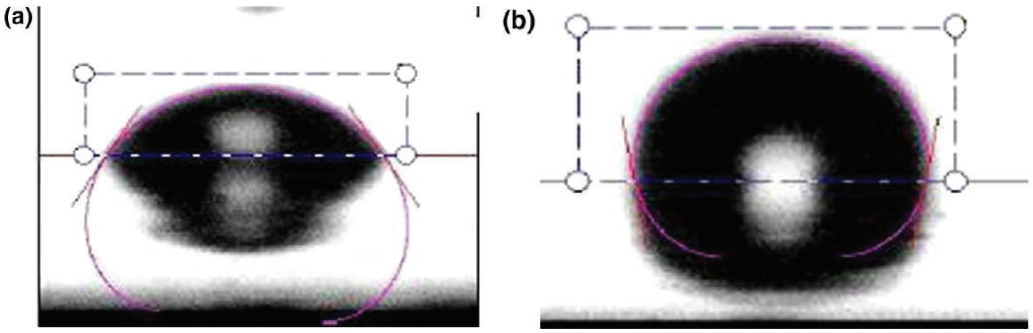

Figure I.14: Photograph of water droplet on the coated copper panels with (a) neat polyester and (b) PDMS modified polyester coatings [80].

PDMS containing materials was also used to improve hydrophobicity of textiles. As reported by Chen *et* al. [81] who found oligomer UV-curable PDMS-containing polyurethane

(PU), (UV-PDMS-PU), preparing through an addition of 2-hydroxyethyl methacrylate (2-HEMA) to NCO-terminated PDMS-containing PU, pre-polymer (NCO-PDMS-PU), can be applied to textile (PET and Nylon) surface treatment. They coated UV-PDMS-PU on textile and then cured it by UV-radiation. After this modification, PET and Nylon textiles both showed a long lasting hydrophobic property. To be more exact, the untreated PET textile absorbs water drops completely due to the capillary effect of the fibers. When PET was treated with PDMS-PU, the contact angle was measured as 128° before washing and then decreased to 124° after five or ten cycle water washings (Figure I.15-left). Similar phenomenon was also observed in Nylon textile as shown in Figure I.15-right.

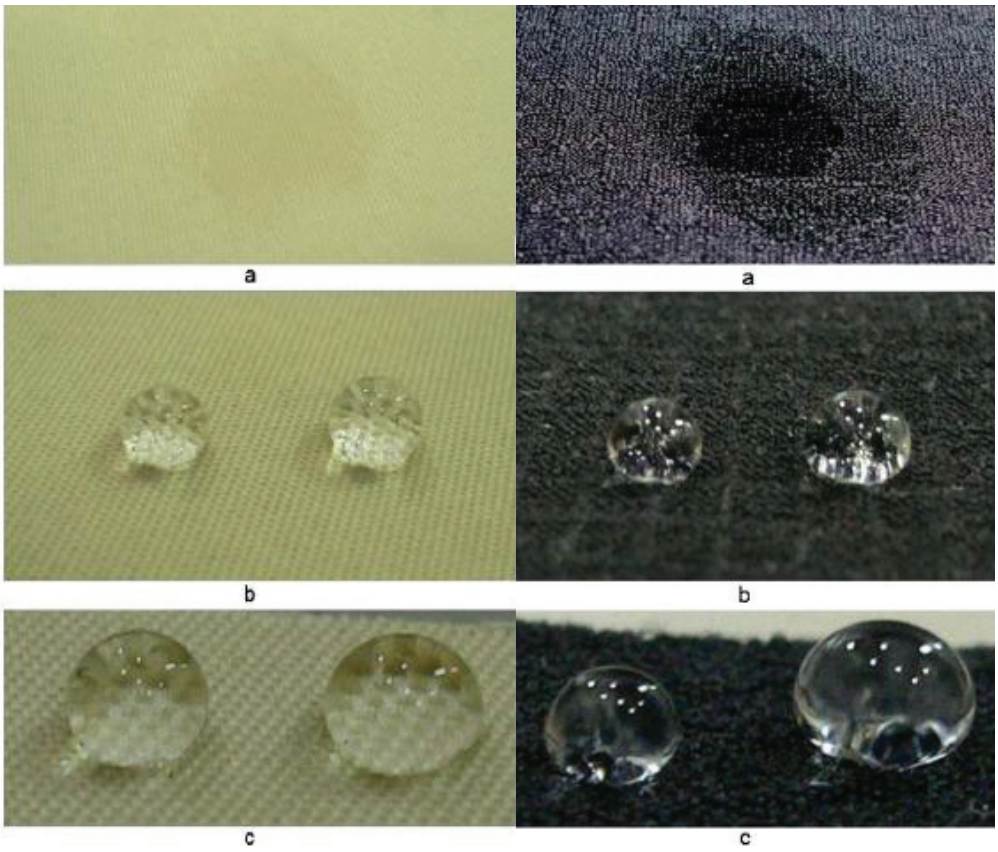

Figure I.15: Water drops on PET(left) and Nylon (right), a) textile original b) textile treated with PDMS-PU before washing c) treated textile after ten water washing cycles [81].

As mentioned before, there are a lot of researches around the introduction of PDMS to achieve hydrophobic or even superhydrophobic materials which can be used as coating or film for anticorrosive, self-cleaning, wettability decrease, *etc*., especially for polyester or polyamide which are not hydrophobic themselves. PDMS works well and has potential in more extensive application of hydrophobicity due to its low-cost and reactivity. However

there are still some problems to be solves like simplify the preparation process, improve the miscibility with other polymer and the stability of final products.

I.4.3 Gas separation of PDMS containing materials

For gas separation (GS) membrane both its permeability and selectivity influence the economics of a GS membrane process. Permeability is the rate at which any compound permeates through a membrane; it depends upon a thermodynamic factor (partitioning of species between membrane phase and feed phase) and a kinetic factor (diffusion in a microporous membrane or diffusion in a dense membrane). The selectivity is the ability of a membrane to accomplish a given separation (relative permeability of the membrane for the feed species). Selectivity is a key parameter to achieve high product purity at high recoveries [82].

PDMS is well known for its application in gas permeability. Rubbery membrane PDMS has weak molecular sieves ability due to its weak intermolecular forces, resulting in broad distribution of intersegmental gap sizes responsible for gas diffusion [83]. However, PDMS homopolymers are mechanically weak and also do not show high selectivities towards different gases. Even PDMS containing polymers can increase mechanical strength of membranes using for gas separation, they are also weak in gas selectivity. For example, Chen *et* al. [84] reported the synthesis of polysiloxaneimide (PSI) membrane for gas (O_2/N_2) separation. This polysiloxaneimide (PSI) polymer was prepared by condensation of pyromellitic dianhydride (PMDA), amine-terminated PDMS A and 4, 4'-oxydianiline (ODA). It was found that the PDMS content played an important role in the packing of PSI polymer chains, the addition of PDMS moiety in polyimide matrix probably increased the polymer free volume and disrupted its packing. This result can also be attributed to the flexibility of the introduced siloxane linkage which affects the packing of the polymer chain. Therefore, the effects of the membrane composition on the gas permeability and O_2/N_2 selectivity were significant. If the diffusion-solution model was adopted, the increase in PDMS content greatly increased the gas permeability and the gas diffusivity. However, the sacrifice of the gas selectivity cannot be avoided as the flexibility of PDMS tended to enlarge the gas pathway in the membrane and therefore results in the decrease of O_2/N_2 selectivity. But through careful

selection and design of material structure, it is also possible to improve the gas selectivity. There are some PDMS containing copolymers which have been evaluated as gas separation membranes with good selectivities. For instance, Park *et* al. [85] prepared polyurethane ureas (PUUs) which are multiblock copolymers consisting of hard segments [4,4-diphenylmethane diisocyanate (MDI)] and soft segments [poly(tetramethylene oxide), poly(ethylene oxide) or PDMS]. When the single soft segment is PDMS-type, they found that the small introduction of PDMS into PUU led to both gas permeabilities and selectivities of O_2/N_2 and CO_2/N_2. This might be due to the incorporation of PDMS which led to the phase separation in both hard segment (MDI) and soft segment due to the difference of the solubility parameter, and thus dispersed PDMS phases might serve to produce a more tortuous route for diffusing molecules as shown in Figure I.16.

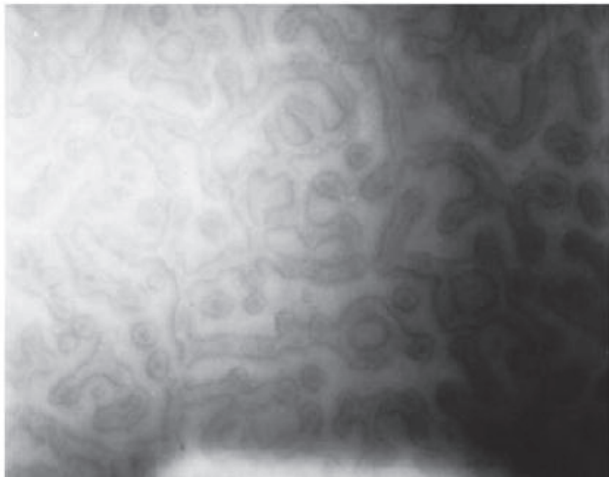

Figure I.16: Transmission electron micrographs of copolymers PUU(PDMS) [85].

Reijerkerk *et* al. [86] reported that they prepared blend membrane through solution consisting PEBAX® 1657 [a polyether-block-amide comprising 60 wt% poly(ethyleneglycol) (PEG) and 40 wt% aliphatic polyamide (PA6)] and PDMS-PEG copolymer. The additive (PDMS-PEG) consists for 80 wt% of PEG and the remaining 20 wt% is PDMS, which is highly flexible and permeable. As such, they combine the high selectivity of PEG for CO_2 with the high permeability of PDMS. This membrane shows the strong potential of the concept as a way to significantly increase the gas permeability and gas selectivity as the CO_2/H_2 ideal selectivity increased from 9.5 for PEBAX® 1657 to 10.6 for PEBAX® 1657 with 50 wt% PDMS–PEG additive (at 35 °C and 4 bar feed pressure). In addition, this method provided a new concept to achieve even higher permeabilities combined with good

selectivities when it was applied using even more permeable polymers like blending of the PDMS-PEG additive with the PEO-*ran*-PPO-T6T6T (aromatic polyamide) block copolymers [87] and so on.

In general, due to the high gas permeability of PDMS, it is suitable and has much potential in gas separation application. But there are still some aspects need to be noted, like mechanical properties, stability and the key problem as mentioned before about how to obtain both good gas permeability and selectivity of such PDMS containing organic materials.

I.4.4 Other applications

PDMS containing materials also have some applications on biological area, such as siloxane-urethane segmented copolymers, or their blends with conventional polyurethane/ polyurethane ureas, which have very good mechanical, surface and fatigue properties [74], have been successfully used in the production of intra-aortic balloons, blood pumps and artificial hearts [74, 88, 89]. Another well-established application is in contact lenses since its extremely high oxygen permeability [90].

Incorporation of PDMS into various organic polymer backbones has been shown to improve the flame resistance. Detailed studies on the flammability and limited oxygen indices of various PDMS-polycarbonate copolymers have been carried out [74, 91]. A synergistic enhancement in limiting oxygen indices of several polymeric systems has been shown to vary with the hard segment type in the following order [91]: bisphenol-A polycarbonate > polystyrene > poly(methyl methacrylate). In addition, incorporation of PDMS into polycarbonates also improves their environmental stress crack resistance and toughness. As a result, this type of material was evaluated for possible use in the aircraft canopy [92].

A submicron pattern with a high aspect ratio was fabricated using the PDMS copolymer as the top layer in a multilayer resist system. Chlorinated poly(methyl styrene)-PDMS block copolymers were shown to function as single component bi-level resists [93]. These materials exhibited both O_2 reactive ion etch resistance and electron beam sensitivity. Graft copolymers of poly(methyl methacrylate) and PDMS were also evaluated as deep UV positive photoresists [94].

PDMS containing poly(alkylene oxide), polyester and polystyrene type copolymers have been used to improve the lubrication, flow and heat resistance properties of epoxy resin powder coatings [95]. Thermally stable polyester-polysiloxane segmented copolymers have been shown to improve the antifriction, flow properties and scratch resistance of acrylic based auto repair lacquers [96].

Poly(n-butyl methacrylate-acrylic acid)-PDMS graft copolymers [74] and polystyrene-PDMS block copolymers [97] have been used as pressure sensitive adhesives. Hot melt adhesives based on polycarbonate-PDMS segmented copolymers [98] showed very good adhesion to substrates with low surface free energy without the need for surface preparation, such as etching.

Introduction of flexible PDMS spacers into main chain or side chain liquid crystalline polymers have been shown to significantly reduce the transition temperatures [26, 99] and increase the response time of the resultant systems to the applied thermal, optical or electrical filed [100, 101]. Besides, PDMS also provided elastomeric properties and improved the processibility of the resulting liquid crystalline copolymers.

I.5 Objective

Through the study of review, it is clear that with its unique and some excellent properties, PDMS had been used or has a potential to be used in a wide range of applications like biomaterials, superhydrophobic and self-cleaning materials, gas separation membranes, adhesive, *etc.* Such properties are close to the material structure and morphology. However, single segment of PDMS is weak in mechanical properties. Therefore, such materials are most achieving from copolymer synthesis which can combine both properties of PDMS and the mechanical properties of commercial polymer like PU, PEG, PC or other kinds of polyester, polyamide. Synthesis of PDMS containing copolymers is useful way to design the materials what we want, like the proportion of soft and hard segments, final microstructure and properties. But through synthesis, it is hard to satisfy the increasing need of PDMS containing materials since the limited yield and high-cost. Another more efficient way to achieve such material is through blending directly.

The reports about PDMS containing materials through blending are not as many as

through synthesis. Because of one hand the difficulty to solve the incompatible problem between PDMS and other polymers, and in the other hand the difficulty to control the final microstructure of the materials during blending process. At recent, the studies of PDMS containing blends are mainly focused on the two problems. For instance, adding amphiphilic copolymer or *in situ* forming copolymer which can work as compatibilizer was considered.

According to the publications, we find an efficient reaction between SiH and carbonyl groups. It is ruthenium catalyzed carbonyl hydrosilylation reaction. We want to apply such reaction to *in situ* compatibilization between PDMS and carbonyl containing polymers like polyester, polyamide to achieve new PDMS containing blends efficiently. Besides, there is few work concerns about the use of multifunctional PDMS like PMHS for polymer chemical modifications, almost all of such works were carried out by functional terminated PDMS. So it is interesting, initial and challenging to investigate such application of PMHS. In order to achieve the goal, there are several aspects to be concerned:

1) Well understand the possibility, efficiency and mechanism of ruthenium catalyzed carbonyl hydrosilylation.

2) Extend such reaction to polyester like PBT or polyamide like PA12. Investigate the optimal processing parameters and physico-chemical parameters which will influence the microstructure of the blends.

3) Study the properties of such blends like surface free energy and ability of gas separation. Combine the properties with material microstructure and try to design materials according to the final properties we need.

4) Investigate the behavior of PMHS in the chemical modification with PBT or PA12 and compare with that of PDMS-SiH to understand better about the role of physico-chemical parameters in controlling the final properties of blends.

I.6 References

[1] S.J. Clarson, J.A. Semlyen, Siloxane polymers, Prentice Hall1993.

[2] S.J. Clarson, Synthesis and properties of silicones and silicone-modified materials, American Chemical Society2003.

[3] A. Noshay, J.E. McGrath, Block copolymers: overview and critical survey, Elsevier2013.

[4] E.L. Thomas, D.M. Anderson, C.S. Henkee, D. Hoffman, Periodic area-minimizing surfaces in block copolymers, (1988).

[5] R. Richards, Small angle neutron scattering from block copolymers, Analysis/Reactions/Morphology, Springer1985, pp. 1-39.

[6] Ì. Yílgör, K. Ahmad, W.P. Steckle, D. Tyagi, G.L. Wilkes, J.E. McGrath, Segmented organosiloxane copolymers. 1. Synthesis of siloxane—urea copolymers, Polymer 25(12) (1984) 1800-1806.

[7] R.G. Jones, W. Ando, J. Chojnowski, Silicon-containing polymers: the science and technology of their synthesis and applications, Springer Science & Business Media2013.

[8] J. McGrath, P. Sormani, C. Elsbernd, S. Kilic, Kinetics, mechanisms, and synthesis studies of difunctional aminopropyl terminated polydimethylsiloxane oligomers, Makromolekulare Chemie. Macromolecular Symposia, Wiley Online Library, 1986, pp. 67-80.

[9] G. Belorgey, G. Sauvet, Organosiloxane block and graft copolymers, Silicon-containing polymers, Springer2000, pp. 43-78.

[10] J. O'Malley, T.J. Pacansky, W. Stauffer, Synthesis and Characterization of Poly (hexamethylene sebacate)-Poly (dimethylsiloxane) Block Copolymers, Macromolecules 10(6) (1977) 1197-1199.

[11] P. Bajaj, S. Varshney, A. Misra, Block copolymers of polystyrene and poly (dimethyl siloxane). I. Synthesis and characterization, Journal of Polymer Science: Polymer Chemistry Edition 18(1) (1980) 295-309.

[12] H.A. Vaughn, The synthesis and properties of alternating block polymers of dimethylsiloxane and bisphenol‐A carbonate, Journal of Polymer Science Part B: Polymer Letters 7(8) (1969) 569-572.

[13] I. Fellegvári, K. Valkó, G. Váradi, P. Bauer, M. Kramer, Purification of human chorionic gonadotropin hormone by anion-exchange high-performance liquid chromatography, Chromatographia 27(11-12) (1989) 601-604.

[14] D. Webster, P. Andolino, 1. S. Riffle, FL Keohan and JE McGrath, Polym. Preprmts 24(1) (1983) 161.

[15] J. Riffle, R. Freelin, A. Banthia, J. McGrath, Interfacial Synthesis Part II: Phase-Transfer Catalyzed Synthesis of Polycarbonate/Polysiloxane Block Copolymers, Journal of Macromolecular Science—Chemistry 15(5) (1981) 967-998.

[16] R. Hernandez, J. Weksler, A. Padsalgikar, J. Runt, Microstructural organization of three-phase polydimethylsiloxane-based segmented polyurethanes, Macromolecules 40(15) (2007) 5441-5449.

[17] M. Kajiyama, M. Kakimoto, Y. Imai, Synthesis and properties of new multiblock copolymers based on dimethyl siloxane and N-phenylated polyureas, Macromolecules 23(5) (1990) 1244-1248.

[18] J. McGrath, L. Wang, J. Mecham, Q. Ji, Synthesis and characterization of segmented siloxane copolymers, Polymer Preprints(USA) 39(1) (1998) 455-456.

[19] G.J. Murphy, D.M. Kirkham, M.A. Cawthorne, P. Young, Correlation of β3-adrenoceptor-induced activation of cyclic AMP-dependent protein kinase with activation of lipolysis in rat white adipocytes, Biochemical pharmacology 46(4) (1993) 575-581.

[20] P.J. Madec, E. Marechal, Synthesis and study of block copolycondensates containing polysiloxane and unsaturated polyester blocks in the chain. II. Poly (unsaturated esters‐b‐siloxanes) with blocks linked by Si C bonds and poly (butadienes‐b‐siloxanes), Journal of Polymer Science: Polymer Chemistry Edition 16(12) (1978) 3165-3172.

[21] D. Tyagi, J. Hedrick, D. Webster, J. McGrath, G. Wilkes, Structure—property relationships in perfectly alternating segmented polysulphone/poly (dimethylsiloxane) copolymers, Polymer 29(5) (1988) 833-844.
[22] L.M. Robeson, A. Noshay, M. Matzner, C.N. Merriam, Physical property characteristics of polysulfone/poly‐(dimethylsiloxane) block copolymers, Die Angewandte Makromolekulare Chemie 29(1) (1973) 47-62.
[23] P. Sormani, R. Minton, I. Yilgor, P.A. Brandt, C. TRAN, J. RIFFLE, J. McGrath, Ring-opening polymerization of cyclic siloxanes in the presence of fnctional disiloxanes, abstract of papers of the american chemical society, AMER CHEMICAL SOC 1155 16TH ST, Nw, Washinton, DC 20036, 1984, pp. 131-POLY.
[24] P. Juliano, T. Mitchell, SYNTHESIS, Physical-properties and crystallization studies on poly (2, 6-diphenyphenyene oxide-dimethylsiloxane) block copolymers, abstract of papers of the american chemical society, AMER CHEMICAL SOC 1155 16TH ST, Nw, Washinton, DC 20036, 1980, pp. 27-POLY.
[25] C. Aguilera, J. Bartulin, B. Hisgen, H. Ringsdorf, Liquid crystalline main chain polymers with highly flexible siloxane spacers, Die Makromolekulare Chemie 184(2) (1983) 253-262.
[26] H. Finkelmann, H.J. Kock, G. Rehage, Investigations on liquid crystalline polysiloxanes 3. Liquid crystalline elastomers—a new type of liquid crystalline material, Die Makromolekulare Chemie, Rapid Communications 2(4) (1981) 317-322.
[27] G. Torrès, P.J. Madec, E. Maréchal, Synthesis of polysulfone‐block‐polysiloxane copolymers, 4. A model study of the limitation of hydrosilylation coupling, Die Makromolekulare Chemie 190(1) (1989) 203-212.
[28] P. Chaumont, G. Beinert, J. Herz, P. Rempp, Synthesis and characterization of multiblock copolymers containing poly (dimethyl siloxane) blocks, Polymer 22(5) (1981) 663-666.
[29] J. Parameswaranpillai, S. Thomas, Y. Grohens, Polymer Blends: State of the Art, New Challenges, and Opportunities, Characterization of Polymer Blends: Miscibility, Morphology and Interfaces (2014) 1-6.
[30] R. Jiang, R.P. Quirk, J.L. White, K. Min, Polycarbonate‐polystyrene block copolymers and their application as compatibilzing agents in polymer blends, Polymer Engineering & Science 31(21) (1991) 1545-1548.
[31] S.M. George, D. Puglia, J.M. Kenny, V. Causin, J. Parameswaranpillai, S. Thomas, Morphological and mechanical characterization of nanostructured thermosets from epoxy and styrene-block-butadiene-block-styrene triblock copolymer, Industrial & Engineering Chemistry Research 52(26) (2013) 9121-9129.
[32] C. Koning, M. Van Duin, C. Pagnoulle, R. Jerome, Strategies for compatibilization of polymer blends, Progress in Polymer Science 23(4) (1998) 707-757.
[33] U. Sundararaj, C. Macosko, Drop breakup and coalescence in polymer blends: the effects of concentration and compatibilization, Macromolecules 28(8) (1995) 2647-2657.
[34] S.H. Anastasiadis, I. Gancarz, J.T. Koberstein, Compatibilizing effect of block copolymers added to the polymer/polymer interface, Macromolecules 22(3) (1989) 1449-1453.
[35] W. Hu, J.T. Koberstein, J. Lingelser, Y. Gallot, Interfacial tension reduction in polystyrene/poly (dimethylsiloxane) blends by the addition of poly (styrene-b-dimethylsiloxane), Macromolecules 28(15) (1995) 5209-5214.
[36] K. Prakashan, A.K. Gupta, S.N. Maiti, Effect of compatibilizer on micromehanical deformations and morphology of dispersion in PP/PDMS blend, Journal of Applied Polymer Science 105(5) (2007) 2858-2867.
[37] A. Adedeji, S. Lyu, C.W. Macosko, Block copolymers in homopolymer blends: interface vs micelles, Macromolecules 34(25) (2001) 8663-8668.
[38] C. Macosko, P. Guegan, A.K. Khandpur, A. Nakayama, P. Marechal, T. Inoue, Compatibilizers for melt

blending: Premade block copolymers, Macromolecules 29(17) (1996) 5590-5598.
[39] W. Zhou, J. Osby, Siloxane modification of polycarbonate for superior flow and impact toughness, Polymer 51(9) (2010) 1990-1999.
[40] M. Marić, N. Ashurov, C. Macosko, Reactive blending of poly (dimethylsiloxane) with nylon 6 and poly (styrene): effect of reactivity on morphology, Polymer Engineering & Science 41(4) (2001) 631-642.
[41] C. Orr, J. Cernohous, P. Guegan, A. Hirao, H. Jeon, C. Macosko, Homogeneous reactive coupling of terminally functional polymers, Polymer 42(19) (2001) 8171-8178.
[42] J.K. Kim, S. Kim, C. Park, Compatibilization mechanism of polymer blends with an in-situ compatibilizer, Polymer 38(9) (1997) 2155-2164.
[43] K. Dedecker, G. Groeninckx, Reactive compatibilization of A/(B/C) polymer blends. Part 2. Analysis of the phase inversion region and the co-continuous phase morphology, Polymer 39(21) (1998) 4993-5000.
[44] K. Dedecker, G. Groeninckx, Reactive compatibilization of the polyamide 6/poly (phenylene oxide) blend by means of styrene–maleic anhydride copolymer, Journal of applied polymer science 73(6) (1999) 889-898.
[45] L. Jakisch, H. Komber, F. Böhme, Multifunctional coupling agents: Synthesis and model reactions, Journal of Polymer Science Part A: Polymer Chemistry 41(5) (2003) 655-667.
[46] L. Jakisch, H. Komber, L. Häußler, F. Böhme, A new bifunctional coupling agent: synthesis and model reactions, Macromolecular Symposia, Wiley Online Library, 2000, pp. 237-244.
[47] B. Marciniec, Comprehensive handbook on hydrosilylation, Elsevier2013.
[48] H. Brunner, Rhodium Catalysts for Enantioselective Hydrosilylation—A New Concept in the Development of Asymmetric Catalysts, Angewandte Chemie International Edition in English 22(12) (1983) 897-907.
[49] C. Chen, X. Li, S.L. Schreiber, Catalytic asymmetric [3+ 2] cycloaddition of azomethine ylides. Development of a versatile stepwise, three-component reaction for diversity-oriented synthesis, Journal of the American Chemical Society 125(34) (2003) 10174-10175.
[50] R. Noyori, R. Noyori, Asymmetric catalysis in organic synthesis, 1994.
[51] H. Nishiyama, H. Sakaguchi, T. Nakamura, M. Horihata, M. Kondo, K. Itoh, Chiral and C2-symmetrical bis (oxazolinylpyridine) rhodium (III) complexes: Effective catalysts for asymmetric hydrosilylation of ketones, Organometallics 8(3) (1989) 846-848.
[52] M. Sawamura, R. Kuwano, Y. Ito, trans‐Chelating Chiral Diphosphane Ligands Bearing Flexible P‐Alkyl Substituents (AlkylTRAPs) and their Application to the Rhodium‐Catalyzed Asymmetric Hydrosilylation of Simple Ketones, Angewandte Chemie International Edition in English 33(1) (1994) 111-113.
[53] A. Sudo, H. Yoshida, K. Saigo, An efficient phosphorous-containing oxazoline ligand derived from cis-2-amino-3, 3-dimethyl-1-indanol: application to the rhodium-catalyzed enantioselective hydrosilylation of ketones, Tetrahedron: Asymmetry 8(19) (1997) 3205-3208.
[54] I. Ojima, M. Nihonyanagi, T. Kogure, M. Kumagai, S. Horiuchi, K. Nakatsugawa, Y. Nagai, Reduction of carbonyl compounds via hydrosilylation: I. Hydrosilylation of carbonyl compounds catalyzed by tris (triphenylphosphine) chlororhodium, Journal of Organometallic Chemistry 94(3) (1975) 449-461.
[55] M. Anada, M. Tanaka, K. Suzuki, H. Nambu, S. Hashimoto, Dirhodium (II) Tetrakis (perfluorobutyrate)-Catalyzed 1, 4-Hydrosilylation of. ALPHA.,. BETA.-Unsaturated Carbonyl Compounds, Chemical and pharmaceutical bulletin 54(11) (2006) 1622-1623.
[56] R. Kuwano, M. Takahashi, Y. Ito, Reduction of amides to amines via catalytic hydrosilylation by a rhodium complex, Tetrahedron letters 39(9) (1998) 1017-1020.
[57] C.Eaborn, K. Odell, A. Pidcock, Hydroslylation of carbonyl compounds catalysed by ruthenium complexes, Jounal of Organometallic Chemistry 63 (1973)

[58] S. Köytepe, T. Seçkin, S. Yaşar, İ. Özdemir, Polyimide-Supported Dichloro-1, 3-bis (p-dimethylaminobenzyl) benzimidazolidin-2-ilidenruthenium (II) as Effective Catalyst for Hydrosilylation Reactions, Designed Monomers and Polymers 11(5) (2008) 409-422.
[59] M. Igarashi, R. Mizuno, T. Fuchikami, Ruthenium complex catalyzed hydrosilylation of esters: a facile transformation of esters to alkyl silyl acetals and aldehydes, Tetrahedron Letters 42(11) (2001) 2149-2151.
[60] K. Matsubara, T. Iura, T. Maki, H. Nagashima, A triruthenium carbonyl cluster bearing a bridging acenaphthylene ligand: An efficient catalyst for reduction of esters, carboxylic acids, and amides by trialkylsilanes, The Journal of organic chemistry 67(14) (2002) 4985-4988.
[61] S. Hanada, T. Ishida, Y. Motoyama, H. Nagashima, The ruthenium-catalyzed reduction and reductive N-alkylation of secondary amides with hydrosilanes: Practical synthesis of secondary and tertiary amines by judicious choice of hydrosilanes, The Journal of organic chemistry 72(20) (2007) 7551-7559.
[62] X. Verdaguer, M.C. Hansen, S.C. Berk, S.L. Buchwald, Titanocene-catalyzed reduction of lactones to lactols, The Journal of organic chemistry 62(24) (1997) 8522-8528.
[63] S.C. Berk, K.A. Kreutzer, S.L. Buchwald, A catalytic method for the reduction of esters to alcohols, Journal of the American Chemical Society 113(13) (1991) 5093-5095.
[64] S.C. Berk, S.L. Buchwald, An air-stable catalyst system for the conversion of esters to alcohols, The Journal of Organic Chemistry 57(14) (1992) 3751-3753.
[65] K.J. Barr, S.C. Berk, S.L. Buchwald, Titanocene-catalyzed reduction of esters using polymethylhydrosiloxane as the stoichiometric reductant, The Journal of Organic Chemistry 59(15) (1994) 4323-4326.
[66] J. Yang, T.D. Tilley, Efficient Hydrosilylation of Carbonyl Compounds with the Simple Amide Catalyst [Fe {N (SiMe3) 2} 2], Angewandte Chemie International Edition 49(52) (2010) 10186-10188.
[67] H. Brunner, W. Miehling, Asymmetrische katalysen: XXII. Enantioselektive hydrosilylierung von ketonen mit CuI-katalysatoren, Journal of organometallic chemistry 275(2) (1984) c17-c21.
[68] B.H. Lipshutz, W. Chrisman, K. Noson, Hydrosilylation of aldehydes and ketones catalyzed by [Ph 3 P (CuH)] 6, Journal of Organometallic Chemistry 624(1) (2001) 367-371.
[69] S. Sirol, J. Courmarcel, N. Mostefai, O. Riant, Efficient enantioselective hydrosilylation of ketones catalyzed by air stable copper fluoride-phosphine complexes, Organic letters 3(25) (2001) 4111-4113.
[70] P. Goswami, S.K. Bharadwaj, Al (H2PO4) 3: An Efficient and Effective Solid Acid Catalyst for Transesterification of β-keto Esters Under Solvent Free Condition, Catalysis Letters 124(1-2) (2008) 100-104.
[71] E.M. Johnston-Liik, MPs in Dublin: Companion to History of the Irish Parliament, 1692-1800, Ulster Historical Foundation2006.
[72] J. Bonnet, V. Bounor-Legaré, P. Alcouffe, P. Cassagnau, EVA reactive blending with Si–H terminated polysiloxane by carbonyl hydrosilylation reaction: From compatibilised blends to crosslinking networks, Materials Chemistry and Physics 136(2) (2012) 954-962.
[73] J. Bonnet, V. Bounor‐Legaré, F. Boisson, F. Mélis, P. Cassagnau, Efficient carbonyl hydrosilylation reaction: Toward EVA copolymer crosslinking, Journal of Polymer Science Part A: Polymer Chemistry 49(13) (2011) 2899-2907.
[74] İ. Yilgör, J.E. McGrath, Polysiloxane containing copolymers: a survey of recent developments, Polysiloxane Copolymers/Anionic Polymerization, Springer1988, pp. 1-86.
[75] M. Jin, X. Feng, J. Xi, J. Zhai, K. Cho, L. Feng, L. Jiang, Super‐hydrophobic PDMS surface with ultra‐low adhesive force, Macromolecular rapid communications 26(22) (2005) 1805-1809.
[76] M. Khorasani, H. Mirzadeh, Z. Kermani, Wettability of porous polydimethylsiloxane surface: morphology study, Applied Surface Science 242(3) (2005) 339-345.
[77] M. Sun, C. Luo, L. Xu, H. Ji, Q. Ouyang, D. Yu, Y. Chen, Artificial lotus leaf by nanocasting, Langmuir :

the ACS journal of surfaces and colloids 21(19) (2005) 8978-8981.
[78] M. Ma, R.M. Hill, J.L. Lowery, S.V. Fridrikh, G.C. Rutledge, Electrospun poly (styrene-block-dimethylsiloxane) block copolymer fibers exhibiting superhydrophobicity, Langmuir : the ACS journal of surfaces and colloids 21(12) (2005) 5549-5554.
[79] N. Zhao, Q. Xie, L. Weng, S. Wang, X. Zhang, J. Xu, Superhydrophobic surface from vapor-induced phase separation of copolymer micellar solution, Macromolecules 38(22) (2005) 8996-8999.
[80] G. Verma, S. Dhoke, A. Khanna, Polyester based-siloxane modified waterborne anticorrosive hydrophobic coating on copper, Surface and Coatings Technology 212 (2012) 101-108.
[81] W.-H. Chen, P.-C. Chen, S.-C. Wang, J.-T. Yeh, C.-Y. Huang, K.-N. Chen, UV-curable PDMS-containing PU system for hydrophobic textile surface treatment, Journal of polymer research 16(5) (2009) 601-610.
[82] P. Bernardo, E. Drioli, G. Golemme, Membrane gas separation: a review/state of the art, Industrial & Engineering Chemistry Research 48(10) (2009) 4638-4663.
[83] F. Wu, L. Li, Z. Xu, S. Tan, Z. Zhang, Transport study of pure and mixed gases through PDMS membrane, Chemical Engineering Journal 117(1) (2006) 51-59.
[84] S.-H. Chen, M.-H. Lee, J.-Y. Lai, Polysiloxaneimide membranes: gas transport properties, European polymer journal 32(12) (1996) 1403-1408.
[85] H.B. Park, C.K. Kim, Y.M. Lee, Gas separation properties of polysiloxane/polyether mixed soft segment urethane urea membranes, Journal of membrane science 204(1) (2002) 257-269.
[86] S.R. Reijerkerk, M.H. Knoef, K. Nijmeijer, M. Wessling, Poly (ethylene glycol) and poly (dimethyl siloxane): combining their advantages into efficient CO 2 gas separation membranes, Journal of membrane science 352(1) (2010) 126-135.
[87] S.R. Reijerkerk, M. Wessling, K. Nijmeijer, Pushing the limits of block copolymer membranes for CO 2 separation, Journal of membrane science 378(1) (2011) 479-484.
[88] E. Nyilas, Polysiloxane-polyurethane block copolymers, Google Patents, 1971.
[89] B. Arkles, Look what you can make out of silicones, Chemtech 13(9) (1983) 542-55.
[90] W. Noll, Chemistry and Technology of Silicones Academic, New York (1968) 147.
[91] R. Kambour, H. Klopfer, S. Smith, Limiting oxygen indices of silicone block polymer, Journal of Applied Polymer Science 26(3) (1981) 847-859.
[92] R. Kambour, J. Corn, S. Miller, G. Niznik, Tough, transparent heat‐and flame‐resistant thermoplastics via silicone block‐modified bisphenol fluorenone polycarbonate, Journal of Applied Polymer Science 20(12) (1976) 3275-3293.
[93] M. Hartney, A. Novembre, F. Bates, Block copolymers as bilevel resists, Journal of Vacuum Science & Technology B 3(5) (1985) 1346-1351.
[94] K. Sugita, N. Ueno, Resists for microlithography: Present status and recent research trends, Progress in polymer science 17(3) (1992) 319-360.
[95] G. Riess, G. Hurtrez, P. Bahadur, Encyclopedia of polymer science and engineering, Wiley, New York 2 (1985) 324.
[96] K. Haubennestel, A. Bubat, Coating and molding compositions with spreadability improving and lubrication increasing siloxanes and use of such siloxanes as coating and molding composition additives, Google Patents, 1986.
[97] J.R. Hahn, J.A. Vallender, Polyorganosiloxane pressure sensitive adhesives and articles therefrom, Google Patents, 1976.
[98] E.F. Johnson, J.S. Carlsen, Thermally stable hot-melt adhesive composition containing polycarbonate-polydimethylsiloxane block copolymer, Google Patents, 1978.
[99] J.W. Huffman, F.J. Matthews, W.H. Balke, Chair-twist equilibria in some tert-butyl octalones, The Journal of Organic Chemistry 49(25) (1984) 4943-4947.

[100] G. Attard, G. Williams, The effect of a directing electric field on the physical structure of a liquid crystalline side chain polymer the preparation of aligned thin films and their study using dielectric relaxation spectroscopy, Polymer communications 27(1) (1986) 2-5.
[101] A. Pinard, J. Attard, 23rd Congress of the European Society of Pediatric Radiology, Pediatr Radiol 16 (1986) 335-355.

Chapter II: Efficient hydrosilylation reaction in polymer blending: An original approach to structure PA12/PDMS blends at multiscales

Abstract

An *in situ* carbonyl hydrosilylation reaction was developed to prepare polyamide 12 (PA12)/polysiloxane blends by reactive blending. This reaction focuses on the addition of hydrogenosilane groups (SiH) from polysiloxane to the carbonyl group from the PA12 amide function. To evidence this carbonyl hydrosilylation onto an amide based polymer, an approach on model compounds (use of *N*-methylpropionamide) was carried out. The mechanism and kinetics were investigated with multinuclear NMR techniques (^{1}H, ^{13}C and ^{29}Si). It could be evidenced that the concentration of *N*-silylated species can reach 70 mol% after 2 hours reaction at 100 °C.

This hydrosilylation reaction was extended to the reactive blending of polyamide 12 with PDMS under molten processing conditions. The evolution of the blend morphology at different scales was investigated by electronic microscopy. The impact of both shearing and hydrosilylation reaction on the final morphology was deeply studied and confirmed the interface enhancement by compatibilization. As a result, the dispersion of PDMS domains decreased from 3-4 µm to around 0.8 µm in diameter forming submicronic morphology. Furthermore, it also confirmed that it is possible to control the dispersion of PDMS at different scales by changing the physico-chemical parameters of the two components (*i.e.,* molar mass and functionality).

Keywords: *hydrosilylation, PA12, PDMS, compatibilization*

Résumé

Une réaction *in situ* d'hydrosilylation de groupement carbonyle a été développée pour élaborer des nouveaux mélanges polyamide 12 (PA12)/polysiloxane-SiH par mélange réactif. Cette réaction consiste en l'addition de groupes hydrogénosilane (SiH) du polysiloxane sur les groupes carbonyle de la fonction amide du PA12. Pour mettre en évidence cette réaction, une approche sur un composé modèle (utilisation du *N*-méthylpropionamide) a été choisie. Le mécanisme et la cinétique ont été analysés par RMN multinucléaire (^{1}H, ^{13}C et ^{29}Si). Il a pu être mis en évidence que la concentration de produits attendus de type composés N-silylés peut atteindre 70mol% après 2 heures de réaction à 100°C.

Cette réaction d'hydrosilylation a été étendue au mélange réactif du polyamide 12 avec le PDMS dans les conditions de mélange fondu. L'évolution de la morphologie des mélanges à différentes échelles a été caractérisée par microscopie électronique. L'impact à la fois du cisaillement et de la réaction d'hydrosilylation sur la morphologie finale a été étudié en détail et a confirmé l'amélioration de l'interface par la compatibilisation. Il en résulte une diminution de la taille des domaines de PDMS de 3-4 microns à environ 0,8 micron. De plus, l'analyse a confirmé qu'il était possible de contrôler la dispersion de PDMS à différentes échelles en changeant les paramètres physico-chimiques des 2 composants (*i.e.,* masse molaire et fonctionnalité).

Mots clés : *hydrosilylation, PA12, PDMS, compatibilisation*

II.1 Introduction

Polymer blending has attracted much attention as an easy and cost-effective method for developing polymeric materials that have versatility for commercial applications. In other words, the properties of the blends can be manipulated according to their end use by correct selection of the component polymers [1, 2]. In this context, blends with thermoplastics and polydimethylsiloxane (PDMS) are of particular interest. PDMS is already widely used in a variety of industrial field because of its well-known unique properties [3]. Indeed, due to the special molecular architecture, composed of highly flexible -O-Si-O- bonds in the main chain with methyl groups attached to the silicone atom [4], their physical and chemical properties combine both organic and inorganic characteristics. For instance, PDMS has excellent thermal properties [6] with a glass transition temperature (T_g) around -125 °C, a melting temperature around -40°C and an onset thermal degradation temperature above 350 °C. Thus PDMS has the one of the widest working temperature range of the commercial polymers. Moreover, it also has UV stability, hydrophobicity, high gas permeability and dielectric properties. But it has low resistance to oil and solvents [7]. Besides, as we know, PA12 has excellent solvent and oil resistance, especially for acid and alkali, and excellent environment stress cracking resistance at elevated temperature [4]. So a blend of PA12 and PDMS will achieve their individual properties and form a new material with special performance in solvent oil resistance, hydrophobicity, gas permeability, *etc*.

However, due to the low surface tension and low viscosity of PDMS, it is highly immiscible and incompatible with the majority of organic polymers such as PA12. In general, the compatibility between the polymer phases decides the properties of a heterogeneous polymer blend [8, 9] and is characterized by the interfacial tension. When the interfacial tension approached to zero, the blend becomes miscible. In other words, if there are strong interactions between the phases. Then the polymer blend will be miscible in nature. Large interfacial tensions lead to phase separation and the phase separated domains perhaps undergoing coalescence. This will result in an increased domain size and, in turn, decreased mechanical properties [1]. For PA12/PDMS blend, the non-miscibility will lead to coarse morphologies, causing fast deterioration of the blend properties due to thermodynamically driven phase separation. In addition, PDMS tends to enrich on the surface since its low

surface free energy (~ 19.9 mN/m) compared with PA12 (~40.7 mN/m). This effect results in a surface covered by a hydrophobic liquid PDMS that cause poor surface properties[10].

Generally speaking, the interfacial tension can be reduced by adding compatibilizers which act as interfacial agent and resulting in the increase of the interface area of the dispersed phase. Consequently, the interfacial adhesion between the components is promoted and finally stabilizes the morphology of dispersed phase [11]. In general, carrying out *in situ* reaction during blending or adding premade copolymers suppresses coalescence resulting in smaller domain size and narrower domain size distribution [12].

In that frame, there are some works about the addition of PDMS based compatibilizer. Xu *et* al. [13] reported that PE-*b*-PDMS diblock copolymer was prepared through the esterification reactions between monohydroxy-terminated poly(dimethylsiloxane) (PDMS-OH) and the corresponding carboxyl terminated polyethylene (PE-COOH) in the presence of tetrabutyl titanate (TBT) firstly. Then the copolymer was used as a compatibilizer in the blends of high-density polyethylene (HDPE) and silicone oil. The copolymer (1 wt%) promoted the dispersion of silicone oil in HDPE from more than 5μm (silicone oil) to no obvious phase segregation through SEM observation and improved the mechanical properties of HDPE/PDMS blends.

Instead of synthesizing the compatibilizer, some polymers which have reactivity with each other can react to achieve *in situ* compatibilization. A few researches have demonstrated the reactive blending of PDMS with organic polymer. For instance, Zhou and Osby [14] reported the *in situ* polycarbonate (PC)/PDMS blends compatibilization through transesterification between PC and hydroxyl-terminated PDMS (PDMS-OH) during twin-screw extrusion. They observed that the formed PC-PDMS copolymer stabilized the sub-micron blend morphology of the immiscible PC/PDMS. As a result the silicone phase was found to be well dispersed in the polycarbonate major phase forming submicron spherical domains (0.2-0.9 μm). Actually, reactive blending of functionalized polysiloxane with organic polymer has attracted much attention nowadays. For example, hydride or vinyl functionalized polysiloxane were reported to modify properties of PBT [15], EVA [16] or polyamide [4] through transition metal compounds catalyzed reaction or peroxide initiated reaction. For example, Mani *et* al. [4] tailored a new thermoplastic vulcanizate (TPV)

composed of PDMS as the rubber phase and PA12 as the thermoplastic phase. PA12 was first functionalized by the reaction of amine (NH_2) and maleic anhydride to form a PA12-grafted-Lotader® copolymer. Such copolymer located between the PA12 and the PDMS phase, reacted with PDMS through a radical reaction initiated by dicumyl peroxide (DCP) and reduced the interfacial tension. Typically, the volume domain radius significantly decreased from 16.5 μm to nearly 0.6 μm.

More recently, Bonnet *et* al. [16] used an original reaction between PDMS and copolymer of ethylene and vinyl acetate (EVA) based on EVA carbonyl hydrosilylation by Si-H groups of hydride terminated PDMS (PDMS-SiH). The occurrence of the hydrosilylation reaction at the EVA/polysiloxane interface promoted a homogenization of the blend depending on the molar ratio SiH/vinyl acetate groups, [SiH]/[VA], and the viscosity ratio of the blend. Two distinct behaviors were observed: i) The formation of a crosslinking network under shear was obtained for a low viscosity ratio between polysiloxane and EVA (polysiloxane/EVA = $4.0x10^{-6}$) with a high concentration of SiH groups ([SiH]/[VA] = 0.5), and ii) the formation of a compatibilized blend was observed for high molar mass polysiloxanes (Mn > 15,000 g mol^{-1}) with a low concentration of SiH ([SiH]/[VA] < $4.0x10^{-3}$).

In this study, we focused on the ruthenium-catalyzed hydrosilylation of PA12 with hydride functionalized PDMS. It notes that this reaction has never been reported before. We used similar but low molar mass compound (*N*-methylpropionamide) to mimic the reaction and investigated the mechanism of reaction. In addition, the reaction was extended to molten condition to confirm its ability of compatibilization. Physico-chemical parameters like viscosity ratio, molar ratio of [NHCO]/[SiH] were studied to understand their role in controlling the morphology development.

II.2 Experiment

II.2.1 Materials and Reagents

N-methylpropionamide, hexafluoro-2-propanol (HFIP), acetone and chloroform were purchased from Aldrich and used without further purification. Anhydrous toluene was

purchased from Acros. Hydride terminated polydimethylsiloxanes (1-PDMS-SiH and 2-PDMS-SiH respectively), and triruthenium dodecacarbonyl [$Ru_3(CO)_{12}$] were commercial products from ABCR. The chemical structures of the reagents used for hydrosilylation reaction are shown in Figure II. 2.

Polyamide 12 was supplied by Arkema (AESNO TL RILSAN®), number average molar mass *Mn* is 26000 $g.mol^{-1}$, weight average molar mass *Mw* is 47000 $g.mol^{-1}$ and the density is 1.01 $g.cm^{-3}$ at room temperature. Characteristics of PA12, PDMS-SiH and blends are listed in Table II.1.

Table II.1: Physico-chemical parameters of PA12, PDMS-SiH and blends.

Parameters	PA12	1-PDMS-SiH	2-PDMS-SiH
Molar mass *(g.mol^{-1})*	26000	726	6000
Viscosity *(10^{-3} Pa.s)*	1x10^{7}	3	100
[SiH] *(%mol)*	/	19.5	3
Molar ratio *[SiH]/[-CONH]*	/	6.7x10^{-2}	8.3x10^{-3}
Viscosity ratio $\eta_{polysiloxane}/\eta_{PA12}$	/	3x10^{-7}	1x10^{-5}

II.2.2 Hydrosilylation reaction with amide compound

N-methylpropionamide was chosen as the amide compound to mimic such hydrosilylation reaction between -SiH and -NH-CO- groups. Equimolar amounts of amide and -SiH groups (0.04 mol) were added in a schlenk. The catalyst $Ru_3(CO)_{12}$ was dissolved in anhydrous toluene (2 ml) first and then added to the amide/ PDMS-SiH mixture. The reactional medium was heated to 100°C from 10 min to 6 h under an argon atmosphere. Aliquots were collected at different reaction times and characterized by ^{1}H, ^{13}C and ^{29}Si NMR.

II.2.3 Hydrosilylation reaction with amide function from Polyamide 12

PA12 pellets were dried in vacuum at 80 °C for 24 h. Melt reactive processing of PA12 and PDMS-SiH was carried out in a Haake Plasticorder intensive batch mixer equipped with a Rheomix 600 internal mixer. The temperature of the mixer chamber was set at 170 °C and the rotation speed was 50 rpm. The resistant torque and temperature were monitored during whole process. In a typical experiment, dried PA12 (40g) was added in the mixer chamber

and first mixed during 3 min to melt the polymer until the torque curve reached a plateau. Then, the catalyst and PDMS-SiH mixture with a predetermined composition (4 g PDMS-SiH and 50 mg $Ru_3(CO)_{12}$) was added in the molten PA12 with a syringe. The extent of the reaction was then qualitatively followed (tracked) from the torque variation and the samples were characterized by FTIR, SEM and TEM.

II.2.4 Characterization

^{1}H and ^{13}C NMR spectroscopy was carried out with a 5-mm BBFO+ probe on a Bruker AVANCE III spectrometer working at 400 MHz for ^{1}H and 100.6 MHz for ^{13}C. ^{29}Si liquid-state NMR spectra were recorded on a Bruker AVANCE II spectrometer (79.5 MHz for ^{29}Si) with a 10 mm ^{29}Si selective probe with a z-gradient coil. Deuterated chloroform，$CDCl_3$ (Aldrich), was used as solvent. All the samples were analyzed at 25 °C. Chemical shift (δ) are given in parts per million (ppm). For silicone analysis, chromium acetylacetonate [$Cr(acac)_3$] was added to shorten the ^{29}Si spin-lattice relaxation times.

Measurements of Attenuated total reflection (ATR) were performed on a Bruker IFS 66/S spectrometer. Spectra were obtained after 64 scans over the range of 4000 cm^{-1} to 400 cm^{-1}. Samples were hot pressed to thin film with a thickness around 0.5mm.

The PA12/PDMS reactive blend solubility was determined after immersion (48 h, 25 °C) of 200 mg blend in HFIP/chloroform (20 ml, 1:4 in volume) mixed solvent and then observe whether there is insoluble matter.

The morphology of the polymer blend was first characterized by scanning electron microscopy (SEM) using a FEI QUANTA 250 microscope with an accelerating voltage of 10 KV. The samples were prepared in two different ways, either fractured in liquid nitrogen or a smooth flat surface of these was obtained by cryo ultramicrotomy at -155 °C with a UC7 LEICA ultramicrotome. Then the surfaces were coated with a gold/palladium thin layer of 10 nm. The morphology was also examined by transmission electron microscopy (TEM). Ultrathin sections of about 80 nm from samples, taken in triplicate throughout the whole materials, were cut by cryo ultramicrotomy at -155 °C and observed using a PHILIPS CM120 microscope operated at an accelerating voltage of 120 KV.

II.3 Results and discussion

II.3.1 N-methylpropionamide/PDMS-SiH hydrosilylation Reaction

The reaction between SiH and -NH-CO- groups in the presence of $Ru_3(CO)_{12}$ is expected to lead to ruthenium-catalyzed reduction. As described in the literature, ruthenium-catalyzed reduction and reductive *N*-Alkylation of secondary amides were achieved with judicious choice of hydrosilanes [17, 18]. In our case, to mimic the reaction between PA12 and 1-PDMS-SiH, *N*-methylpropionamide and the same bifunctional 1-PDMS-SiH (hydride terminated) were first chosen for the mechanism and kinetic studies. Possible reaction pathways are shown below (Figure II.1).

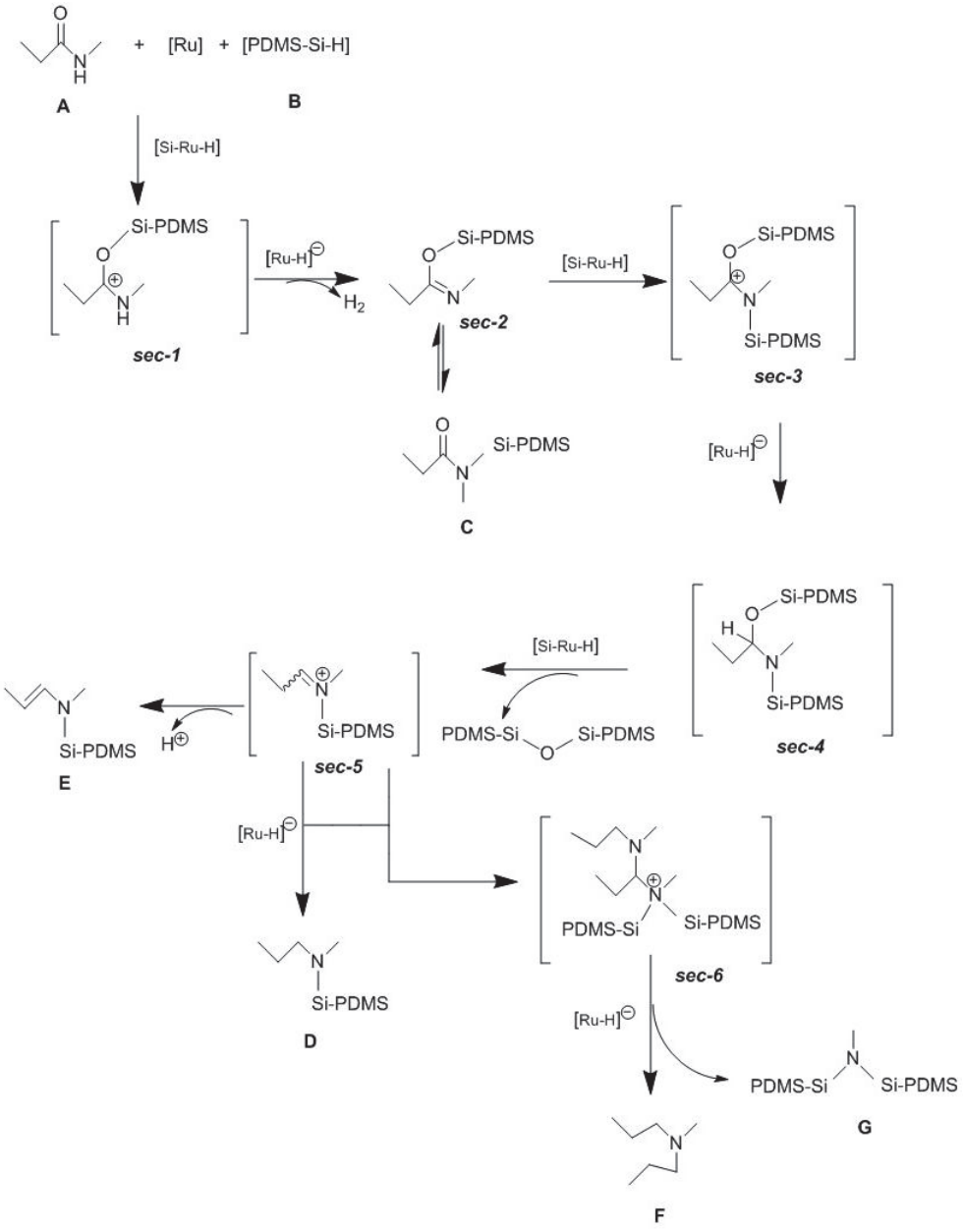

Figure II.1: Possible reaction pathway between *N*-methylpropionamide and PDMS-SiH.

The reaction of *N*-methylpropionamide was initiated from the addition of Si-H to C=O groups to form an intermediate ***sec-1*** and then activated ***sec-1*** changed to another intermediate ***sec-2*** which involves dihydrogen release. The *O*-silyl imidoylester ***sec-2*** can alternatively change to ***C*** which is more stable or can keep reduction and silylation through the addition reaction of Si-H to C=N, forming intermediate ***sec-3***. Followed by the activation with $Ru\text{-}H^-$, activated ***sec-3*** is reduced to ***sec-4***. The third step of the reduction is release of a polysiloxane from ***sec-4***, providing the formation of an imine activated by a cationic silyl group, ***sec-5.*** Finally**,** the target product ***D*** is obtained through reduction of ***sec-5.*** However, since the C=N bond is activated by the $^+$Si-PDMS, two side reactions can take place. One is

the deprotonation of the iminium intermediate ***sec-5*** at α-position leading to compound ***E***. The other side reaction is the formation of ***sec-6,*** which can be explained by the attack of target product ***D*** on the silylated iminium ion ***sec-5.*** After further reduction of the resulting intermediate ***sec-6***, tertiary amine ***F*** and disiloxane tertiary amine ***G*** are formed.

Briefly speaking, the ruthenium-catalyzed reduction and reductive *N*-siloxaneation of *N*-methylpropionamide with 1-PDMS-SiH may form *N*-siloxane-*N*-methylpropionamide (***C***) and *N*-siloxane-*N*-methylpropionamine (***D***) mainly. In addition, during the process three side reactions also took place leading to the formation of *N*-siloxane-*N*-methylpropionenamine (***E***), *N*,*N*-dipropyl-*N*-methylamine (***F***) and *N*,*N*-disiloxane-*N*-methylamine (***G***). The reactions are summarized below (Figure II.2) and confirmed by ^{1}H, ^{13}C and ^{29}Si NMR characterization.

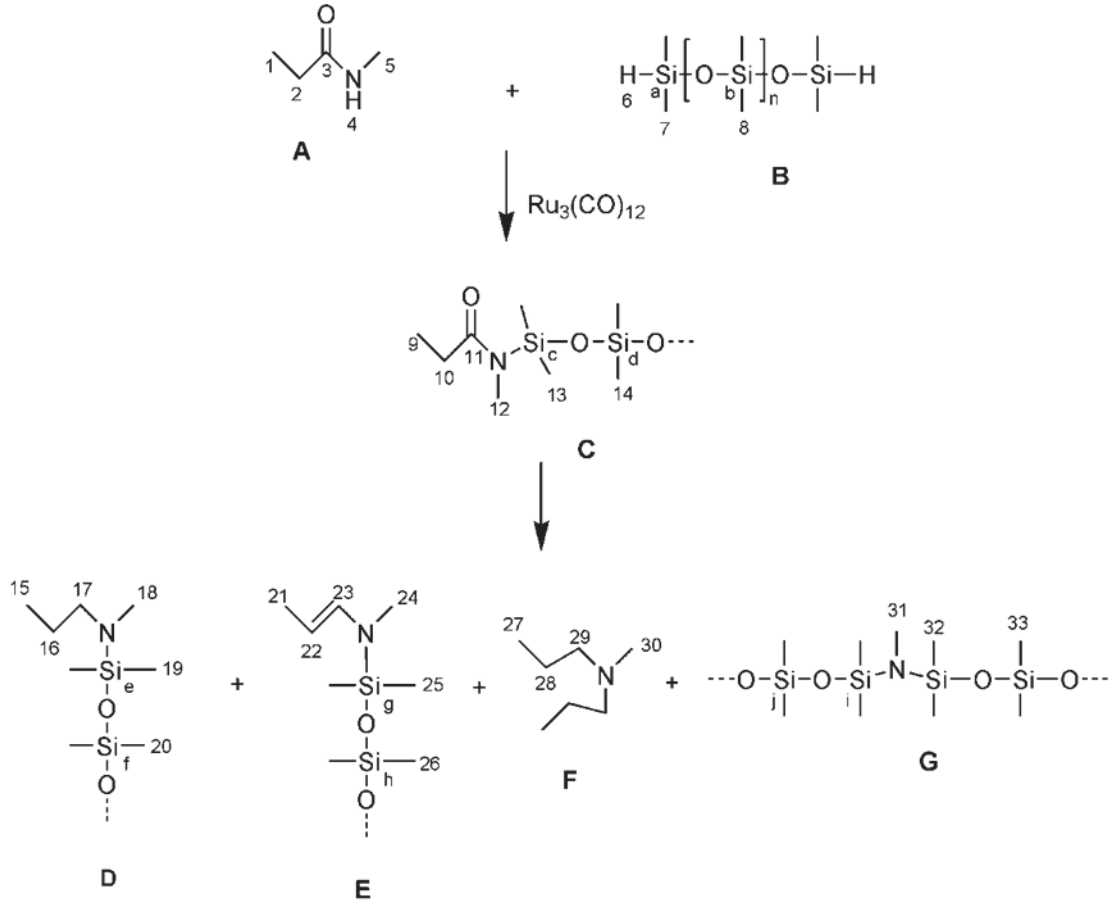

Figure II.2: Expected products from reaction between *N*-methylpropionamide and PDMS-SiH.

Since the main products maybe *N*-silylated, it is not easy to confirm their formation through 1D-NMR only, so 2D-NMR experiment such as $^{1}H/^{29}Si$ HMBC was used to investigate the *N*-silylated structures first. According to the literature, after the reaction, PDMS should be linked to a nitrogen atom and Si chemical shift of such T unit is expected

around -10 ppm. As shown in ^{29}Si NMR spectrum of reactional medium after 2 h, at 100 °C (Figure II.3), we found four main signals at -7.76, -9.27, -9.61 and -11.23 ppm in this area which were attributed to the structures: CON(CH_3)Si- (c), $CH_3N(Si)_2$ (i), CH=CHN(CH_3)Si (g) and RN(CH_3)Si (e), respectively. Through 2D-^{1}H/^{29}Si HMBC correlations (Figure II.4), the silicon signal at -11.23 ppm long range correlated with -CH_2- (H17) and -NCH_3 (H18) protons at 2.71 and 2.38 ppm, was found to come from the secondary amine *N*-siloxane-*N*-methylpropionamine (***D***). The signal at -7.76 ppm showed a cross peak with signal at 2.84 ppm from protons of *N*-methyl (H12) of *N*-siloxane-*N*-methylpropionamide (***C***). Similarly, the correlation between silicon signal at -9.61 ppm and proton signals at 2.58 ppm from H24 and 6.31 ppm from H23 was characterizing the silylation of enamine (***E***). The weak signal at -9.27 ppm exhibiting an obvious cross peak with -NCH_3 at 2.51 ppm (H31) was attributed to *N*, *N*-disiloxane-*N*-methylamine (***G***). However, all the signals with a chemical shift in the range -18 to -26 ppm were assigned to -O$Si(CH_3)_2$O- on the main PDMS chains. Complementary information on the product structures will be shown through ^{1}H and ^{13}C NMR.

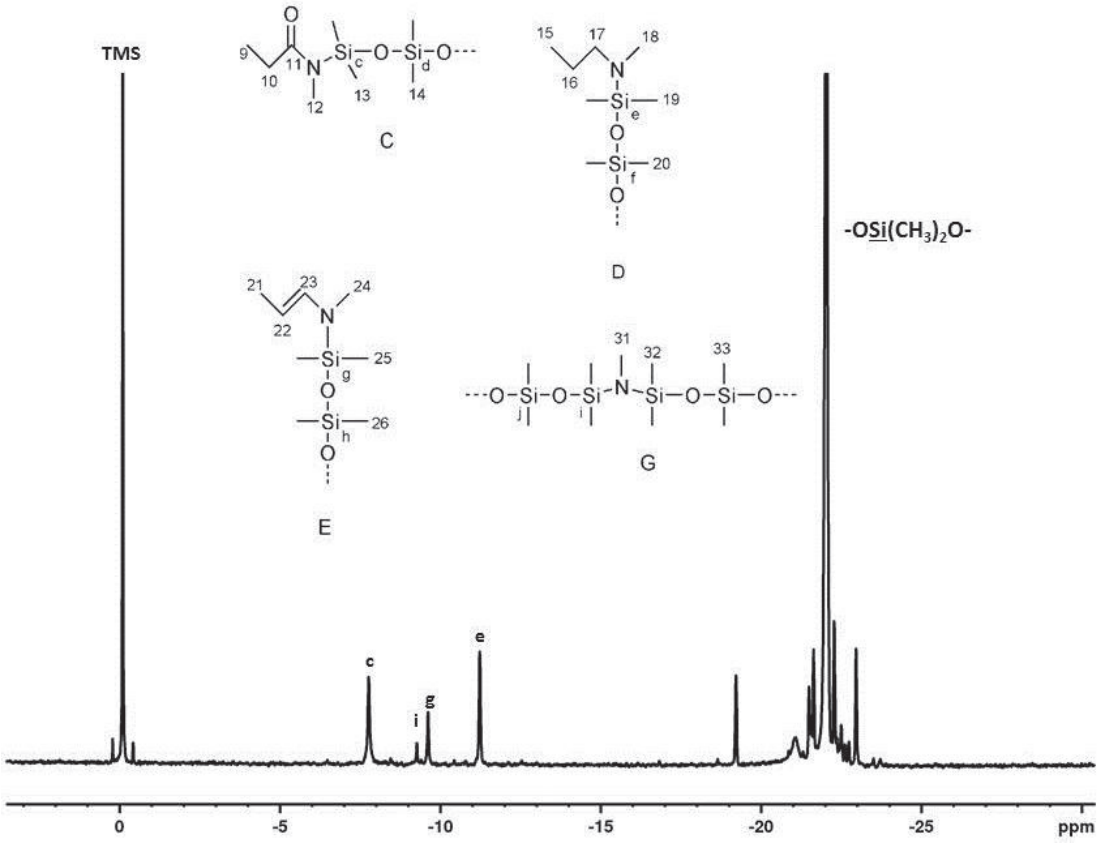

Figure II.3: ^{29}Si NMR spectrum of reactional medium after 2 h reaction at 100 °C, ($CDCl_3$-25°C).

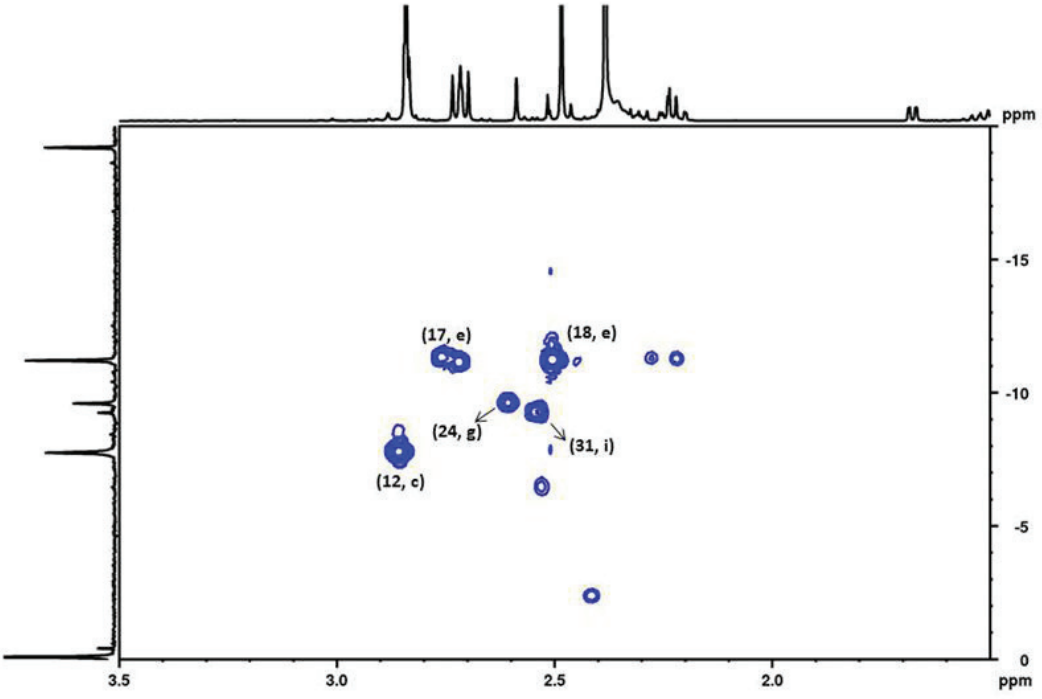

Figure II.4: Zoom of the 2D-NMR HMBC (^{1}H-^{29}Si) of reactional medium after 2 h reaction at 100 °C, ($CDCl_3$-25°C).

The ^{1}H NMR spectrum of reactional medium after 2 h of reaction at 100 °C between *N*-methylpropionamide and hydride terminated PDMS is shown in Figure II.5. *N*-siloxane-*N*-methylpropionamide (C) was characterized by two singlet at 2.84 ppm (H12) from -NC$\underline{H}_3$ protons and 0.35 ppm (H13) from protons of -NSi(C$\underline{H}_3$)$_2$, a triplet at 1.15 ppm and a overlaid signal at 2.36 ppm assigned to protons methyl (H9) and methylene protons (H10) respectively. *N*-siloxane-*N*-methylpropionamine, was confirmed by a singlet at 2.38 ppm (H18) from protons -NC$\underline{H}$3, a triplet at 0.85 ppm (H15), a quartet at 1.45 ppm (H16) and a triplet at 2.71 ppm (H17) from protons of propyl group. Besides, the relative integrals of those proton signals are 3:3:2:2 confirming the structure of secondary amine.

In addition, the spectrum of the reactional medium after 2 h at 100 °C described several other signals assigned to side products. For *N*-siloxane-*N*-methylpropionenamine (E), it can be confirmed by an obvious doublet at 6.29 ppm (H23) and a multiplet at 4.28 ppm (H22) corresponding to the protons of HC=CH, peaks at 1.66 ppm (H21, doublet) and 2.58 ppm (H24, singlet) assigned to methyl protons CH=CHC$\underline{H}_3$ and NC$\underline{H}_3$, respectively. Tertiary amine *N,N*-dipropyl-*N*-methylamine (F) is confirmed from the peaks at 2.23 ppm (H30, singlet), 0.91ppm (H27, triplet), 1.50 ppm (H28, multiplet) , 2.31 ppm (H29, triplet). ^{1}H NMR information of *N,N*-disiloxane-*N*-methylamine (G) is a singlet at 2.51 ppm (H31) for protons of -NC$\underline{H}$3, other information can be achieved from ^{13}C and ^{29}Si NMR. Moreover, the reaction is almost completed since the signal from PDMS-Si$\underline{H}$ (H6) after 2 h reaction is not obvious anymore compared with the spectrum of initial reactional medium (Figure II.5). Methyl protons of the -Si-O- chains, except -CONSi(CH$_3$)$_2$- (C, H13), are not easy to distinguish and they are all in the range [(-0.1)-0.3] ppm.

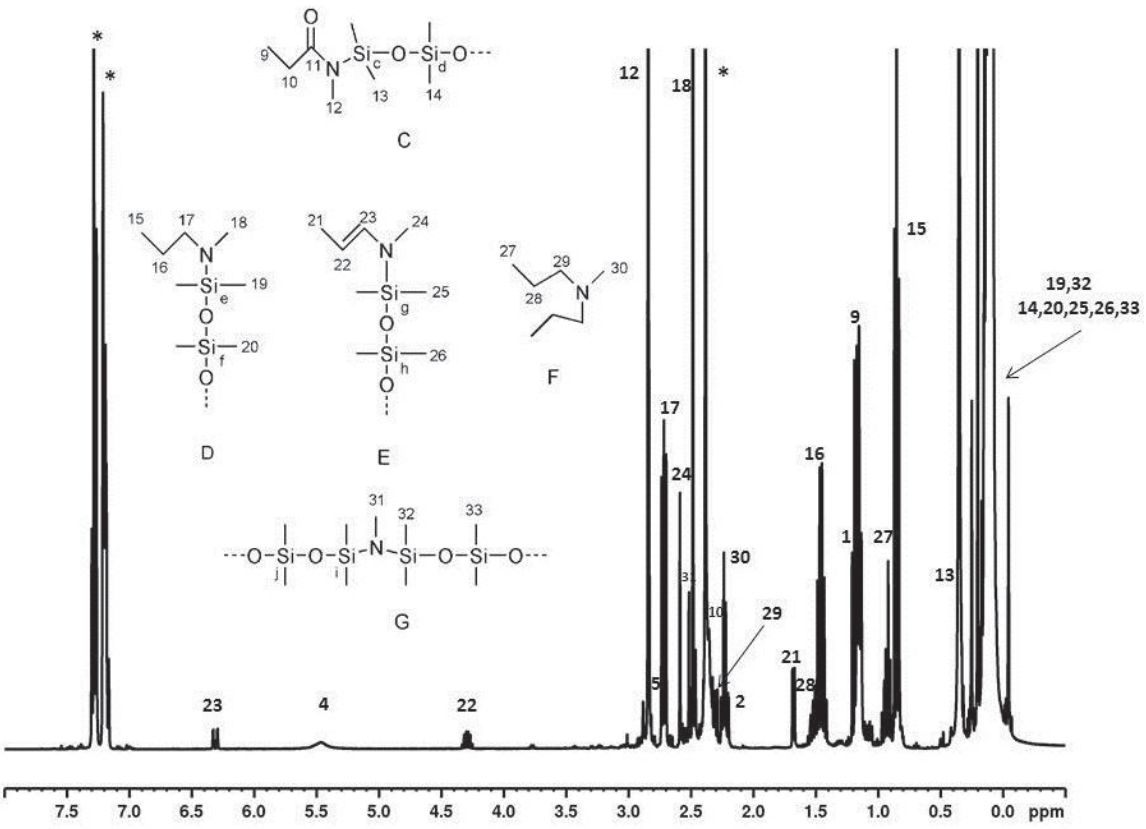
C
D
E
F
G
19,32
14,20,25,26,33
7.5 7.0 6.5 6.0 5.5 5.0 4.5 4.0 3.5 3.0 2.5 2.0 1.5 1.0 0.5 0.0 ppm

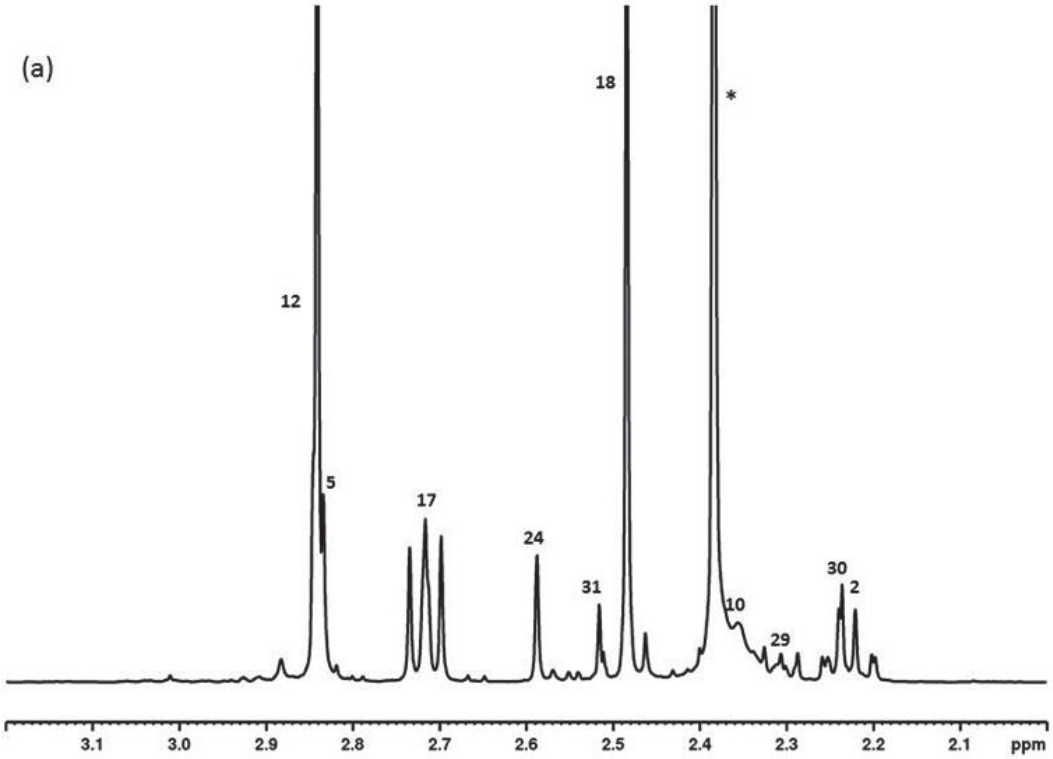
(a)
3.1 3.0 2.9 2.8 2.7 2.6 2.5 2.4 2.3 2.2 2.1 ppm

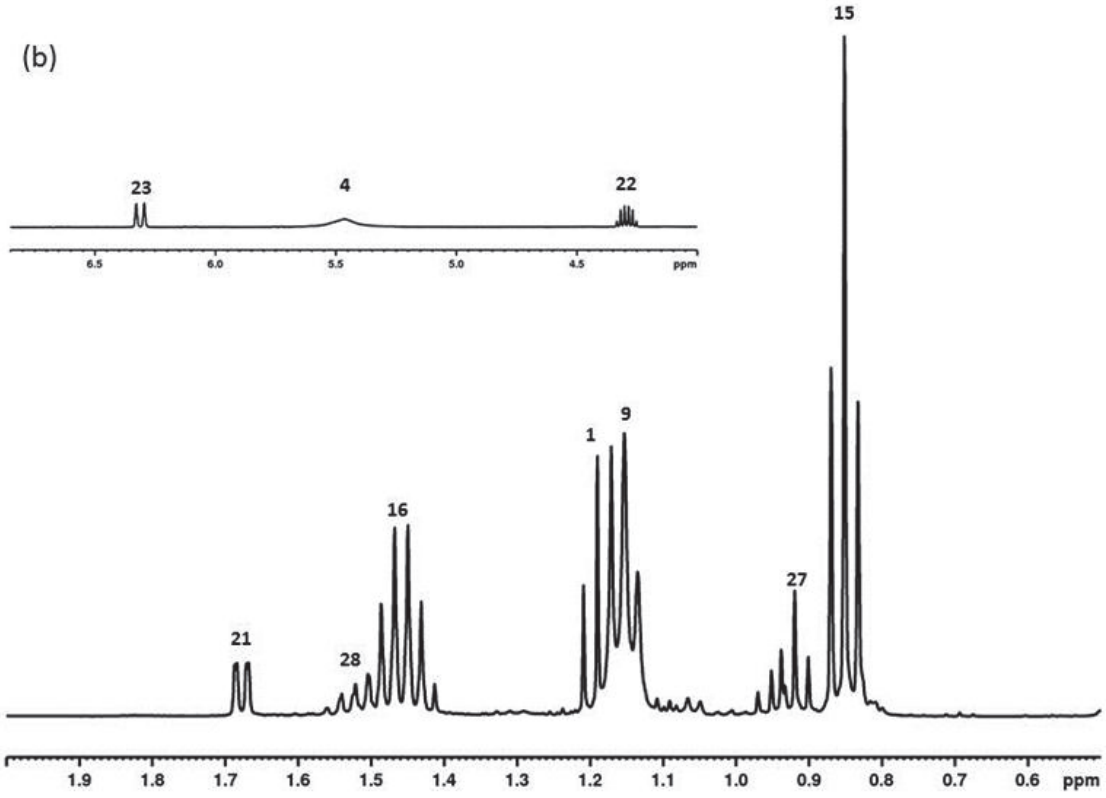

Figure II.5: ^{1}H NMR spectrum of reactional medium after 2 h reaction at 100 °C, full scale and (a) 2.0-3.2 ppm and (b) 0.5-2.0 ppm, ($CDCl_3$-25°C), (*) Toluene.

The formation of all those products was also supported by ^{13}C NMR characterization of the reactional medium after 2h at 100 °C (Figure II.6). *N*-siloxane-*N*-methylpropionamide (***C***) was analyzed by 4 main signals at 8.51, 30.07, 181.58 and 26.91 ppm assigned to carbons of $\underline{C}H_3CH_2$- (C9), $CH_3\underline{C}H_2$- (C10), -$\underline{C}ON(CH)_3$- (C11) and -$CON(\underline{C}H)_3$- (C12), respectively. The other reductive product *N*-siloxane-*N*-methylpropionamine (***D***) was confirmed by the signal at 11.29 ppm from carbons of $\underline{C}H_3CH_2$- (C15) , signal at 21.83 ppm from $CH_3\underline{C}H_2$- (C16) and signals from methylene and methyl combined with nitrogen atom, -$\underline{C}H_2N\underline{C}H_3$ (C17,C18), at 51.59 and 33.63 ppm respectively.

Signals of side products could also be found on the^{13}C NMR spectrum. To be exact, signals at 15.41, 92.77, 135.09 and 30.87 ppm were assigned to carbons from $\underline{C}H_3CH$=CH- (C21), $CH_3\underline{C}H$=CH-(C22), CH_3CH=$\underline{C}H$-(C23) and -$N\underline{C}H_3$(C24) of *N*-siloxane-*N*-methylpropionenamine (***E***). For tertiary amine *N*,*N*-disiloxane-*N*-methylamine (***G***), 4 signals at 11.90, 20.52, 59.92 and 42.30 ppm from carbons $\underline{C}H_3CH_2CH_2$- (C27), $CH_3\underline{C}H_2CH_2$- (C28), $CH_3CH_2\underline{C}H_2$- (C29) and -$N\underline{C}H_3$ (C30) were evidenced. A weak signal at 29.14 ppm corresponding to carbons from -$N\underline{C}H_3$ of *N*, *N*-disiloxane-*N*-methylamine (***G***) was

also found. All those assignments were done with the help of 2D-NMR $^{1}H/^{1}H$ COSY and $^{1}H/^{13}C$ HMBC and HSQC correlations.

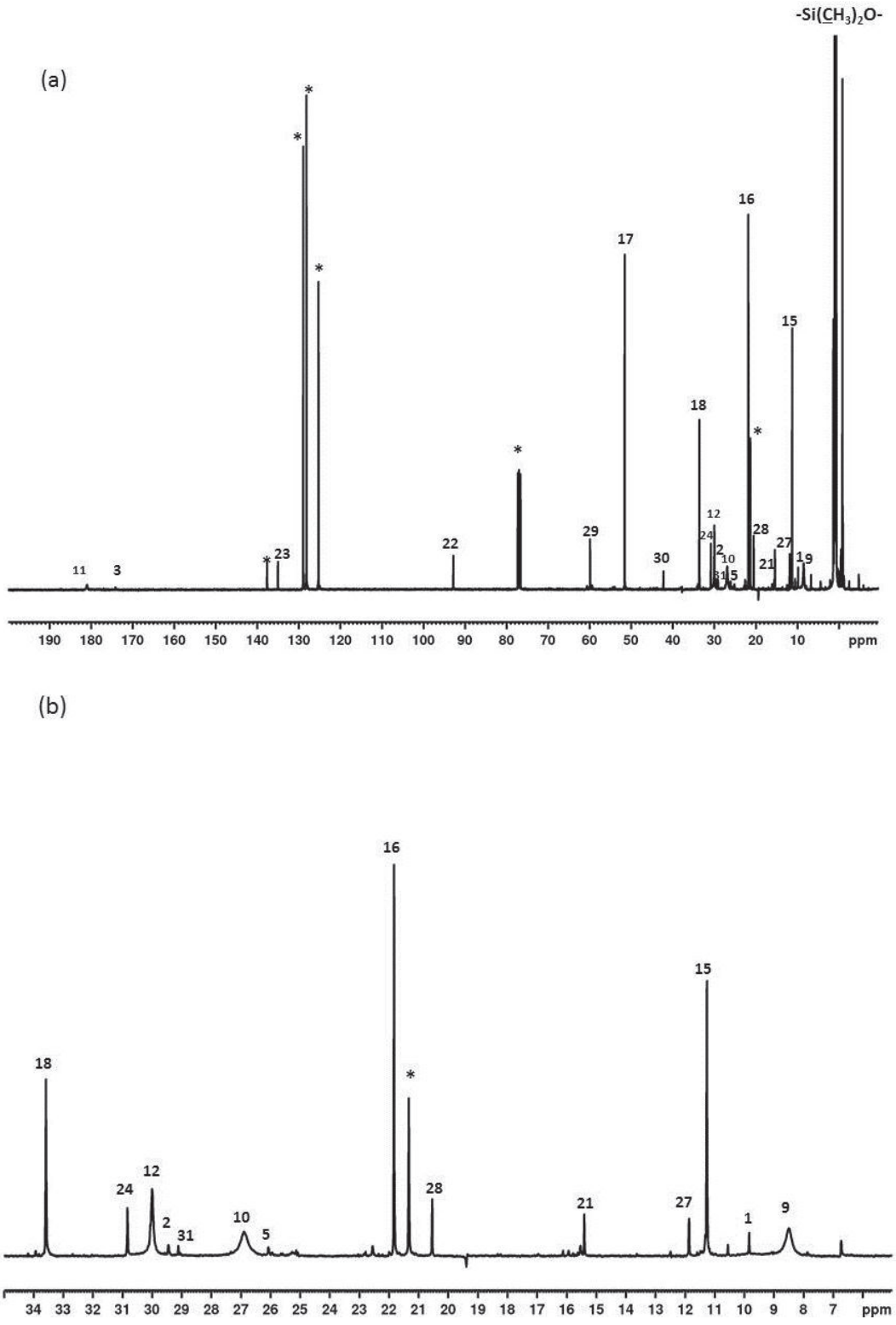

Figure II.6: ^{13}C NMR spectrum of reactional medium after 2 h reaction at 100 °C, (a) full scale, (b) 5-35 ppm, ($CDCl_3$-25°C). (*) Toluene

Finally, through NMR characterization of the reactional medium after 2 h of reaction at

100 °C, previously proposed reaction pathway for ruthenium-catalyzed hydrosilylation reaction between *N*-methylpropionamide and PDMS-SiH was ascertained, the main products are *N*-silylated amide and reductive *N*-silylated amine. At the same time, side products like tertiary amine, *N*-silylated enamine and *N*-disilylated amine were also evidenced.

II.3.2 Kinetics

Kinetics study of ruthenium-catalyzed-reaction between *N*-methylpropionamide and 1-PDMS-SiH were carried out by ^{1}H NMR analysis of reactional medium from 10 min to 6 h. For the quantification, since there is no proton signal keeping the same chemical shift from the beginning up to 6 h, we cannot calibrate a signal to a constant value, however, as all the products have been identified, the proportion can be achieved from the integral value of each one dividing to the sum of whole amine and amide compounds (Table II.2, Figure II.7).

To be specific, excess *N*-methylpropionamide (***A***) was quantified through area of signal H1, even though the peak was partially overlapped by signal H9, we can calculate via splitting rules. The amounts of *N*-siloxane-*N*-methylpropionamine (***D***), *N*-siloxane-*N*-methylpropionenamine (***E***), *N*, *N*-dipropyl-N-methylamine (***F***) and *N*, *N*-disiloxane-N-methylamine (***G***) are obtained by integration of signals H17, H21, H27 and H31, respectively.

Through the evolution of excess initial amide and new formed products, it is clear that the ruthenium-catalyzed reaction is efficient, since there is 15 mol % conversion to the two main products, silylated amide (***C***) and amine (***D***), reached in 10 min. In the early stage of the reaction, high concentration of Si-H promoted the reduction, formed amine and inhibited the change from *O*-silyl imidoylester ***sec-2*** to *N*-siloxane-*N*-methylpropionamide (***C***), so concentration of *N*-siloxane-*N*-methylpropionamine (***D***) increased more quickly than amide ***C***. After 2h the growth speed of *N*-siloxane-*N*-methylpropionamine (***D***) yield decreased with SiH decrease. This phenomenon is consistent with the mechanism described in literature [17-19], if the hydrosilane is bifunctional and their two SiH groups are located near each other, addition of SiH to C=N occurs intramolecularly and accelerate the reaction. Therefore, proportion of *N*-silylated amide and amine is controlled by [SiH], however, high concentration of [SiH] also promote the formation of side products.

Table II.2: Evolution of *N*-methylpropionamide and new species formed during reaction (100 °C).

Time of Reaction(min)	*N*-methylpropionamide (A) (mol%)	*N*-siloxane-*N*-methylpropionamide (C) (mol%)	*N*-siloxane-*N*-methylpropionamine (D) (mol%)	Products (E+F+G) (mol%)
10	80	12	2	6
30	76	7	9	8
60	48	13	30	9
120	17	39	32	12
180	11	41	35	13
240	9	41	37	13
360	9	41	38	12

E: *N*-siloxane-*N*-methylpropionenamine, F: *N, N*-dipropyl-*N*-methylamine, G: *N,N*-disiloxane-*N*-methylamine

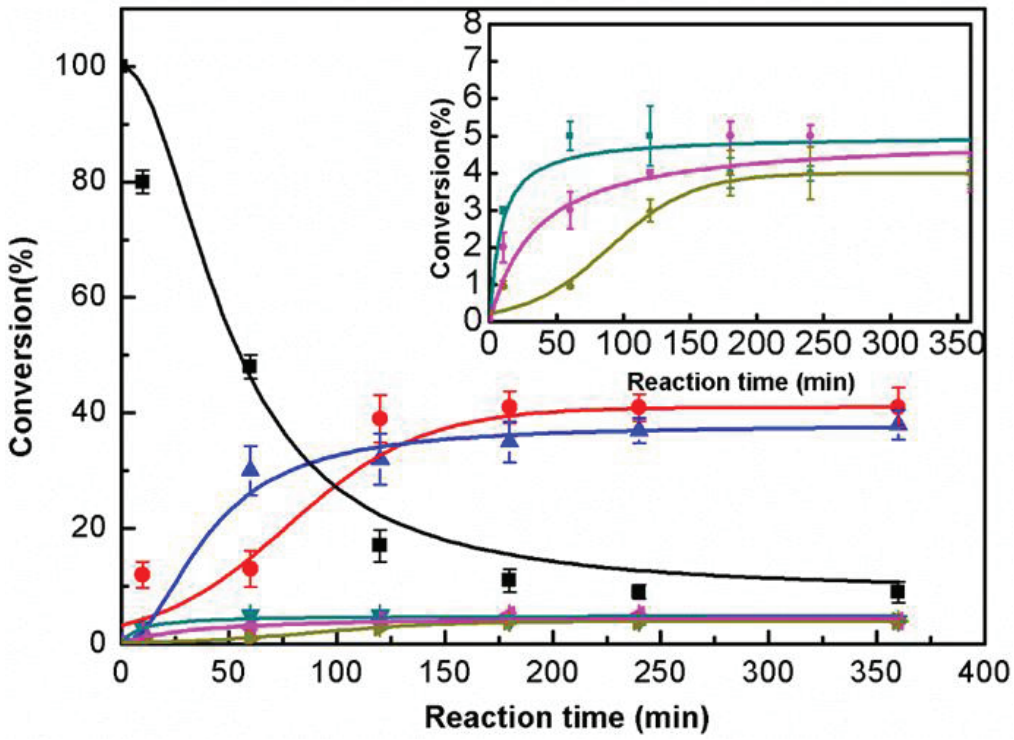

Figure II.7: Proportion of *N*-methylpropionamide and products obtained at 100 °C, *N*-methylpropionamide(■); *N*-siloxane-*N*-methylpropionamide(●);*N*-siloxane-*N*-methylpropionamine (▲), *N*-siloxane-*N*-methylpropionenamine (▼); *N*,*N*-dipropyl-*N*-methylamine (◂); *N*,*N*-disiloxane-*N*-methylamine (▸).

II.3.3 Hydrosilylation reaction with amide functions from PA12

The hydrosilylation reaction between PA12 and PDMS-SiH chains was carried out in a mixer chamber at 170 °C in molten conditions under shear. Based on the previous results from model study, this reaction should lead to mainly form *N*-silylated polyamide and polyamine as illustrated in Figure II.8.

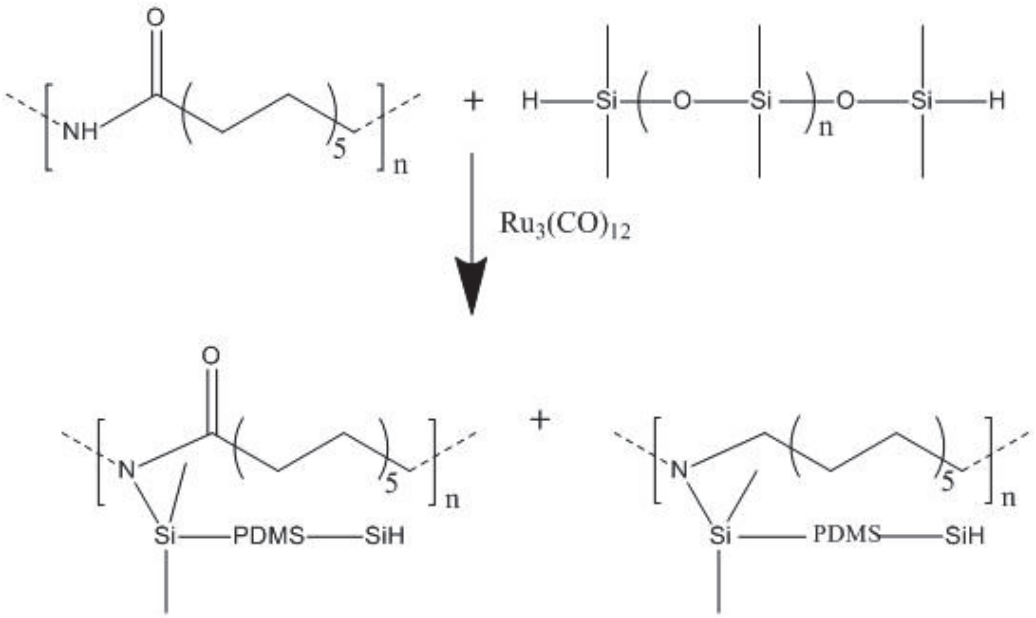

Figure II.8: Scheme of reaction between PA12 and PDMS-SiH chains.

First, we carried out reactive blending between PA12 and 1-PDMS-SiH (viscosity ratio: $\lambda_{1\text{-PDMS-SiH/PA12}} = 3x10^{-7}$, molar ratio: $\lambda_{1\text{-PDMS-SiH/PA12}} = 6.7x10^{-2}$, molar mass of 1-PDMS-SiH is 726 $g.mol^{-1}$). The variation of the torque *versus* time is depicted in Figure II.9. The torque variation corresponding to the variation of the apparent viscosity of the bulk material is relevant to some microstructure development [16, 20]. In the present case, the addition of 1-PDMS-SiH to the molten PA12 first leaded to a torque decrease due to lubricant effect causing by the large difference of viscosity between the molten PA12 and 1-PDMS-SiH. Therefore, the shear deformation was located in the thin film (lubricant effect) and the torque was governed by the rheology of the lowest viscosity fluid.

Few seconds after this drastic drop of the torque, the torque increased rapidly indicating the beginning of PA12/1-PDMS-SiH mixing. Within 6 min, the torque increased to a maximum value, highlighting the occurrence of PA12 modification associated with the reaction. During this processing phase, the reaction at the interface of the immiscible blend was expected. Furthermore, such phenomenon was not observed during the mixing of PA12 and 1-PDMS-SiH in the absence of catalyst. Figure II.9 (SEM pictures) also shows the morphology change between non-reactive and reactive blends. Actually, for non-reactive blend, 1-PDMS-SiH domains dispersed in PA12 phase with a diameter around 4 μm. The nodular morphology is explained by the non-miscibility between PA12 and 1-PDMS-SiH, and the low viscosity ratio. When the hydrosilylation occurs under shearing, the dispersion of

1-PDMS-SiH becomes better as the final submicronic morphology shows the 1-PDMS-SiH dispersed in PA12 matrix with a diameter around 0.8 µm and narrow size distribution.

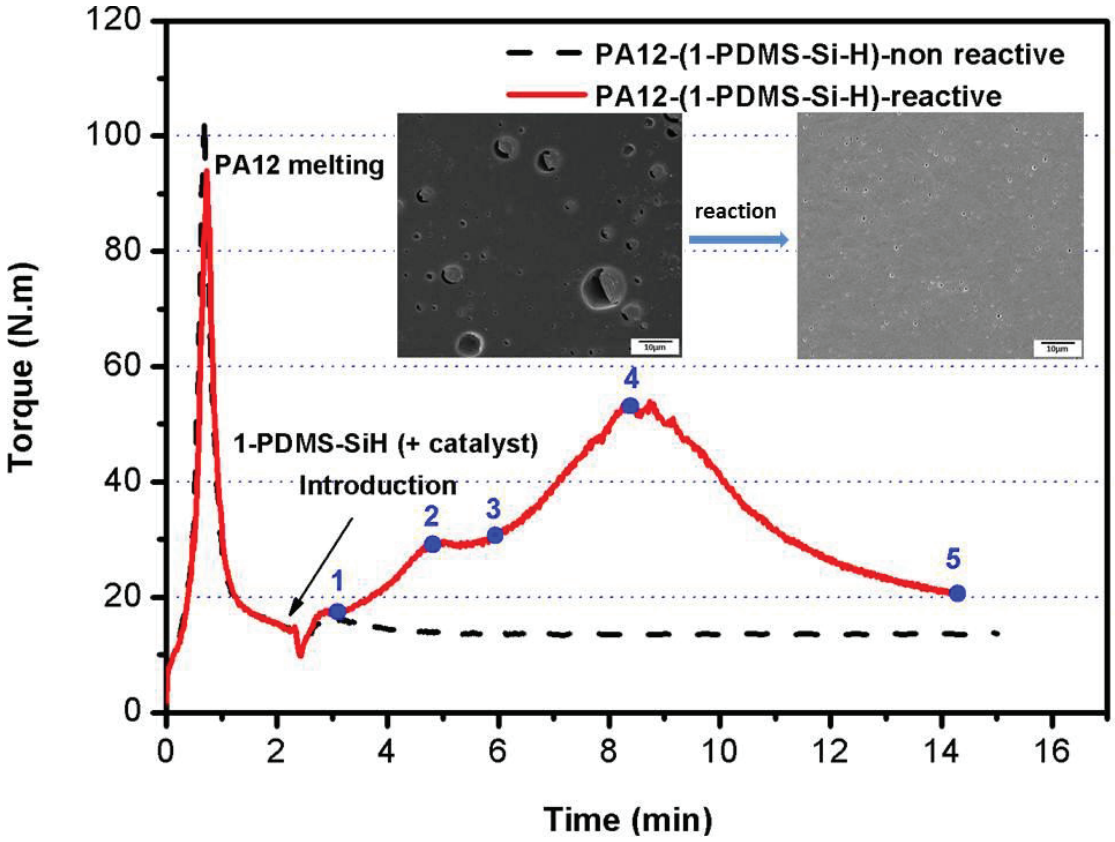

Figure II.9: Variation of the mixing torque versus between PA12 and 1-PDMS-SiH under shear in the internal mixer at 170 °C: reactive blending (solid line) and non-reactive blend (dotted line). SEM micrographs (surface) of both non-reactive and reactive blends.

In order to better understand the action of the hydrosilylation reaction onto the blend compatibilization, evolution of morphology was observed by SEM of PA12/1-PDMS-SiH blends (Figure II. 10). We observed morphologies of samples (1, 2, 3, 4 and 5), removing from different stages of PA12/1-PDMS-SiH reactive mixing (Figure II. 9) process. It is clear that the chemical reaction does not occur in homogeneous conditions at least at the early stages of the process since in Figure II.10-1, there is not too much 1-PDMS-SiH mixed into PA12 and the mixed one dispersed in PA12 presents a large size around 10 µm diameter. With the occurrence of reaction, the torque increased from 18 to 30 N.m (point 1 to 2), and we can find there are more 1-PDMS-SiH domains dispersed in the matrix with a size around 3-4 µm. It means that the reaction at the interface between PA12 and 1-PDMS-SiH promoted their compatibilization. Then the size of 1-PDMS-SiH domains decreased rapidly from 3-4 µm to less than 1 µm, in the meantime, the torque increased rapidly to the top. During this process

the reaction between PA12 and 1-PDMS-SiH occurred at the interface, reducing the interfacial tension and promoting the dispersion of PDMS. With mixing, the torque decreased to a steady value around 20 N.m meaning the bulk viscosity was constant and achieved a stable blend with a submicronic morphology of PDMS (size of PDMS domains are 0.8 μm) after reactive compatibilization. Therefore, combing the previous reaction mechanism study, during the whole reactive blending process, hydrosilylation of PA12 and 1-PDMS-SiH formed *N*-silylated copolymers working as compatibilizer at the interface and promoted the dispersion and stability of PDMS in PA12.

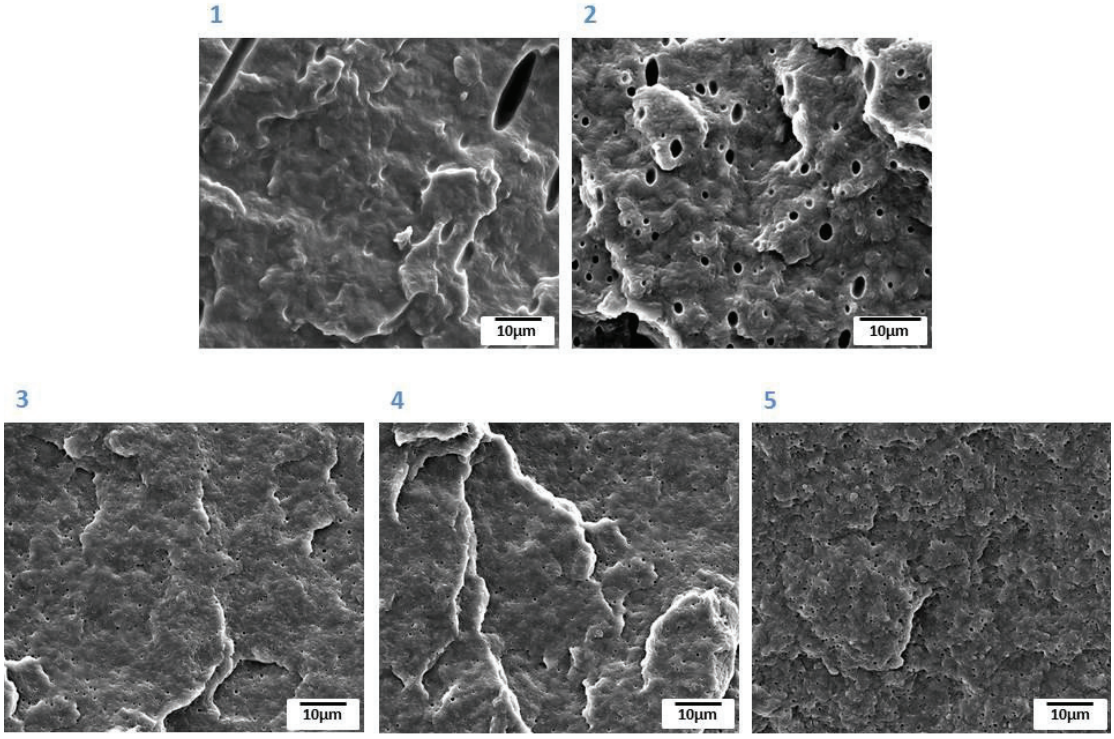

Figure II.10: Evolution of SEM micrographs (fracture) of PA12/1-PDMS-SiH reactive blend at different stage of process related to torque variation.

To confirm the hypothesis that new copolymers are formed, PA12, PA12-1-PDMS-SiH-reactive and PA12-1-PDMS-SiH-non reactive materials were pressed to 0.50 mm films for ATR characterization (Figure II. 11). For PA12, as secondary amide [21, 22], there are stretching and bending band of -NH appearing at 3288 and 1558 cm^{-1}, respectively, and a strong -C=O band at 1635 cm^{-1} due to stretching vibration. Two bands of strong intensity owning to the stretching vibration of the C-H bonds from $-CH_2$ and $-CH_3$ of the polymer chain are observed at 2850 and 2919 cm^{-1} respectively with their corresponding bending vibration at 1464 cm^{-1}. For PDMS [15, 21, 23], the band due to the asymmetric

Si-O-Si stretching vibration is at 1062 cm^{-1}, the band due to the methyl rocking vibration and the Si-C stretching vibration occur at 797 cm^{-1}. These bands can all be found in both spectra of PA12-1-PDMS-SiH-reactive and PA12-1-PDMS-SiH-non reactive blends. The difference of them is the disappearance of Si-H band (2159 cm^{-1}, since the low concentration and a part was shielded by vibration of H_2O, the difference is not very obvious) and appearance of Si-N after reaction. Specifically, the band due to the deformation vibration of Si-H groups appearing at 908 cm^{-1} [15] disappeared after reaction. Otherwise, a new band at 892 cm^{-1} due to Si-N stretching vibration on the spectrum of PA12 and 1-PDMS-SiH reactive blend is observed. This new bond proves the formation of the *N*-silylated product through reactive processing as predicted in previous model study. However, during the process only 10wt% 1-PDMS-SiH was introduced, and as previously observed the kinetic data (Table II.2), so the concentration of *N*-silylated copolymer cannot be high. Furthermore, the reaction takes place in a non-homogenous media as it occurs at the interface between PA12 and PDMS chains. It is the reason why the band of Si-N is not significant. The low concentration of *in situ* formed compatibilizer is common [22, 24]. As reported by Stiubianu *et* al. [24], cellulose acetate was reacted with poly[dimethyl(methyl-H)siloxane] containing 25 mol% Si–H side groups along the chain to modify its thermal and surface properties. The dehydrocoupling reaction between Si–H and C–OH groups occurred in presence of Karstedt's catalyst, leading to the formation of Si–O–C bond and being proved by ATR spectrum. Even though the signal of Si-O-C bond is quite weak at 857 cm^{-1}, similar to our observation, the modification of surface properties is obvious. A number of research reported sometimes about 2 wt% of a typical diblock copolymer is enough to cover completely the interface of 1 μm size particles [25, 26].

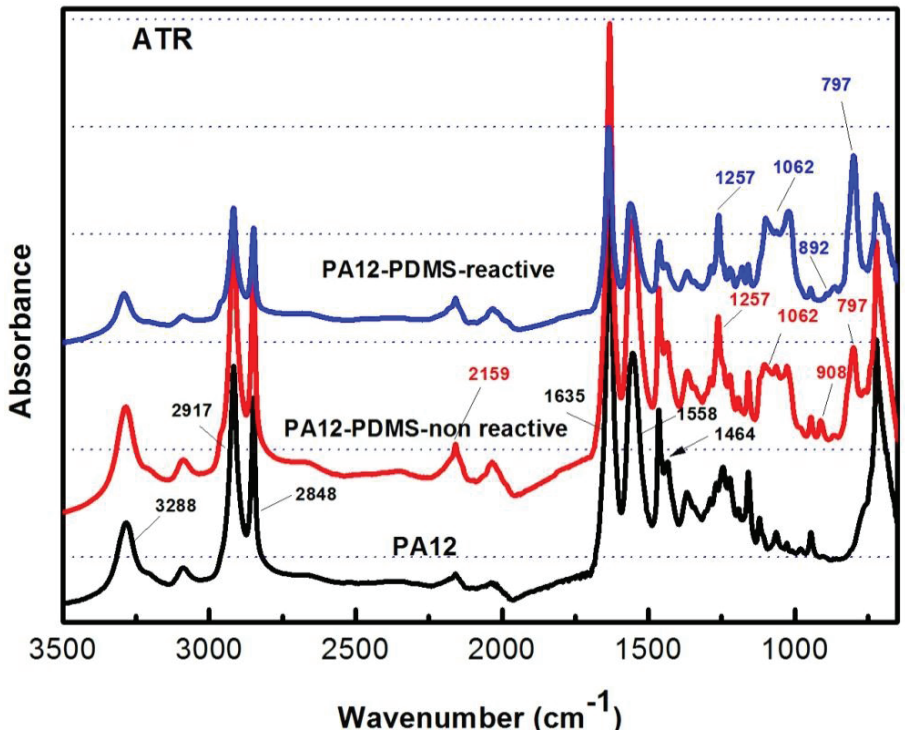

Figure II.11: ATR spectra of PA12, PA12-1-PDMS-SiH-reactive and PA12-1-PDMS-SiH-non reactive films.

In addition, we also compared the solubility of non-reactive and reactive blends. 200 mg blend was added in HFIP/chloroform solvent. After 48h, there is no insoluble matter in both solutions meaning there is at least no crosslinking network formed between PA12 and 1-PDMS-SiH even though the torque increased rapidly when the reaction was carried out. However, comparing the two kinds of solutions, the one corresponding to the reactive blend is turbid and not as clear as the one corresponding to the non-reactive one. In order to understand the origin of this observation, the morphology variation of PA12/1-PDMS-SiH non-reactive and reactive blends was investigated by TEM micrographs in Figure II.12(a-c) depicted the morphologies of compatibilized PA12/1-PDMS-SiH blend. Figure II.12(e-g) is corresponding to non compatibilized blend. Comparing Figure II.12a with Figure II.12e, it can be observed that the dispersion of 1-PDMS-SiH in PA12 matrix is promoted by reactive compatibilization resulting in PDMS domains sizes around 0.5-0.8 µm diameter. Regarding non- reactive blend, just a few PDMS domains can be observed in the blend [Figure II. 12(e-g)]. Actually, without compatibilization, PDMS tends to enrich the surface of blend during mixing as previously discussed from torque variation. For PA12/1-PDMS-SiH reactive blend, the *in situ* copolymer acts as an efficient compatibilizer at the interface between PA12 and PDMS, reducing the interfacial tension and stabilizing the blend. As reported by Hu *et* al.

[27], a critical concentration of 0.002% diblock poly(styrene-*b*-dimethylsiloxane) can achieve maximum 82% reduction of interfacial tension in PS/PDMS blend. Macosko *et* al. [28] also reported a proportion of 1% copolymer can lead to a significant reduction of PMMA particle size in poly(methyl methacrylate)/polystyrene (30:70) blend.

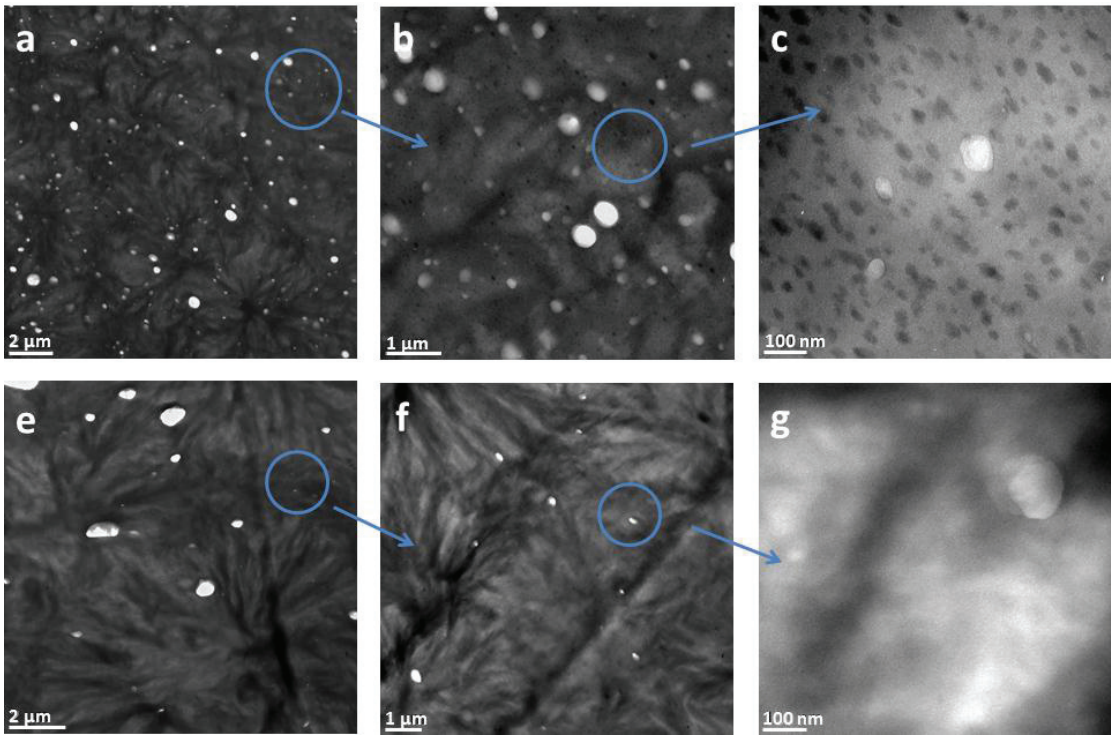

Figure II.12: TEM micrographs of PA12-1-PDMS-SiH-reactive blend (a, b and c) and PA12-1-PDMS-SiH-non reactive blend (e, f and g).

The obvious difference between reactive and non-reactive PA12/1-PDMS-SiH blends is, through magnifying the image, the observation of a lot of small nano size (~30nm) particles existing in the reactive blend (Figure II. 12c). It is clear that beside the expected compatibilizer copolymers, there are some extra products formed during the reactive process. The nano size particles probably coming from PDMS, but they are not smooth and round like initial PDMS domains. As mentioned in literatures [18, 29-31], in the presence of ruthenium or platinum catalyst, functionalized PDMS can graft or even crosslink themselves. Satyanarayana *et* al. [31] reported that rhodium catalyzed modification of poly(methylhydrosiloxane) (PMHS) via a dehydrogenative coupling reaction followed by *in situ* oxidation under mild conditions (80°C, 4h) which lead to a thermally stable and crosslinking polysiloxane. In addition, Hanada *et* al. [29] also proved that, ruthenium-catalyzed in presence of silicone containing more than two SiH is an efficient

catalyst system for the reduction of amide to amine involving self-encapsulation of the catalyst species into the insoluble silicone resin formed by oxidation. So it is quite probable that the nano particles in PA12/1-PDMS-SiH reactive blend is new formed silicone resin species obtained through PDMS-SiH oxidation reaction. Due to the low concentration of such nano particles (less than 10 wt%), it is difficult to confirm its exact chemical structure .

In order to confirm this hypothesis, we carried out complementary experiments. First, 1-PDMS-SiH and $Ru_3(CO)_{12}$ (4g/50mg) were heated at 170 °C in a schlenk with stirring under air atmosphere. After 15 min, the viscosity of the solution increases and a gel is formed. Then this mixture was introduced in molten PA12 and process for 15 min (conditions are the same as previously used for the reactive blend preparation). Finally, the blend was analyzed by TEM, and a few PDMS domains around 3µm diameter are observed. Moreover, the PDMS is not liquid with smooth and round surface anymore but looks like solid with sharp surface. Keeping magnifying the observation (Figure II.13c), we found the same nano particles as the ones depicted in Figure II.12c. The phenomenon confirms that the oxidation reaction of PDMS-SiH catalyzed by the ruthenium is at the origin of the nanometric phase dispersed in the PA12.

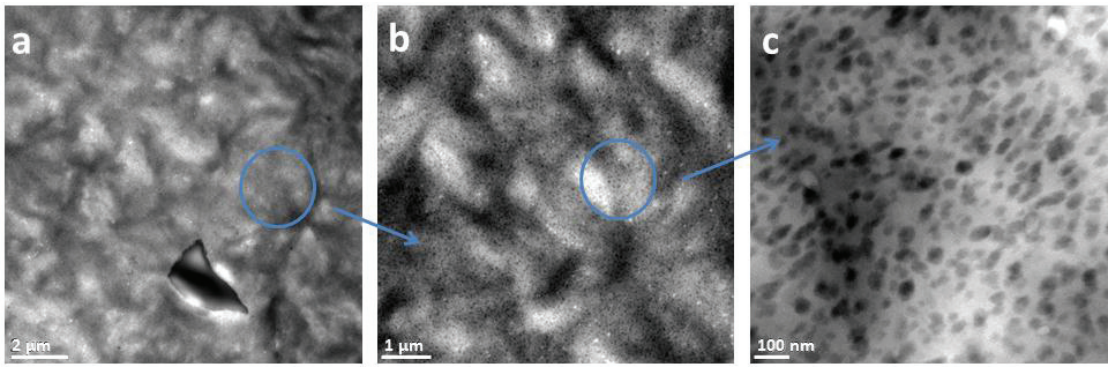

Figure II.13: TEM micrographs of PA12 and 1-PDMS-SiH-catalyst.Preheated blend (a', b' and c'): 1-PDMS-SiH and catalyst was heated 15min then introduced to melt PA12 in mix chamber at 170 °C.

Therefore, during the polymer blending, two kinds of modification were carried out. One is reactive compatibilization between PA12 and PDMS, *in situ* formed *N*-silylated copolymer promoted the dispersion of PDMS in PA12 matrix. Another is the evolution of a part of PDMS changed from liquid to gel-like nanoparticles due to self-crosslinking. Figure II.14-a represents the TEM micrograph of sample 3 (Figure II.9, 3 min after the introduction of PDMS/catalyst). It was the early stage of PDMS self-crosslinking since the edge of the

domains were still smooth. Through the increase of torque, the reaction was enhanced and PDMS changed to particles with a diameter around 100 nm and sharp edge (Figure II.14-b, sample 4, the second top on the torque curve). Then, under shearing the crosslinking network changed to smaller size around 30 nm (Figure II.12-c) and the torque value decreased again (Figure II.9). So the drastic torque variation was due to the both modification.

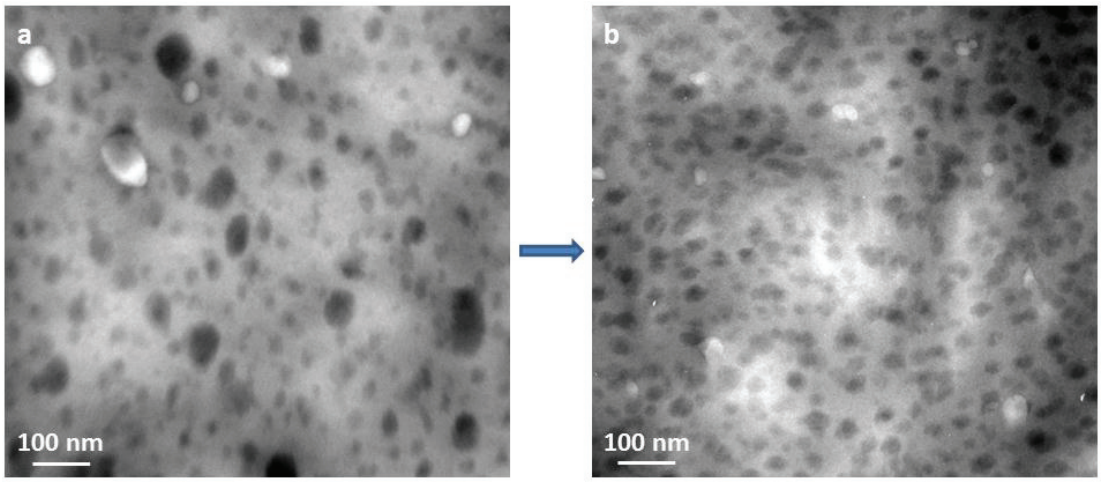

Figure II.14: TEM micrographs represent PA12-1-PDMS-SiH-reactive blend at different stages: a) sample 3 and b) sample 4 according to the torque curve (Figure II.9).

Finally, through previous study like using model compounds to understand the mechanism and the reactive processing in molten conditions, we confirm that the ruthenium catalyst in presence of PA12/PDMS-SiH blend caused hydrosilylation and promoted the dispersion of PDMS in PA12 and stabilized such blend. Specifically, new formed *N*-silylated polyamide and *N*-silylated polyamine copolymers by hydrosilylation acted as compatibilizer and modified the interface between the two immiscible phases, reducing the interfacial tension and increasing the interfacial adhesion. It is a typical and efficient reactive compatibilization [16, 32]. In the meantime, due to the nature of functionalized PDMS and ruthenium catalyst, a portion of PDMS changed to silicone resin caused by oxidation involving self-encapsulation of the catalyst species and evenly distributed with a nanostructure in the matrix. Figure II.15 illustrated the mechanism of the reactive blending in detail.

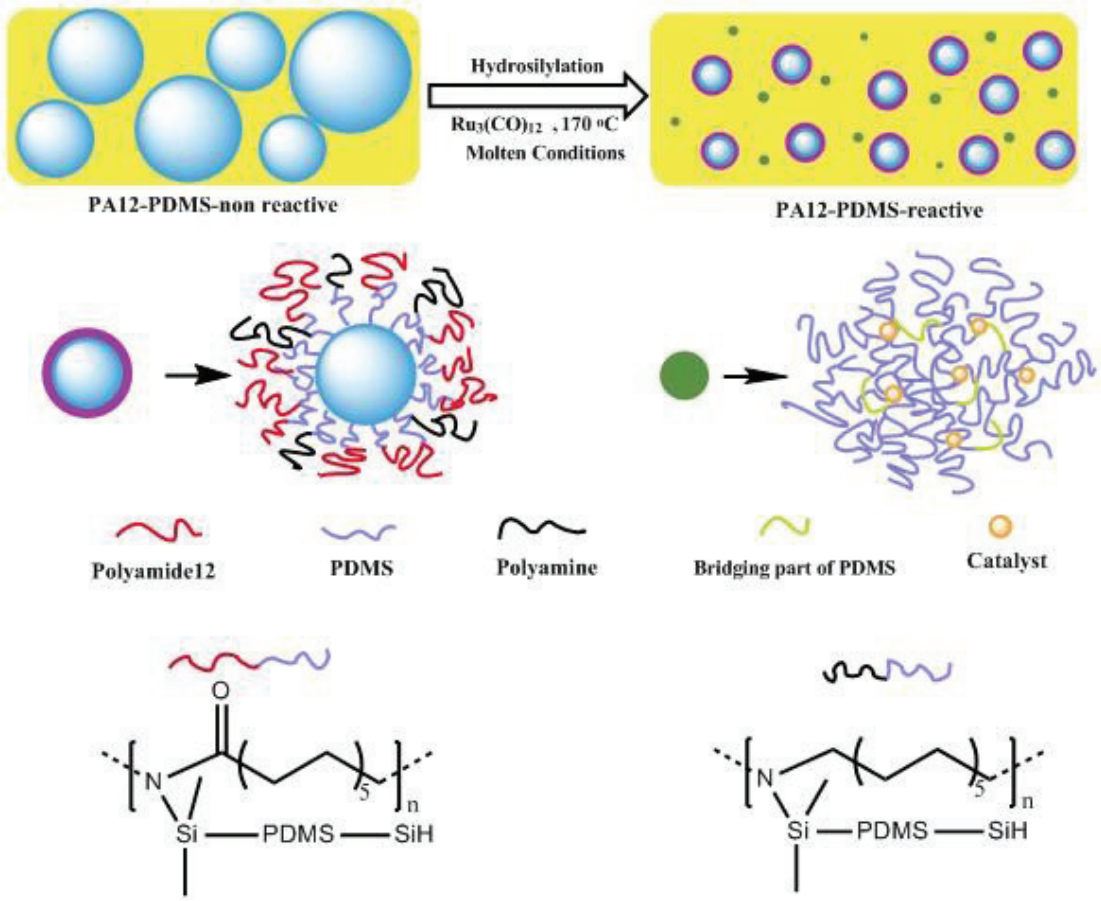

Figure II.15: Schematic of morphological development for PA12/PDMS-SiH reactive blend in the melt and the proposed mechanism.

II.3.4 Effect of physico-chemical parameters on compatibilization

Generally speaking, there are different parameters such as diffusion, viscosity ratio and interfacial tension which have to be considered for polymer blends. Furthermore, for reactive blending, ratio of functionalized groups and concentration of the *in situ* formed compatibilizer also act important role in such system. The present reactive system can be used as a model system to study the mixing of fluid of low viscosity ratios. To investigate the influence of the nature of polysiloxane on the blending of PA12 and PDMS, the experiments were also carried out with another hydride functionalized PDMS. It is a hydride terminated 2-PDMS-SiH of higher molar mass (6000 $g.mol^{-1}$). The viscosity ratio is $\lambda_{2\text{-PDMS-SiH/PA12}}= 1x10^{-5}$, and the molar ratio is $\lambda_{2\text{-PDMS-SiH/PA12}}=8.3x10^{-3}$.

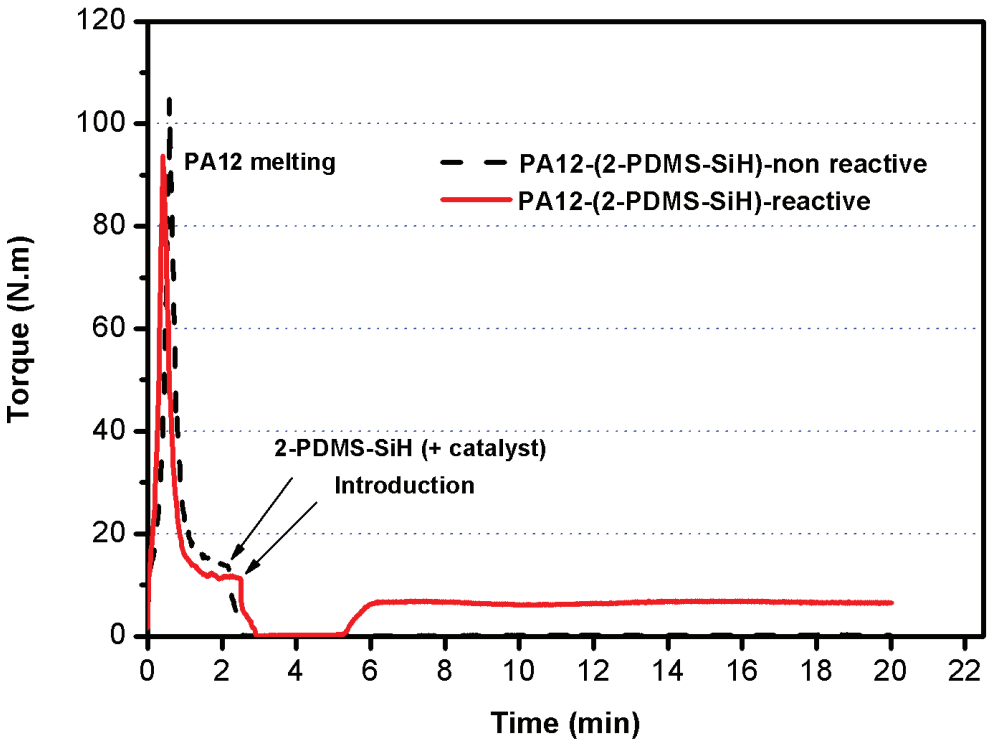

Figure II.16: Variation of the mixing torque between PA12 and 2-PDMS-SiH (10 wt%) under shear in the internal mixer at 170 °C: reactive blending (solid line) and non-reactive blend (dotted line).

Figure II.16 shows the variation of the torque for the non-reactive and reactive PA12/2-PDMS-SiH blends. The addition of 2-PDMS-SiH in molten PA12 leads to a sharp decrease in the torque, because the PDMS acted as lubricant coating on the wall of the mixing chamber as mentioned before. The torque remained equal to zero even after 20 min of mixing meaning that there was no effective mixing and the blend was totally phase separated at the macroscale. From Figure II.17c, it can be clearly observed a few large PDMS domains (~50 µm) dispersed in the blend confirming the weak mixing and obviously phase separation.

However, the torque of PA12/1-PDMS-SiH reactive sample (Figure II.9: dotted line) increased soon in a few seconds after a slight decrease and reached a steady plateau around 15 N.m. Scott and Macosko [20] confirmed that this mixing torque variation was primarily due to a change in blend rheology caused by a morphology transformation related to a phase inversion in the blend. Sample after the blending was investigated by SEM (Figure II.17a), it shows the domains dispersed in PA12 matrix with a diameter around 4-5 µm indicating mixing had occurred. For PA12/1-PDMS-SiH non-reactive systems, the viscosity ratios are lower than one for PA12/2-PDMS-SiH and we found that the rotor was not totally controlled by lubrication, mixing was also observed. Therefore, for PA12/1-PDMS-SiH system ($3x10^{-7}$),

mixing can be more efficient than for PA12/2-PDMS-SiH ($1x10^{-5}$). In some publications [33] they also demonstrated that for PDMS with lower molar mass, the better dispersion of the PDMS domains in the matrix is observed.

Through investigating the physical parameters between PA12 and PDMS, we found that PDMS with quite low viscosity and molar mass can get better dispersion in PA12 matrix and form more interface between them than those with higher molar mass. It is beneficial for later *in situ* compatibilization as the reaction can only occurred at the interface [34]. This result is the same as described in a number of research when viscosity will influence the drop size [35].

Figure II.9 (solid line) and Figure II.16 (solid line) show the variation of the mixing torque for PA12/1-PDMS-SiH and PA12/2-PDMS-SiH reactive blends, respectively. The chemical reaction between PA12 and PDMS-SiH by hydrosilylation reaction occurred as expected. Compared the torque between reactive and non-reactive one, the mixing of PA12 and PDMS-SiH was accelerated in the case of reactive blends. To be more exact, PA12/2-PDMS-SiH mixing was observed 2 min later after the introduction of 2-PDMS-SiH/$Ru_3(CO)_{12}$ mixture. Finally, the value of the steady torque at the plateau was 8 N.m, suggesting that the bulk viscosity of the blend was constant and close to the viscosity of PA12 matrix (about 11 N.m), but such mixing step never appeared in non-reactive blend. As described before, the same accelerated mixing phenomenon was observed in PA12/1-PDMS-SiH reactive blend and more significant since the torque increased more sharply. Morphology analysis of such blends confirmed the modification of dispersion and the difference between the two systems. Figure II.17b and Figure II.17d corresponding to PA12/1-PDMS-SiH and PA12/2-PDMS-SiH reactive blends clearly evidenced that after the reaction the PDMS-SiH morphology was considerable reduced to size 0.8 μm and 4μm, respectively. In addition, the surface of PA12/2-PDMS-SiH reactive blend is a little bit oily after the process confirmed the imperfect compatibilization comparing with PA12/1-PDMS-SiH reactive blend.

The difference of compatibilization efficiency between PA12/1-PDMS-SiH and PA12/2-PDMS-SiH reactive blends should come from the interface area and reactivity of the blend. Since interfacial reaction kinetics [36] under mixing has been studied by assuming that

the reaction is second order and that it occurred only in the interfacial volume. The interfacial volume is defined by the surface area of the minor phase and an interfacial thickness, λ [25, 37].

$$\frac{dC_A}{dt} = k_1 C_A C_B \phi_1 \qquad (1)$$

Where C_A and C_B are the concentrations of functionalized groups A and B, k_1 is the rate constant for the interfacial coupling reaction, and ϕ_1 is the interfacial volume fraction ($=\lambda a_v$ where a_v is the interfacial area per unit volume). Simply, the factors impact of the reactive efficiency comes from viscosity ratio and molar ratio of functionalized groups.

It should be noted again that the functional group molar ratio of the two reactive blends varied from $6.7x10^{-2}$ (PA12/1-PDMS-SiH) to $8.3x10^{-3}$ (PA12/2-PDMS-SiH). The viscosity ratio increased also from $3x10^{-7}$ (PA12/1-PDMS-SiH) to $1x10^{-5}$ (PA12/2-PDMS-SiH). Consequently, the formation of PA12/PDMS coupling was not the same. Since the concentration of SiH coming from 2-PDMS-SiH is lower for the reaction and interfacial volume fraction is also smaller, reactive compatibilization of the blend was observed but not as efficient as in the case of PA12/1-PDMS-SiH reactive one. So better diffusion (lower viscosity) and higher reactivity (high concentration of functional group) of PDMS can provide better conditions for reactive blending. Besides, the reactivity of PDMS also significantly affects its oxidation reaction. Through comparing the TEM micrographs of two reactive blends (Figure II.17-e and Figure II.17-f), it is clear that PA12/2-PDMS-SiH reactive blend has less silicon resin particles dispersed in the matrix. Therefore, high reactivity of PDMS not only weaken the reactive compatibilization but also PDMS self-oxidation reaction which leads to form gel-like phase. It is also the reason why the torque variation of PA12/2-PDMS-SiH reactive blend is not as drastic as the one of PA12/1-PDMS-SiH reactive blend.

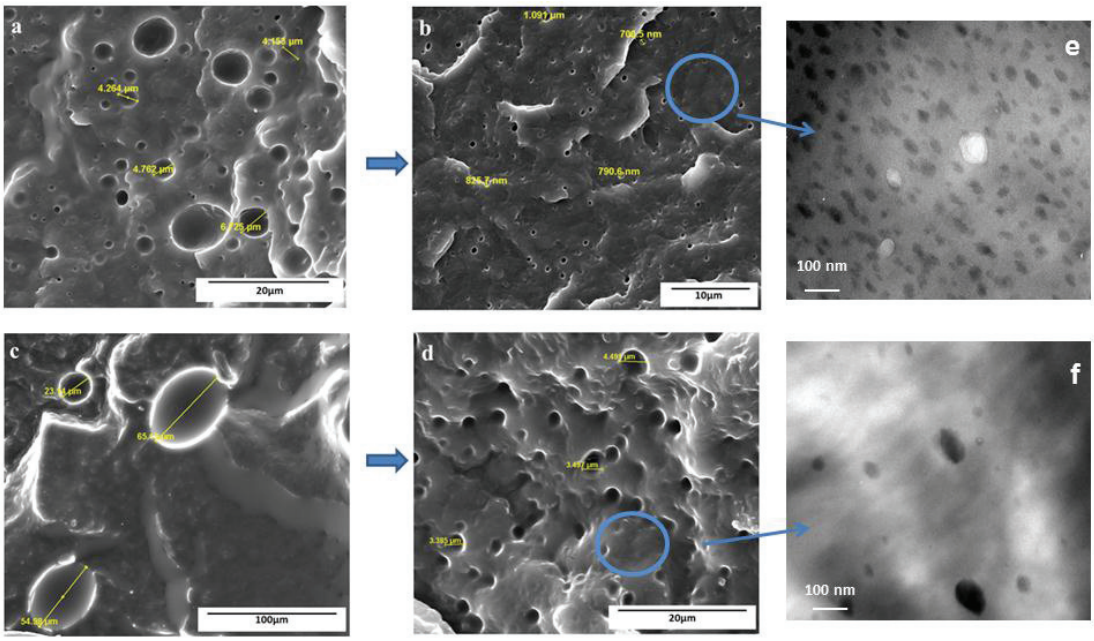

Figure II.17: Representative SEM micrographs of PA12/PDMS blends: a) PA12/1-PDMS-SiH non-reactive blend, b) PA12/1-PDMS-SiH reactive blend, c) PA12/2-PDMS-SiH non-reactive blend, d) PA12/2-PDMS-SiH reactive blend, and TEM micrographs of reactive blends: e) PA12/1-PDMS-SiH reactive blend, f) PA12/2-PDMS-SiH reactive blend.

In general, these processing and morphological behaviors clearly indicated the reactive compatibilization of the blends obtaining with ruthenium catalyst. The new formed copolymer at the interface reduced the interfacial tension between the two immiscible phases. The results produced the same observation and conclusion derived by Zhou *et* al. [14]. They reported that the dispersion of siloxane domains in PC matrix is 15-20 µm without *in situ* reaction. Differently, the reactive dispersion of 5 wt% of PDMS-OH in PC formed small spherical domains with a length about 0.2-0.9 µm. In addition, physico and chemical parameters such as viscosity ratio, diffusion and reactivity act important role in reactive efficiency and controlling the final morphology.

II.4 Conclusion

Ruthenium-catalyzed hydrosilylation between amide and PDMS-SiH was evidenced at high temperature. Mechanism and efficiency were investigated through model reaction. Yield of *N*-silylated amide and *N*-silylated amine can be totally more than 70 mol% after 2h reaction, meaning such reaction is efficient.

From amide hydrosilylation reaction, a new method for PA12/polysiloxane one-step

compatibilization was proposed. During process, compatibilization was carried out in PA12 molten condition directly through ruthenium-catalyzed reaction between PA12 and -SiH at the interface. The dispersion of PDMS in PA12 matrix was significantly promoted. Interfacial tension was reduced by the acting of copolymer. The size of 1-PDMS-SiH domains decreased rapidly from 4 μm to 0.8 μm and finally achieved stable blend with submicronic morphology. Besides, in such reactive conditions and in presence of ruthenium catalyst, PDMS-SiH oxidation reaction was partially observed. This phenomenon leads to a second PDMS gel based dispersion with a size around 20-30 nm diameter. We also investigated the influence of physico-chemical parameters of both PA12 and hydride functionalized PDMS to the reactive compatibilization by using higher viscosity and lower reactivity 2-PDMS-SiH. We found that it is possible to control the morphology and microstructure of such blend through modifying such parameters.

II.5 References

[1] J. Parameswaranpillai, S. Thomas, Y. Grohens, Polymer Blends: State of the Art, New Challenges, and Opportunities, Characterization of Polymer Blends: Miscibility, Morphology and Interfaces (2015) 1-6.
[2] D.R. Paul, Control of phase structure in polymer blends, Springer1989.
[3] C.-L. Chang, T.-M. Don, H.S.-J. Lee, Y.-O. Sha, Studies on the aminolysis of RTV silicone rubber and modifications of degradation products, Polymer degradation and stability 85(2) (2004) 769-777.
[4] S. Mani, P. Cassagnau, M. Bousmina, P. Chaumont, Morphology development in novel composition of thermoplastic vulcanizates based on PA12/PDMS reactive blends, Macromolecular Materials and Engineering 296(10) (2011) 909-920.
[5] N. Sheremetyeva, N. Voronina, A. Bystrova, V. Miakushev, M. Buzin, A. Muzafarov, Advances in Sili cones and Silicone Modified Materials, ACS Symposium Se Received July 27, 2011; in revised form October 6, 2011 ries, p. 111.
[6] L. Yang, Y. Hu, H. Lu, L. Song, Morphology, thermal, and mechanical properties of flame-retardant silicone rubber/montmorillonite nanocomposites, Journal of Applied Polymer Science 99(6) (2006) 3275-3280.
[7] R.N. Santra, P. Mukunda, G. Nando, T. Chaki, Thermogravimetric studies on miscible blends of ethylene-methyl acrylate copolymer (EMA) and polydimethylsiloxane rubber (PDMS), Thermochimica acta 219 (1993) 283-292.
[8] R. Jiang, R.P. Quirk, J.L. White, K. Min, Polycarbonate-polystyrene block copolymers and their application as compatibilzing agents in polymer blends, Polymer Engineering & Science 31(21) (1991) 1545-1548.
[9] S.M. George, D. Puglia, J.M. Kenny, V. Causin, J. Parameswaranpillai, S. Thomas, Morphological and mechanical characterization of nanostructured thermosets from epoxy and styrene-block-butadiene-block-styrene triblock copolymer, Industrial & Engineering Chemistry Research 52(26) (2013) 9121-9129.
[10] N.T. McManus, S.H. Zhu, C. Tzoganakis, A. Penlidis, Grafting of ethylene–ethyl acrylate–maleic anhydride terpolymer with amino-terminated polydimethylsiloxane during reactive processing, Journal of Applied Polymer Science 101(6) (2006) 4230-4237.
[11] L. Utracki, Melt flow of polymer blends, Polymer Engineering & Science 23(11) (1983) 602-609.
[12] U. Sundararaj, C. Macosko, Drop breakup and coalescence in polymer blends: the effects of concentration and compatibilization, Macromolecules 28(8) (1995) 2647-2657.
[13] Z. Xu, S. Jie, B.G. Li, Well-defined PE-b-PDMS diblock copolymers via the combination of thiol-ene click and esterification reactions: Facile synthesis and compatibilization for HDPE/silicone oil blends, Journal of Polymer Science Part A: Polymer Chemistry 52(22) (2014) 3205-3212.
[14] W. Zhou, J. Osby, Siloxane modification of polycarbonate for superior flow and impact toughness, Polymer 51(9) (2010) 1990-1999.
[15] C.-A. Fustin, M. Sclavons, N. Pantoustier, S. Bebelman, D. Truffier-Blanc, C. Bailly, P. Merlin, Reactivity of Si-H and Si-vinyl end functionalized siloxanes toward PBT: A model system study, Polymer Engineering & Science 45(8) (2005) 1067-1072.
[16] J. Bonnet, V. Bounor-Legaré, P. Alcouffe, P. Cassagnau, EVA reactive blending with Si–H terminated polysiloxane by carbonyl hydrosilylation reaction: From compatibilised blends to crosslinking networks, Materials Chemistry and Physics 136(2-3) (2012) 954-962.
[17] S. Hanada, T. Ishida, Y. Motoyama, H. Nagashima, The ruthenium-catalyzed reduction and reductive N-alkylation of secondary amides with hydrosilanes: Practical synthesis of secondary and tertiary amines by judicious choice of hydrosilanes, The Journal of organic chemistry 72(20) (2007) 7551-7559.

[18] Y. Motoyama, K. Mitsui, T. Ishida, H. Nagashima, Self-encapsulation of homogeneous catalyst species into polymer gel leading to a facile and efficient separation system of amine products in the Ru-catalyzed reduction of carboxamides with polymethylhydrosiloxane (PMHS), Journal of the American Chemical Society 127(38) (2005) 13150-13151.
[19] S. Hanada, E. Tsutsumi, Y. Motoyama, H. Nagashima, Practical Access to Amines by Platinum-Catalyzed Reduction of Carboxamides with Hydrosilanes: Synergy of Dual Si− H Groups Leads to High Efficiency and Selectivity, Journal of the American Chemical Society 131(41) (2009) 15032-15040.
[20] C.E. Scott, C.W. Macosko, Morphology development during reactive and non-reactive blending of an ethylene-propylene rubber with two thermoplastic matrices, Polymer 35(25) (1994) 5422-5433.
[21] G. Socrates, Infrared and Raman characteristic group frequencies: tables and charts, John Wiley & Sons2004.
[22] H. Kim, C. Lim, S.-I. Hong, Gas permeation properties of organic-inorganic hybrid membranes prepared from hydroxyl-terminated polyether and 3-isocyanatopropyltriethoxysilane, Journal of sol-gel science and technology 36(2) (2005) 213-221.
[23] N. Risangud, Z. Li, A. Anastasaki, P. Wilson, K. Kempe, D.M. Haddleton, Hydrosilylation as an efficient tool for polymer synthesis and modification with methacrylates, RSC Advances 5(8) (2015) 5879-5885.
[24] G. Stiubianu, C. Racles, M. Cazacu, B.C. Simionescu, Silicone-modified cellulose. Crosslinking of cellulose acetate with poly[dimethyl(methyl-H)siloxane] by Pt-catalyzed dehydrogenative coupling, Journal of Materials Science 45(15) (2010) 4141-4150.
[25] P. Guégan, C. Macosko, T. Ishizone, A. Hirao, S. Nakahama, Kinetics of chain coupling at melt interfaces, Macromolecules 27(18) (1994) 4993-4997.
[26] F. Ide, A. Hasegawa, Studies on polymer blend of nylon 6 and polypropylene or nylon 6 and polystyrene using the reaction of polymer, Journal of applied polymer science 18(4) (1974) 963-974.
[27] W. Hu, J.T. Koberstein, J. Lingelser, Y. Gallot, Interfacial tension reduction in polystyrene/poly (dimethylsiloxane) blends by the addition of poly (styrene-b-dimethylsiloxane), Macromolecules 28(15) (1995) 5209-5214.
[28] C. Macosko, P. Guegan, A.K. Khandpur, A. Nakayama, P. Marechal, T. Inoue, Compatibilizers for melt blending: Premade block copolymers, Macromolecules 29(17) (1996) 5590-5598.
[29] S. Hanada, Y. Motoyama, H. Nagashima, Dual Si–H effects in platinum-catalyzed silane reduction of carboxamides leading to a practical synthetic process of tertiary-amines involving self-encapsulation of the catalyst species into the insoluble silicone resin formed, Tetrahedron Letters 47(35) (2006) 6173-6177.
[30] W. Fortuniak, S. Slomkowski, J. Chojnowski, J. Kurjata, A. Tracz, U. Mizerska, Synthesis of a paraffin phase change material microencapsulated in a siloxane polymer, Colloid and polymer science 291(3) (2013) 725-733.
[31] N. Satyanarayana, H. Alper, Rhodium-catalyzed modification of poly (methylhydrosiloxane) into a highly cross-linked polysiloxane, Macromolecules 28(1) (1995) 281-283.
[32] C. DeLeo, K. Walsh, S. Velankar, Effect of compatibilizer concentration and weight fraction on model immiscible blends with interfacial crosslinking, Journal of Rheology 55(4) (2011) 713.
[33] Z.-y. Zhao, W.-w. Yao, R.-n. Du, Q. Zhang, Q. Fu, Z.-h. Qiu, S.-l. Yuan, Effect of molecular weight of PDMS on morphology and mechanical properties of PP/PDMS blends, Chinese Journal of Polymer Science 27(01) (2009) 137-143.
[34] J.M. Raquez, Y. Nabar, R. Narayan, P. Dubois, In situ compatibilization of maleated thermoplastic starch/polyester melt-blends by reactive extrusion, Polymer Engineering & Science 48(9) (2008) 1747-1754.
[35] L. Utracki, Z. Shi, Development of polymer blend morphology during compounding in a twin-screw extruder. Part I: Droplet dispersion and coalescence—a review, Polymer Engineering & Science 32(24)

(1992) 1824-1833.
[36] C.W. Macosko, H.K. Jeon, T.R. Hoye, Reactions at polymer–polymer interfaces for blend compatibilization, Progress in Polymer Science 30(8-9) (2005) 939-947.
[37] H.K. Jeon, C.W. Macosko, B. Moon, T.R. Hoye, Z. Yin, Coupling reactions of end-vs mid-functional polymers, Macromolecules 37(7) (2004) 2563-2571.

Chapter III: Study of physical properties of PA12/PDMS blend preparing via ruthenium-catalyzed in situ compatibilization

Abstract

Hydrosilylation reaction catalyzed by triruthenium dodecacarbonyl ($Ru_3(CO)_{12}$) between SiH and amide group was developed to prepare compatibilized blends of polyamide (PA12) and hydride terminated polydimethylsiloxane (PDMS-SiH). N-silylated copolymers were formed at the interface during the process, when using 1wt% of catalyst and 10wt% to 20wt% of PDMS-SiH. In addition, the dispersed PDMS-SiH domains' size decreased and the interfacial adhesion between the two immiscible phases increased. More specifically, the size of PDMS-SiH domains in PA12/PDMS-SiH with 10 wt% of PDMS-SiH decreased from around 4 μm to 800 nm after compatibilization and similarly, for the reactive blend with 20wt% PDMS-SiH, the size of dispersed phase decreased from more than 30 μm to 1 μm.

The reactive route permitted to avoid PDMS leaching phenomenon and allowed incorporation of higher amount of PDMS within PA12 while keeping stable materials. Thermal stability was improved after compatibilization as the initial degradation temperature of reactive blends obviously increased compared with non-reactive ones.

Finally the impacts of compatibilization were studied on materials' surface properties, mechanical properties and gas permeability. The introduction of PDMS lowered the surface free energy and the PA12-based blend turned from hydrophilic to hydrophobic, as evidenced by the water contact angle measurement. Gas permeability and CO_2/H_2 and CO_2/He selectivity were also improved with the increase of PDMS content. The mechanical properties were enhanced with 13 % increase of Young's modulus after *in situ* compatibilization with 15 wt% PDMS-SiH.

Keywords: *PA12, PDMS, hydrosilylation, polymer blend, gas permeability, surface free energy*

Résumé

La réaction d'hydrosilylation catalysée par le triruthénium dodecacarbonyle ($Ru_3(CO)_{12}$) entre le SiH et le groupe amide a été développée pour comparer les mélanges compatibilisés de polyamide (PA12) et de polydiméthylsiloxane terminé hydride (PDMS-SiH). Les copolymères N-silylés sont formés à l'interface pendant le procédé lorsque sont ajoutés 1m% de catalyseur et entre 10 et 20m% de PDMS-SiH. La taille des domaines de PDMS-SiH dispersé diminue et l'adhésion interfaciale entre les 2 phases immiscibles est améliorée. Plus précisément, après compatibilisation, la taille des domaines de PDMS-SiH dans le PA12/PDMS-SiH avec 10m% de PDMS-SiH (respectivement 20m%) diminue environ de 4 microns à 0,8 micron (respectivement de 30 micron à 1 micron).

L'approche réactive permis d'éviter phénomène de lessivage PDMS et a permis l'incorporation d'une quantité plus élevée de PDMS dans les PA12 tout en gardant des matériaux stables. La stabilité thermique a été améliorée après compatibilisation étant donné que la température de dégradation initiale des mélanges réactifs est augmentée par rapport à celle pour les systèmes non réactifs. Enfin, les impacts de compatibilisation ont été étudiés sur lespropriétés de surface, les propriétés mécaniques et la perméabilité aux gaz. L'introduction de PDMS réduit l'énergie libre de surface et le mélange à base de PA12 présente un léger comportement hydrophobe, comme en témoigne la mesure de l'angle de contact de l'eau. La perméabilité au gaz CO_2/H_2 et CO_2/He a également été améliorée grâce à l'augmentation de la teneur en PDMS. Les propriétés mécaniques ont été renforcées avec une augmentation du module de Young de 13% après compatibilisation *in situ* avec 15% en masse de PDMS dans le PA12 .

***Mots clés** : PA12, PDMS, hydrosilylation, mélange de polymères, perméabilité aux gaz, énergie libre de surface.*

III.1 Introduction

Polydimethylsiloxanes (PDMS) are of particular interest since it has a wide range of commercial applications resulting from its special properties [1]. These include high chemical and thermal stability and low toxicity. The linear polymer is liquid with low freezing point

and low surface tension. Its physical properties show only small changes with change in temperature [2]. There are some examples of the commercial applications of PDMS as follows: water repellent, dielectric fluid, release agent, antifoam, polishes, lubricants and medical or pharmaceutical use [1]. The properties such as water repellent or gas permeability of PDMS are outstanding. However, as most PDMS are liquid or gum, their mechanical properties are weak and the applications are limited. Therefore, PDMS combining the requested mechanical properties is an ideal solution. To achieve this object, synthesis of PDMS based copolymers is widely reported. For example, Ho *et* al. [3] synthesized poly(dimethylsiloxane-urethane-urea) (PDMS-PUU) segmented block copolymers based on aminopropyl endcapped dimethylsiloxane [$H_2N(CH_2)_3(Si(CH_3)_2O)_nSi(CH_3)_2(CH_2)_3$-$NH_2$], isophorone diisocyanate [5-isocyanato-1-(isocyanatomethyl)-1,3,3-trimethylcyclohexane] and 1,4-benzenedimethanol by a two-step polymerization. The surface properties [4] of various segmented block copolymers had been studied using dynamic contact angle analysis. They proposed that the surfaces reorganize by a mechanism in which the hard block urethane-urea domains migrate through the soft block silicone to the polymer-water interface, and established development of nontoxic, antifouling coatings for use in marine environments. Otherwise, Miyata *et* al. [5] synthesized different kinds of membranes, consisting in ethanol-permselective PDMS and water-permselective poly(methylmethacrylate) (PMMA), using PDMS macro-azoinitiator initiating the addition reaction between vinyl-ester terminated PDMS and MMA in solution. The copolymers were prepared into membranes to investigate the relationship between their microphase separation and their permselectivity for aqueous ethanol solutions during pervaporation. They found that the PMMA-g-PDMS membranes changed from water- to ethanol-permselective at a PDMS content of 35 mol %. Synthesis of such PDMS containing copolymers allows combining both properties of PDMS and thermoplastics. However, due to the cost and complex synthesis steps, the use of polymer blends seems to be the trend of application. As most of the polymer blends, the immiscible problem is obvious between PDMS and most thermoplastics, due to the low surface tension and low viscosity of PDMS. There are two common routes for polymer blends compatibilization, one is adding amphiphilic copolymer working as interfacial agent and it is widely used. As represented by Xu. *et* al. [6], a proportion of PE-b-PDMS diblock copolymer achieving through the esterification reactions between monohydroxy-terminated

poly(dimethylsiloxane) (PDMS-OH) and the corresponding carboxyl terminated polyethylene (PE-COOH) in the presence of tetrabutyl titanate (TBT), was used as a compatibilizer in the blends of high-density polyethylene (HDPE) and silicone oil. The copolymer (1wt%) promoted the dispersion of silicone oil in HDPE from more than 5 μm (silicone oil) to no obvious phase segregation approaching by SEM observation and improved the mechanical properties of HDPE/PDMS blends. The other method of blend compatibilization is reactive blending. It is effective to control morphology and to design new materials without previous compatibilizer synthesis. This method had been used by Zhou *et* al. [7] for the formation of polycarbonate (PC)/PDMS compatibilized blends through the use of hydroxyl-terminated PDMS (PDMS-OH) reacting with PC through twin-screw extrusion at 280 °C. The new formed PC-PDMS copolymer provides a compatibilization effect for the stable sub-micron blend morphology in an otherwise immiscible PC/PDMS blend system. Silicone material was found to be well dispersed in the polycarbonate major phase forming small spherical domains with the domain size of about 0.2-0.9 μm.

Our work was inspired by an earlier study conducted by Bonnet *et* al. [8]. They developed a new and original reactive blending between PDMS and EVA based on EVA carbonyl hydrosilylation by Si-H groups of hydride-terminated PDMS (PDMS-SiH). The occurrence of the hydrosilylation reaction at the EVA/polysiloxane interface promoted a homogenization of the blend. The efficiency of compatibilization depends on the molar ratio SiH/vinyl acetate groups, [SiH]/[VA], and the viscosity ratio of the blend. Two distinct behaviors were observed. The formation of a crosslinking network under shear was obtained for a low viscosity ratio between polysiloxane and EVA (polysiloxane/EVA = $4.0x10^{-6}$) with a high concentration of SiH groups ([SiH]/[VA] =0.5), while the formation of a compatibilized blend was observed for high molar mass polysiloxanes (Mn > 15,000 g mol^{-1}) with a low concentration of SiH ([SiH]/[VA] < $4.0x10^{-3}$). In addition, Igarashi *et* al. [9] found that ruthenium catalyst could be used for hydrosilylation between amide and SiH functional PDMS. Therefore, the aim of our work is expanding the application of ruthenium-catalyzed hydrosilylation to reactive blending containing PDMS. In a previous work, we had confirmed the efficiency of the reaction in PA12/PDMS compatibilization and the morphology of a stable blend with well dispersed PDMS phase in PA12 matrix, especially with the use of

hydride terminated PDMS with a low viscosity (726 g.mol^{-1}, 3x10^{-3} Pa.s). The present work aims at investigating the processability and morphological behavior of PA12/PDMS blends with various PDMS contents. It is also focused on the impact of the PDMS content and PDMS/PA12 interface on the blend properties, such as thermal stability, hydrophobicity, gas permeability and mechanical properties. We tried to investigate the relationship between properties and morphology and find an efficient way to control such properties of the new materials.

III.2 Experimental Part

III.2.1 Materials

PA12 was supplied by Arkema (AESNO TL RILSAN®). The melting point is 170 °C, number average molar mass *Mn* is 26000 g.mol^{-1}, weight average molar mass *Mw* is 47000 g.mol^{-1} and the density is 1.01 g.cm^{-3} at room temperature.

Hydride-terminated polydimethylsiloxane (PDMS-SiH) and triruthenium dodecacarbonyl [$Ru_3(CO)_{12}$] were commercial products from ABCR. Moreover, viscosity ratio of PDMS and PA12 ($\lambda_{PDMS\text{-}SiH/PA12}$) is 3x10^{-7}, molar ratio of functional groups ($\lambda_{PDMS\text{-}SiH/PA12}$) is 6.7x10^{-2}.

III.2.2 Processing of PA12/PDMS-SiH blends

PA12 pellets were dried in vacuum at 80°C for 24 h. Melt reactive processing of PA12 and PDMS-SiH was carried out in a Haake Plasticorder intensive batch mixer equipped with a Rheomix 600 internal mixer. The temperature of the mixer chamber was set at 170 °C and the rotation speed was 50 rpm. The resistant torque and temperature were monitored during whole process. In a typical experiment, dried PA12 was added in the mixer chamber and first mixed for 3 min to melt the polymer until the torque curve reached a plateau. Then, the catalyst and PDMS-SiH mixture with a predetermined composition (Table III.1) was added in the molten PA12 by syringe. Furthermore, non-reactive PA12/PDMS-SiH blend and pure PA12 were prepared with the same processing parameters to work as references.

Samples for mechanical measurement were prepared using a 15 g-capacity DSM micro-extruder (Midi 2000 Heerlen, NL) with co-rotating screws (length/diameter (L/D) ratio=18). PA12 pellets were added in the extruder first, then PDMS-SiH and catalyst mixture was introduced by syringe from the top gap between the screw and chamber surface. The blends were processed at 200 °C for 5 min under a 100 rpm speed and injected in a 10 cm^3 mold at 80 °C to obtain dumbbell-shaped specimens (ISO 527 -Type 5A: dumbbell-shaped, 25x4x2mm^3). In addition, we confirmed by SEM that the processing methods (Haake plasticorder and micro-extruder) have no effect on the morphologies.

Table III.1: Composition of the PA12/PDMS-SiH polymer blends

	Sample	Designation	m(PA12) : m(PDMS-SiH) : m(catalyst)
Internal mixer	PA12-PDMS(10%)-non reactive	PA12 : PDMS-SiH	90 : 10
	PA12-PDMS(10%)-reactive	PA12 : PDMS-SiH : catalyst	90 : 10 : 1
	PA12-PDMS(20%)-reactive	PA12 : PDMS-SiH : catalyst	80 : 20 : 1
Micro-extruder	PA12-PDMS(10%)-non reactive	PA12 : PDMS-SiH	90 : 10
	PA12-PDMS(10%)-reactive	PA12 : PDMS-SiH : catalyst	90 : 10 : 1
	PA12-PDMS(15%)-reactive	PA12 : PDMS-SiH : catalyst	85 : 15 : 1

III.2.3 Methods of characterization

The morphology of the polymer blend was characterized by scanning electron microscopy (SEM), the samples were fractured in liquid nitrogen and sputter coated with gold/palladium. The morphology was analyzed using a QUANTA 250 microscope with an accelerating voltage of 10kV.

Differential Scanning Calorimetry (DSC) measurements were performed on a Q20 (TA instruments) from 30 to 200 °C for PA12 and PA12/PDMS-SiH blends. The samples were kept for 3 min at 200 °C to erase the thermal history before being cooled and then heated at a rate of 10 $Kmin^{-1}$ under Helium flow 40 $ml.min^{-1}$. The crystallinity was calculated using the crystallization enthalpy for a 100% crystalline yield to PA12 of 95 J/g [10, 11].

Thermo gravimetric analysis (TGA) measurements of PA12 and PA12/PDMS-SiH blends were performed on a TA Q500 at a heating rate of 10 $°C.min^{-1}$. The samples were heated from 30 to 700 °C at a rate of 10 $°C.min^{-1}$ under helium flow.

Rheological measurements of the samples were carried out using a Rheometer ARES. The samples were first molded as disk (d=25 mm, h=1mm). The samples were heated at

200 °C for 5 min until equilibrium was reached and the gap between the two plates was adjusted to 1 mm. Then the samples were equilibrated for 2 min before starting the test. Nitrogen gas was used to prevent thermal oxidation of the samples. The linear complex shear modulus ($G^*(\omega)=G'(\omega)+jG''(\omega)$, $j^2=-1$) was measured at 200 °C.

Uniaxial tensile tests of PA12/PDMS-SiH blends were performed in a Shimadzu universal testing machine model AG – 10 KN, speed of 30 mm. min^{-1} until fracture. For calculation of the elasticity modulus, speed of 2 mm. min^{-1} was used, using segment mode between 0.05 and 0.25% of strain (among elastic deformation). The tabulated results are average of at least five measurements.

The water uptake measurements were carried out after 12-day long immersion of test samples (hot pressed film, thickness: around 0.5 mm) in distilled water, at room temperature. It was checked that this immersion time was high enough to reach water sorption equilibrium for all studied samples.

Surface free energy of modified PA12 was determined with the sessile drop method using a Dataphysics Digidrop contact angle meter equipped with a CDD2/3 camera. From contact angle measurements performed with water ($\gamma_l = 72.8$ mN/m, $\gamma_l^d = 21.8$ mN/, $\gamma_l^p = 51$ mN/m) and diiodomethane ($\gamma_l = 50.8$ mN/m, $\gamma_l^d = 48.5$ mN/m, $\gamma_l^p = 2.3$ mN/m) as probe liquids on films with smooth surface. Polar and dispersive components of surface free energy were determined by using Owens – Wendt theory [12]. The tabulated results are average of at least five measurements on different parts of each sample.

Gas permeation experiments were carried out for He, H_2, and CO_2 at 20 °C under an upstream pressure equal to 3 bars. The permeation cell consisted of two compartments separated by the studied membrane. The pressure variations in the downstream compartment were measured as a function of time. The permeability coefficient, *P*, expressed in barrier units was calculated from the slope of the straight line in the steady state.

III.3 Results and discussion

III.3.1 Processability and morphological behavior

Reactive compatibilization of PA12/PDMS-SiH carried out in a Haake plasticorder at 170 °C in molten conditions under shear was evidenced in our previous work. Figure III. 1 illustrated the reaction. It aimed to form N-silylated polyamide and polyamine at the interface to decrease the interfacial tension and increase the interfacial adhesion between the two immiscible polymers, and finally promote the dispersion of PDMS-SiH into the PA12 matrix.

Figure III.1 also presents the variation of torque during polymer blending. It is clear that after the introduction of PDMS-SiH to molten PA12, the torque value decreased due to the PDMS-SiH lubrication. Then it increased to around 17 N.m for both in non-reactive and reactive system. As reported by Scott *et* al. [13], the mixing torque variation was primarily due to the change in blend rheology caused by a morphological transformation in such blend (from SEM, Figure III.2a, PDMS-SiH domains were with a diameter around 3 μm dispersed in PA12). This means the occurrence of mixing in such immiscible blend due to the lower molar mass (726 $g.mol^{-1}$) of PDMS-SiH leading to a better dispersion [14]. However, the torque value of PA12/PDMS-SiH reactive blend did not reach a steady plateau as for the non-reactive one but increased rapidly again from 17 to 53 N.m before decreasing again. The torque variation corresponds to the variation of the apparent viscosity of the bulk material and consequently to some relevant microstructure development [8, 13]. Comparing the morphology (Figure III.2), it is clear that in presence of catalyst, new formed copolymers such as N-silylated polyamide and N-silylated polyamine act as compatibilizer. The mixing became effective and the morphology changed drastically until the torque reached a plateau. Then the torque decreased and finally compatibilized blend with a decrease of the PDMS-SiH domain size (around 0.8 μm) and narrow domain size distribution of PDMS-SiH in PA12 matrix is obtained.

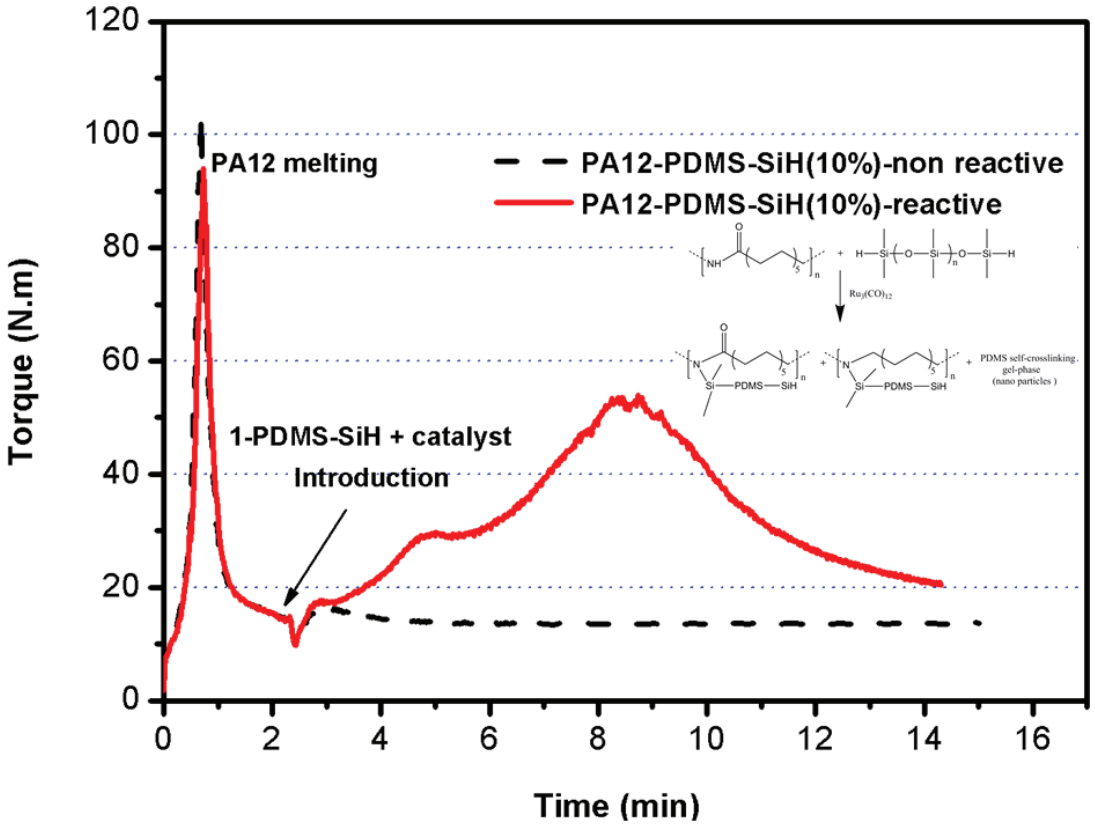

Figure III.1 Scheme of reaction between PA12 and PDMS-SiH and variation of the mixing torque between PA12 and PDMS-SiH (10 wt%) under shear in the internal mixer at 170 °C: reactive blending (solid line) and non-reactive blend (dotted line).

As PDMS has a lot of unique properties, theoretically the more PDMS is introduced the more modification of organic polymer will be obvious as shown by Liddell *et* al. [15], who found that the organically modified silicates take on a more flexible nature as the PDMS concentration was increased. In our processing conditions, it was possible to increase PDMS-SiH content up to 20 wt%, but with a specific recipe. As mentioned before, the PDMS-SiH acting as a lubricant, the shear rate was located in the PDMS-SiH fluid which coated the wall of mixing chamber. When the concentration is not high, due to the nature of PDMS-SiH, effective mixing can be carried out. However, along with the PDMS-SiH amount increasing, lubrication is more pronounced and there is only a part of PDMS which can be mixed into molten PA12. Even though the reaction is efficient, the formed compatibilizers were not in high concentration enough to promote the dispersion of whole PDMS as reported in some literatures [16]. Thus the whole addition of PDMS-SiH which resulted in a poor mixing and total phase separation (the PDMS-SiH gathered on the blend oily surface). To solve the problem, first we added 10 wt% PDMS-SiH and catalyst mixture in the molten

PA12. In such conditions efficient reactive blending was observed. When the torque tended to reach a steady plateau, another 10 wt% of pure PDMS-SiH (without catalyst) was introduced. The morphology of PA12/PDMS-SiH (20%)-reactive blend (Figure III.2c) proved the efficient blending, PDMS-SiH domains dispersed in the matrix with a diameter around 1 μm and the size distribution was narrow. In addition through simply comparing 10 and 20 wt% PDMS based blends morphology, we found a higher concentration of PDMS-SiH phase in the one with 20 wt% PDMS-SiH (Figure III.2c). It should be mentioned that the sample is not oily like the one with poor mixing and it is an efficient way to increase PDMS-SiH content by introducing it step by step.

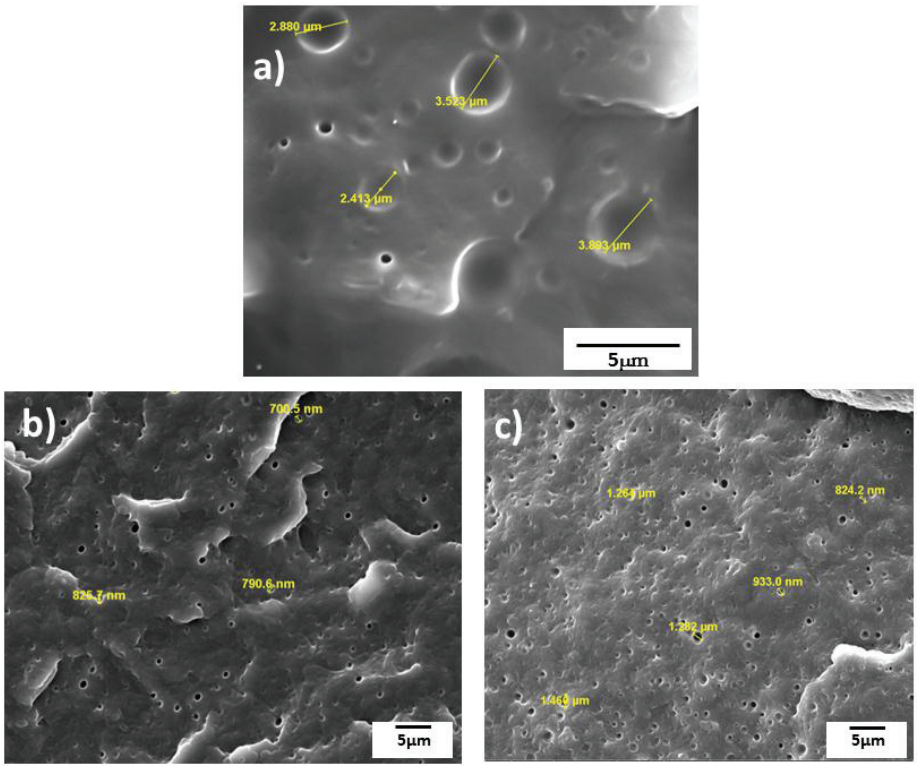

Figure III.2: Representative SEM morphology: a), PA12/PDMS-SiH (10%)-Non reactive, b) PA12/PDMS-SiH (10%)-Reactive, c) PA12/PDMS-SiH (20%)-Reactive.

The study of torque variation and morphology confirmed the reactive compatibilization between PA12 and PDMS-SiH catalyzed by ruthenium catalyst. The *in situ* formed copolymers worked at the interface promoted the dispersion of PDMS-SiH in PA12 matrix. We obtained PA12/PDMS-SiH blends with a reduction of domains size and a narrow size distribution of PDMS phase. Specifically, the PDMS domain sizes of reactive blends with 10 wt % and 20 wt % contents decreased to 0.8 μm and 1 μm, respectively. In general, the compatibility between the polymer phases decides the properties of the polymer blend [17,

18]. So rheological, thermal, mechanical and gas permeability properties were investigated to understand the morphology-property relationship of such PA12/PDMS-SiH blend.

III.3.2 Rheological behavior

The rheological behavior of two-phase polymer blends is affected by the flow-induced changes in morphology. Compatibilizer leads to smaller domain size and narrower size distribution of the dispersed phase. In physical compatibilized blends (compatibilization through adding premade copolymers), the rheological properties are influenced by the amount, molar mass and the architecture of the added copolymers [19]. Some researchers [20] proved that the conclusion about rheological properties obtained on physically compatibilized blends are also valid in such reactive compatibilization method.

Figure III.3a and Figure III.3b shown typical behavior of the dynamic modulus for the matrix and the compatibilized blends. Results show that the two modulus increase at low frequency, the storage increased more rapidly than the loss one. The addition of PDMS-SiH in PA12 matrix significantly affected the frequency dependence of G' and G'' especially for compatibilized PA12/ PDMS-SiH blend with the highest concentration (20 wt%). This means that the blends have additional relaxation process [21, 22] and stronger ability to resist to the shear that is absent in the pure PA12. As reported in the literatures, this additional relaxation could be attributed to the shape-relaxation of drops [23, 24] and to the interfacial viscoelasticity of compatibilizer [25, 26] in the blend. But in this case only the shape relaxation cannot explain this viscoelastic behavior (see also shear thinning behavior and yield stress behaviors at low frequency in Figure III.3c). Actually, this behavior is attributed to the blend morphology at the nanoscale (Figure III.3d), to be more exact, nano structure of PDMS (gel particles around 20-30 nm) formed through oxidation reaction. Finally as shown previously, during the polymer blending, there were two kinds of modification. One is reactive compatibilization between PA12 and PDMS, in situ formed N-silylated copolymer promoted the dispersion of PDMS in PA12 matrix. Another is the evolution of a part of PDMS changed from liquid to gel-like nano particles since self-crosslink

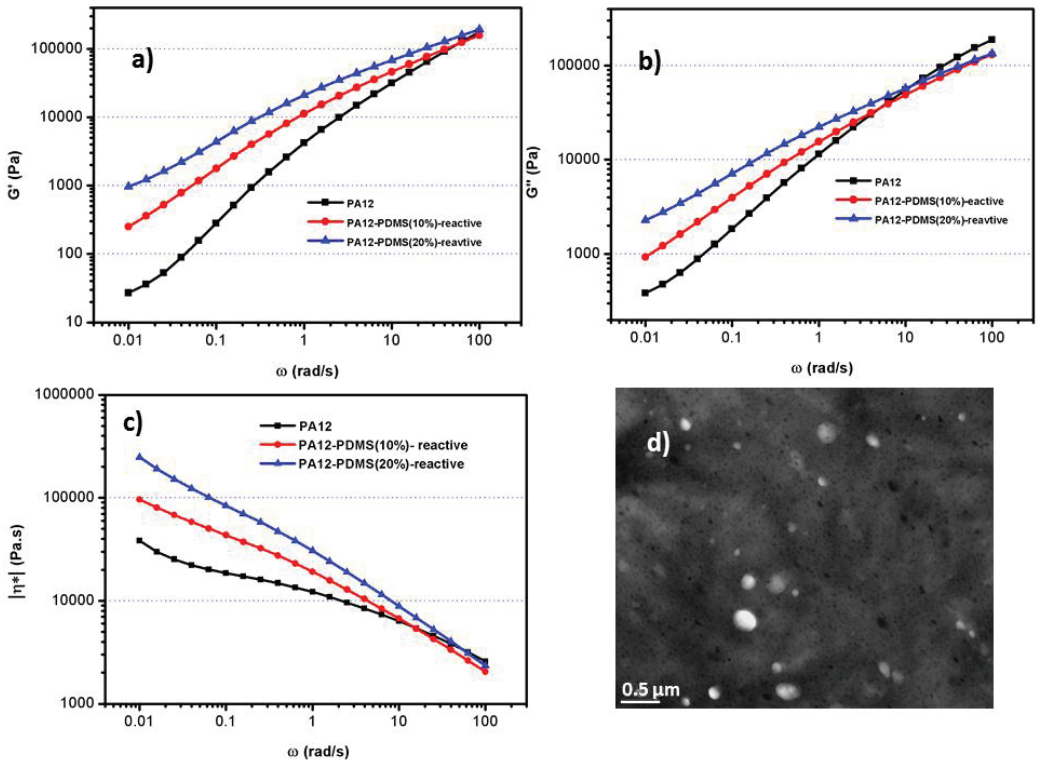

Figure III.3: Rheological behaviors as a function of frequency for PA12, PA12-PDMS (10%) and PA12-PDMS (20%) reactive blends: a) variation of storage modulus, b) variation of loss modulus, c) complex viscosity and d) TEM morphology of PA12-PDMS (10%) reactive blend.

III.3.3 Thermal properties: TGA and DSC

Blending polymers has been reported to have much influence on the degradation and thermal properties, and compatibility plays an important role in the degradation and thermal behavior of the blends [27, 28]. The comparison of thermal stability among PA12, PA12/PDMS-SH non-reactive and reactive was shown in Figure III.4. The initial degradation temperature shifted toward higher temperature for the reactive blend catalyzed by $Ru_3(CO)_{12}$, blend catalyzed by $Ru_3(CO)_{12}$ in comparison with the non-catalyzed blend, which indicated that compatibilized blend was relatively more stable than the non-reactive one. More precisely, the weight loss at around 419 °C for non-reactive blend coming from the degradation of PDMS phase was no more observed for the reactive blend. This indicated the improvement of PDMS phase stability in the blend, because the formed PA12-PDMS copolymer by hydrosilylation reaction enhanced the interaction between phases. Furthermore, as described before, a part of PDMS-SiH changed to gel-like nano particles due to oxidation reaction in the presence of ruthenium catalyst also leading to enhance the thermal stability. Our results are in

agreement with observations of other researchers such as Giri *et* al. [27]. They found that the initial degradation temperature improved with the increase of in situ formed ethylene-methylacrylate (EMA)-g-PDMS copolymers concentration until reaching a maximum value. Such increase was also founded in PA12/PDMS-SiH (20%) reactive blend, confirming that compatibilization also promoted the thermal stability even when the PDMS content increased.

The residues of PA12/PDMS-SiH reactive blends at 700 °C are also more important than the ones for pure PA12 and PA12/PDMS-SiH non-reactive blend. As shown in Figure III.4 the residue at 700 °C increased from 0.29% to 0.65% for PA12/PDMS-SiH (10 wt%) reactive blend and kept increasing with the increase of PDMS content (0.82% for the one containing 20 wt% PDMS). Satyanarayana *et* al. [29] proved that in the presence of rhodium catalyst, PDMS formed crosslinking network which exhibited both higher thermal stability and residue. In their system, residue of PDMS/catalyst shifted from 67.7% to 95.1% depending on the kinds of catalyst. In our case, as there is also a part of PDMS formed crosslinking network (nano particles) by oxidation reaction in the presence of $Ru_3(CO)_{12}$, the residue increased after reaction.

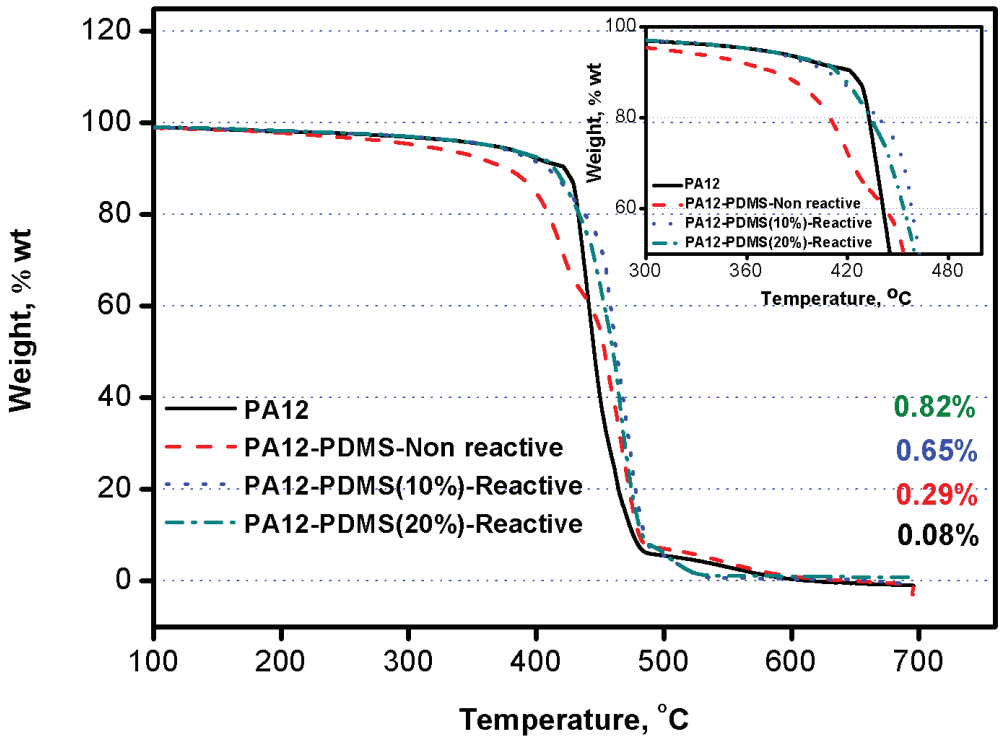

Figure III.4: TGA curves of pure PA12, PA12/PDMS-SiH non-reactive and reactive blends under helium atmosphere.

The effect of PDMS introduction and compatibilization on the melting and crystalline properties of PA12/PDMS-SiH blends can be evaluated from the DSC heating and cooling curves given in Figure III.5, respectively. It is seen that the introduction of PDMS does not affect the main melting temperature, but decreased the formation of PA12 γ crystalline structure which has a lower melting temperature than α crystalline one [30], especially when PDMS concentration increased to 20 wt% (almost no melting peak of γ crystal). However, after the introduction of PDMS, crystalline temperature shifted from 145 °C to 150 °C meaning that it promoted the formation of α crystalline. However, in general compatibilization and introduction of PDMS-SiH have no notable influence on the X_c of the PA12 matrix may due to that PDMS promoted the formation of α crystalline but inhibit the formation of γ crystal. The DSC results implied that the PDMS has no significant influence on PA12 crystalline behaviors.

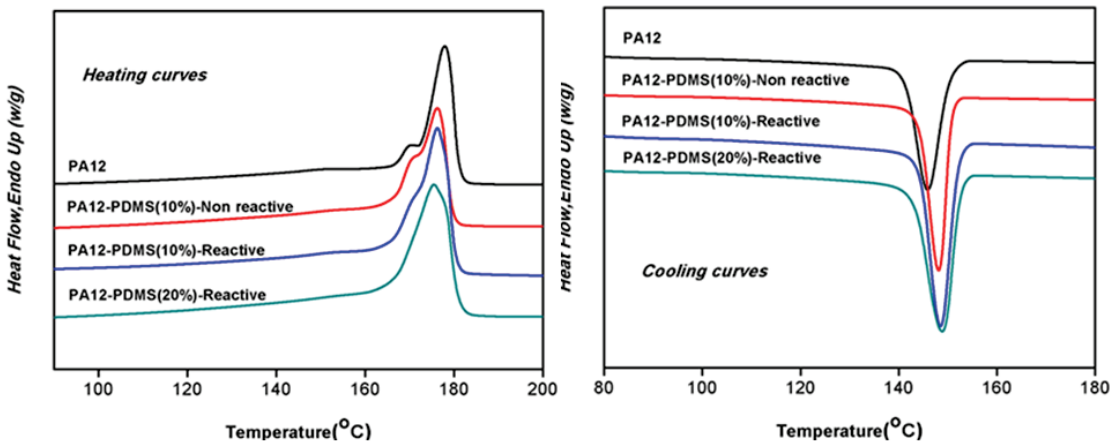

Figure III.5: DSC thermo grams of pure PA12, PA12/PDMS-SiH non-reactive and reactive blends: cooling curves (left) and heating curves (right).

Table III.2 : Crystalline properties of pure PA12, PA12/PDMS-SiH non-reactive and reactive blends.

Crystallization	PA12-Pure	PA12-PDMS(10%)-Non reactive	PA12-PDMS(10%)-Reactive	PA12-PDMS(20%)-Reactive
*T*m (°C)	177	176	176	175
*T*c (°C)	145	148	151	150
*T*onset (°C)	153	152	157	156
*T*endset (°C)	138	142	145	143
Δ*H*m (J.g^{-1})	57.6	49.8	52.7	44.2
*X*c (%)	61	58	61	58

$$X_c = \Delta H_m/(\omega_c \cdot \Delta H_m^o) \quad \Delta H_m^o = 95\ J.g^{-1}$$

As a consequence, the *in situ* formed compatibilizer stabilized the dispersion of PDMS in PA12 matrix, enhanced the interface between the two phases. Therefore, such compatibilized PA12/PDMS blends performed higher thermal stability comparing with pure PA12 but almost no change of crystalline degree is observed.

III.3.4 Water uptake and surface free energy

PDMS exhibits hydrophobic behavior and poor wettability. The introduction of PDMS can modify the hydrophilic character of PA12. Such modification was first proved by water uptake measurement. As shown in Table III.3, there is a relationship between water uptake and PDMS content, specifically, the water uptake decreased with increasing PDMS proportion in PA12/PDMS blend. Through comparing with pure PA12, it decreased from 1.23% to 1.11% [PA12-PDMS(10%)-reactive blend] and 0.92% [PA12-PDMS(20%)-reactive blend], respectively. Such decrease of water uptake in PA12-PDMS blend is due to the hydrophobicity of PDMS.

Table III.3: Relative water uptake for PA12 and PA12/PDMS compatibilized blends at room temperature.

Time (Day)	PA12-pure (wt%)	PA12-PDMS(10%)-Reactive (wt%)	PA12-PDMS(20%)-Reactive (wt%)
1	0.53	0.38	0.35
2	0.61	0.53	0.49
4	0.87	0.83	0.75
6	1.06	0.98	0.87
8	1.14	1.09	0.87
10	1.22	1.11	0.90
12	1.23	1.11	0.92

The surface free energy of PA12/PDMS compatibilized blends were calculated by Owens – Wendt theory [12] based on contact angle results with water and diiodomethane. PA12 and PA12/PDMS compatibilized blends show different wettability depending on the different polarity of the two solvents. The static water and diiodomethane contact angle measurement results are shown in Figure III.8 and Figure III.9, respectively. For pure PA12, the water contact angle (CA) is around 80±4.5^{o} thus less than 90^{o} , this last CA value being often considered to determine the limit between wettability and non-wettability [31]. The PA12/PDMS compatibilized blends are both hydrophobic since the corresponding water CA are both larger than 90^{o} and improved from 100±2.1^{o} to 106±1.8^{o} with PDMS content increasing from 10wt% to 20wt%. For diiodomethane an increase of CA is also observed as PDMS is introduced in the PA12 matrix. Specifically, the diiodomethane CA increased from 45±2.2^{o} for pure PA12 to 63±1.3^{o} and 68±1.5^{o} for compatibilized PDMS phase 10wt% and 20wt%, respectively. It has to be noted that the measurement of non-reactive blend was not carried out since its surface appears oily causing by PDMS migration. Similar result was achieved by Zhang *et* al. [32], they found a phenoxy base polymer which is hydrophilic (water CA 74^{o}) changed to hydrophobic with a water CA 94^{o} after the introduction of 1.7 wt%

PDMS copolymer. They proved that the change of surface property is due to the surface enrichment of the low surface energy component such as PDMS in order to minimize the overall surface free energy of the binary macromolecular system.

There are several methods to estimate the solid surface free energy through contact angles, [33-35]. In this work, we used the Owens – Wendt theory which is the most general one which was used to determine the surface free energy. The surface free energy at room temperature was derived as follows: pure PA12 38.0 mN/m [36], PA12/PDMS (10 wt%)-reactive blend 26.9 mN/m and PA12/PDMS (20 wt%)-reactive blend 24.5 mN/m. Besides, there are also decreases of both dispersion force (γ_s^d) and polar force (γ_s^p). γ_s^d decreased from 33 mN/m to 26.1 mN/m (with 10 wt% PDMS) and to 24.3 mN/m (with 20 wt% PDMS). γ_s^p decreased from 5 mN/m of pure PA12 to 0.8 mN/m (10 wt%) and to 0.2 mN/m (20 wt%), respectively. It is clear that, the introduction of PDMS significantly decreased the surface free energy of PA12. These results further supported the above discussion of wettability of such materials.

The achievement of hydrophobicity due to PDMS introduction was also published in a lot of literatures. For instance, Chen *et* al. [37] prepared UV-curable PDMS-containing polyurethane (PU) oligomer (UV-PDMS-PU) where such UV-PDMS-PU system consisted in 1% (w/w) photo-initiator was coated either on PET or Nylon textile surface and then cured by UV-radiation. They found the washing stability was improved since the water CA is around 130^o. They also mentioned that the observed higher contact angles were probably due to the micro-phase separation of PDMS moiety in different polymers matrix. This mechanism is also suitable for our PA12/PDMS compatibilized blends, since SEM results confirmed the micro-morphology of the samples that both of them show a well dispersed PDMS in PA12 matrix with a diameter around 0.8 μm to 1 μm. This micro-structure provides hydrophobicity to PA12/PDMS blend and such property increased with increasing of PDMS content.

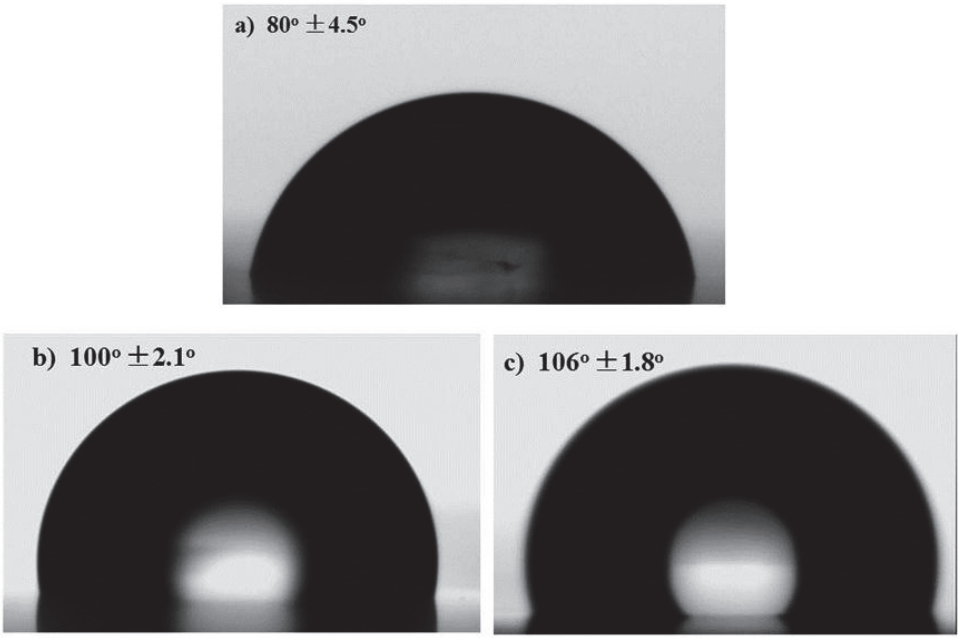

Figure III.6: Water contact angle of pressed films: a) pure PA12, b) PA12-PDMS10%-reactive, c) PA12-PDMS20%-reactive.

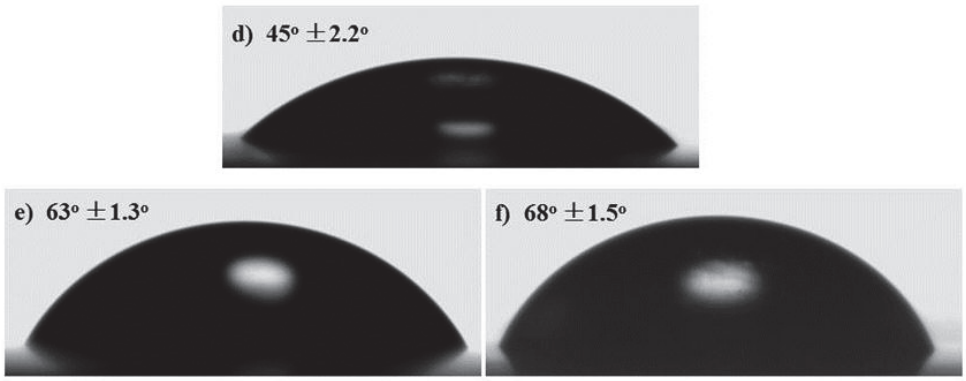

Figure III.7: Diiodomethane contact angle of pressed films: d) pure PA12, e) PA12-PDMS10%-reactive, f) PA12-PDMS20%-reactive.

Table III.4: Surface properties of PA12 and PA12/PDMS blends after compatibilization.

	θ_{water}(°)	$\theta_{diiodomethane}$(°)	γ_S (mN/m)	γ_S^d (mN/m)	γ_S^p (mN/m)
PA12-pure	80±4.5	45±2.2	38.0±1.3	33.0±0.1	5.0±1.2
PA12-PDMS(10%)-reactiv	100±2.1	63±1.3	26.9±0.5	26.1±0.3	0.8±0.2
PA12-PDMS(20%)-reactiv	106±1.8	68±1.5	24.5±0.4	24.3±0.5	0.2±0.1

III.3.5 Gas permeability

PDMS as mentioned in the introduction is a polymer well known to have the highest gas permeability and diffusivity among all of the polymers manufactured on an industrial scale

[38, 39]. Therefore, an increase of gas permeability is expected for the PA12 based materials with introduction of PDMS. The evolution of CO_2 permeability coefficients as a function of the blend composition is presented in Figure III.8. As expected, the permeability increased as the PDMS content increased. However, significant differences were observed between the reactive and non-reactive PA12-PDMS blends. Higher permeability values were obtained for the reactive system. To discuss more deeply the impact of the type of blends (non-compatibilized vs compatibilized) on the gas transport properties, we also indicated the permeability values calculated from Maxwell law in the Figure III.8.

The Maxwell model developed in 1954 [40, 41], originally used for electrical conductivity of particulate composites, can be adapted to gas permeability of mixed materials membranes as equation 1:

$$\frac{P}{P_m} = \frac{1 + 2\emptyset(\lambda_d - 1)/(\lambda_d + 2)}{1 - \emptyset(\lambda_d - 1)/(\lambda_d + 2)} \quad (1)$$

Where P is the effective permeability of the blend, P_m is the permeability of the continuous phase (PA12 matrix), ϕ is the volume fraction of the dispersed phase, known as loading. λ_d is the permeability ratio P_d/P_m where P_d is the permeability of the dispersed phase (PDMS).

The permeability coefficient values determined on both systems (reactive and non-reactive blends) were lying below the theoretical curve.

Maxwell law was developed for ideal binary systems, meaning that it neither takes into account an eventual modification of the matrix due to the presence of the dispersed phase nor potential interfacial effects. [42]. The former factor can be important especially for semi-crystalline polymer. Actually, the polymer crystalline regions are considered to be impermeable to small molecules such as gases and thus change in crystallinity degree can lead to a modification of the final permeability. However, in our case through the DSC analysis we found no notable changes in PA12 crystallinity after the introduction of PDMS. The PA12 matrix still maintained its individual property and kept the crystalline degree around 60%.

For the reactive PDMS-SiH/PA12 system, *in situ* compatibilization took place leading to the coexistence of micrometer and nanometer sized PDMS rich domains dispersed within the PA12 matrix. One could expect a high gas diffusion rate in such materials due to the formation of more interconnected permeable phases. However, it was shown that PA12/PDMS interfacial interactions were reinforced in these systems. Moreover, the presence of crosslinked PDMS rich nanoparticles was also evidenced. These last phenomena have a

detrimental effect on gas diffusion and could explain the slightly lower values of permeability obtained with respect to the theoretical ones. For PA12/PDMS non-reactive blend, P_{CO_2} is 1.3 barrer. This value is lower than the one of the reactive PA12/PDMS with the same composition (1.6 barrer) and lower than the theortical value (1.75 barrer).This is due to that without compatibilization, PDMS is easy to leach out and enrich on the blend surface driving by the significant difference between PA12 and PDMS. Therefore, there are only a part of PDMS actually dispersed in PA12.

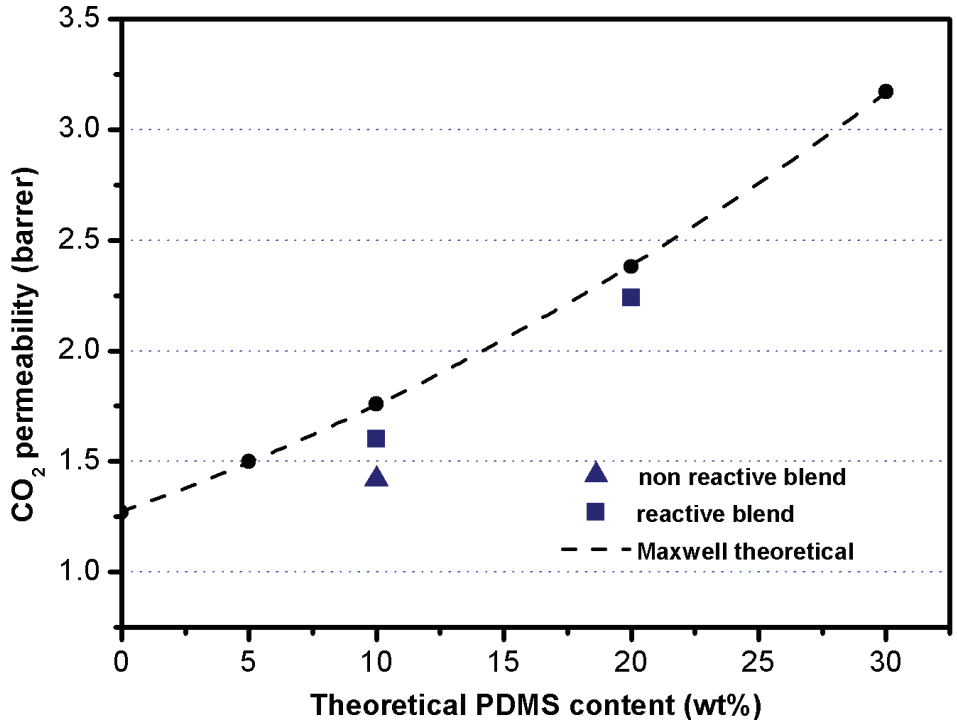

Figure III.8: Evolution of the CO_2 permeability coefficient as a function of PDMS content in PA12/PDMS blends. (▲) is representative of P_{CO_2} of PA12/PDMS(10%)-non reactive blend, (■)is representative of P_{CO_2} of PA12/PDMS- reactive blend. The dotted line is Maxwell theoretical value tendency of P_{CO_2}.

The gas transport study was enlarged to H_2 and He for the reactive PA12/PDMS blend and the relative permeability (the permeability of the blend ratioed to the permeability of the neat PA12) was reported for each gas and each blend composition in Figure III.9. The relative permeability of H_2 and He are very close to each other, since these two gases have similar kinetic diameters of 2.34 and 2.65 Å [42], respectively. Furthermore, all gas permeability increased as a function of PDMS content. However, the CO_2 relative permeability values are always higher than those measured for He and H_2. This result can be assigned to the high solubility (S) of CO_2 in PDMS resulting in a higher P, as in a fickian transport mechanism.

$$P=SD \qquad (2)$$

with D the diffusion coefficient. According to the literature[43, 44], a penetrant's relative permeability in PDMS can be largely determined by its relative solubility. Specifically, the

solubility of CO_2 in PDMS is much higher than the one of H_2 [1.29 and 0.05 cm^3 (STP)/cm^3 atm, respectively]. Different gas permeability coefficients of CO_2, He and H_2 provides a potential application as gas selectivities for PA12/PDMS blends.

In general, the introduction of PDMS phase to PA12 with a well and stable dispersion can significantly modify the gas permeability of PA12. We confirm the improvement of gas permeability with increase of PDMS content. Therefore, PA12/PDMS compatibilized blend through hydrosilylation provide a new route for polyamide achieving better gas permeability and gas selectivity.

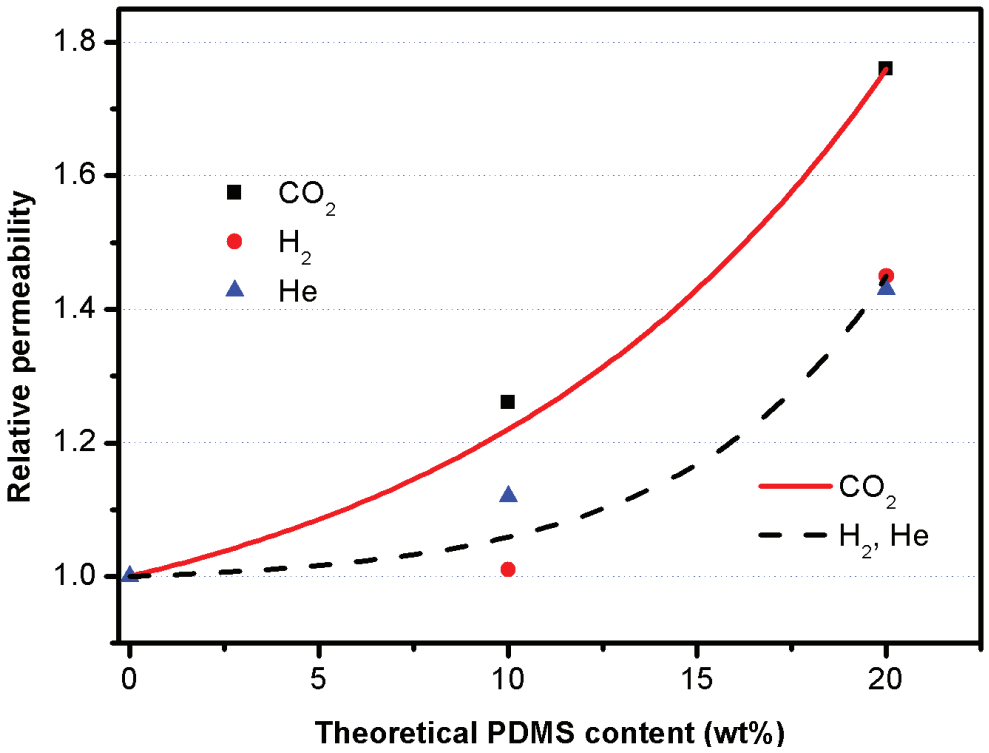

Figure III.9: Evolution of the relative permeability (CO_2, He, H_2) of the PA12/PDMS compatibilized blend as a function of PDMS content.

The mechanical properties of pure PA12, PA12/PDMS-non reactive and PA12/PDMS-reactive with different PDMS contents were carefully analyzed and shown in Figure III.10 and Table III.5 (10 wt% and 15 wt%). Firstly, the Young's modulus, elongation at break and tensile stress decreased (50% elongation at break, 21% tensile stress and 6% Young's modulus decrease) as PDMS was introduced without compatibilization comparing with pure PA12. As no change in the crystalline behavior of PA12 matrix, it is obvious that the decrease of mechanical properties is most due to a weak interfacial adhesion between PDMS and PA12. This had been proved by a lot of researches such as Prakashan *et* al. [45] who found that PP/PDMS blend in absence of compatibilizer was easy to cause debonding at

the elastomer-matrix interface. On the contrary, PA12/PDMS blend after compatibilization shows higher Young's modulus (890 MPa) than pure PA12 (750 MPa) and PA12/PDMS non-reactive blend (700 MPa). The yield stress almost kept the same before and after introduction of PDMS. The increase of Young's modulus is related to the *in situ* formed copolymers promoting the compatibilization and enhancing the interfacial adhesion. In addition, a part of PDMS changed from liquid to gel through oxidation reaction in the presence of $Ru_3(CO)_{12}$ forming a second nano size gel based dispersion which also promoted the mechanical properties comparing with non-reactive blend. The decrease of elongation at break after introduction of PDMS especially for non-reactive blend is due to the defects causing by the significant difference of viscosity between PA12 and PDMS.

Through increasing the PDMS content in PA12/PDMS compatibilized blend, the mechanical properties decreased slightly (5% for the Young's modulus and 7% for both the elongation at break and tensile stress) compared with PA12/PDMS (10 wt%)-reactive blend. This decreased had been discussed in some publications as Bremner *et* al. [46] who found that polyurethanes/PDMS blend existed an optimal level of PDMS concentration around 1.5-2%, lead to an enhancement of the mechanical properties. Over this concentration, phase separation of PDMS became significant leading to a decrease of the mechanical properties. It can be used to explain the decrease of mechanical properties of PA12/PDMS (15wt%)-reactive blend in our system, because the size of PDMS domain increased with PDMS content increase which had been confirmed by SEM study.

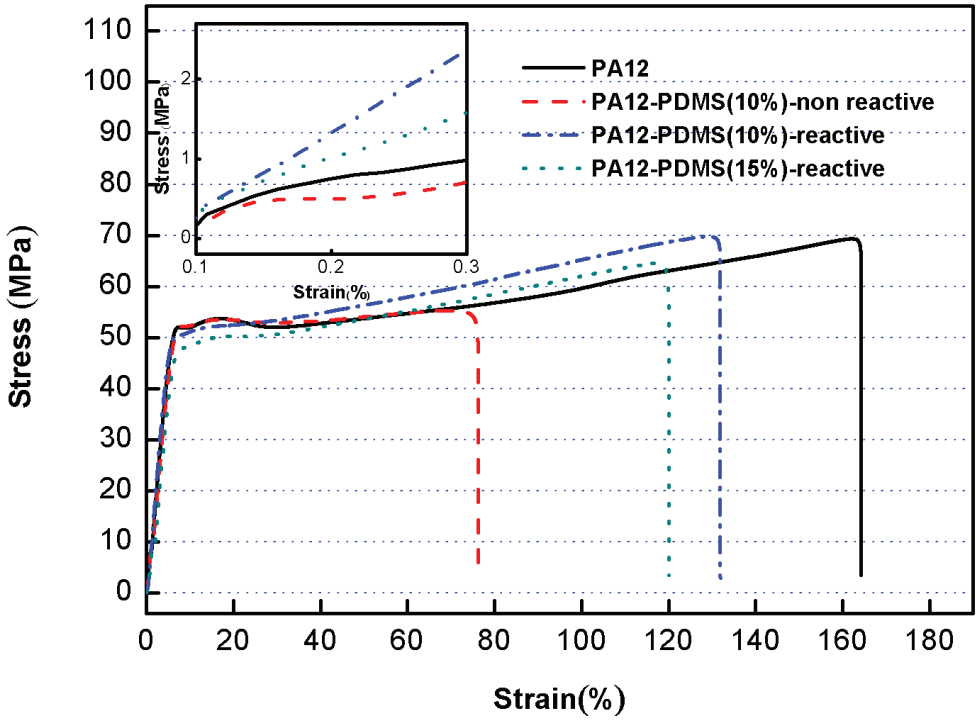

Figure III.10: Stress-strain curve of PA12 and PA12-PDMS blends and zoom of elastic deformation.

Table III. 5: Mechanical properties of PA12 and PA12-PDMS blends.

Sample name	Young's modulus (MPa)	Yield stress (MPa)	Elongation at break (%)	Tensil stress (Mpa)
PA12	750±14	52±0.3	160±4	70±0.6
PA12-PDMS(10%)-non reactive	700±25	53±1.4	80±10	55±1.1
PA12-PDMS(10%)-reactive	890±20	51±0.8	130±10	70±1.1
PA12-PDMS(15%)-reactive	850±21	50±1.1	120±9	65±1.3

III.4 Conclusion

The ruthenium-catalyzed hydrosilylation can be used to compatibilize the PA12 and PDMS-SiH blend, promoted the PDMS dispersion in PA12 matrix and increased the interfacial adhesion of the two immiscible phases comparing with non-reactive blend. PDMS domains' size decreased from 3 µm to 0.8 µm (10 wt% PDMS) and 1 µm (20 wt% PDMS) and finally we achieved a stable PA12/PDMS blend. Through characterization, we found the compatibilized PA12/PDMS blend has a better hydrophobicity with a water contact angle over 100^{o} and a better gas permeability comparing with pure PA12 due to the introduction of PDMS phase. In addition, the thermal stability of PA12/PDMS blends was enhanced after compatibilization with a similar initial degradation temperature as PA12 but an increase of solid residue due to the formation of N-silylated copolymers and PDMS self-crosslinking. The introduction of PDMS does not have significant effect of crystalline degree of PA12

since either pure PA12 or PA12/PDMS has a crystalline degree around 60%. Besides, the mechanical properties were enhanced with 13 % increase of Young's modulus after *in situ* compatibilization with 15 wt% PDMS-SiH.

III.5 References

[1] S.J. Clarson, J.A. Semlyen, Siloxane polymers, Prentice Hall1993.

[2] D. Scott, J. Messerly, S. Todd, G. Guthrie, I. Hossenlopp, R. Moore, A. Osborn, W. Berg, J. McCullough, Hexamethyldisiloxan: chemical thermodynamic properties and internal rotation about the siloxane linkage1, The Journal of Physical Chemistry 65(8) (1961) 1320-1326.

[3] T. Ho, K.J. Wynne, R.A. Nissan, Polydimethylsiloxane-urea-urethane copolymers with 1, 4-benzenedimethanol as chain extender, Macromolecules 26(25) (1993) 7029-7036.

[4] J.K. Pike, T. Ho, K.J. Wynne, Water-induced surface rearrangements of poly (dimethylsiloxane-urea-urethane) segmented block copolymers, Chemistry of materials 8(4) (1996) 856-860.

[5] T. Uragami, E. Fukuyama, T. Miyata, Selective removal of dilute benzene from water by poly (methyl methacrylate)-graft-poly (dimethylsiloxane) membranes containing hydrophobic ionic liquid by pervaporation, Journal of Membrane Science 510 (2016) 131-140.

[6] Z. Xu, S. Jie, B.G. Li, Well‐defined PE‐b‐PDMS diblock copolymers via the combination of thiol‐ene click and esterification reactions: Facile synthesis and compatibilization for HDPE/silicone oil blends, Journal of Polymer Science Part A: Polymer Chemistry 52(22) (2014) 3205-3212.

[7] W. Zhou, J. Osby, Siloxane modification of polycarbonate for superior flow and impact toughness, Polymer 51(9) (2010) 1990-1999.

[8] J. Bonnet, V. Bounor-Legaré, P. Alcouffe, P. Cassagnau, EVA reactive blending with Si–H terminated polysiloxane by carbonyl hydrosilylation reaction: From compatibilised blends to crosslinking networks, Materials Chemistry and Physics 136(2) (2012) 954-962.

[9] Y. Motoyama, K. Mitsui, T. Ishida, H. Nagashima, Self-encapsulation of homogeneous catalyst species into polymer gel leading to a facile and efficient separation system of amine products in the Ru-catalyzed reduction of carboxamides with polymethylhydrosiloxane (PMHS), Journal of the American Chemical Society 127(38) (2005) 13150-13151.

[10] E.S. Ogunniran, R. Sadiku, S. Sinha Ray, N. Luruli, Morphology and thermal properties of compatibilized PA12/PP blends with boehmite alumina nanofiller inclusions, Macromolecular Materials and Engineering 297(7) (2012) 627-638.

[11] S. Jose, S. Thomas, P. Biju, P. Koshy, J. Karger-Kocsis, Thermal degradation and crystallisation studies of reactively compatibilised polymer blends, Polymer Degradation and Stability 93(6) (2008) 1176-1187.

[12] D.K. Owens, R.C. Wendt, Estimation of the surface free energy of polymers, Journal of applied polymer science 13(8) (1969) 1741-1747.

[13] C.E. Scott, C.W. Macosko, Morphology development during reactive and non-reactive blending of an ethylene-propylene rubber with two thermoplastic matrices, Polymer 35(25) (1994) 5422-5433.

[14] Z.-y. Zhao, W.-w. Yao, R.-n. Du, Q. Zhang, Q. Fu, Z.-h. Qiu, S.-l. Yuan, Effect of molecular weight of PDMS on morphology and mechanical properties of PP/PDMS blends, Chinese Journal of Polymer Science 27(01) (2009) 137-143.

[15] HG. Liddell, R. Scott, HS. Jones, Mackenzie 1996.

[16] C. DeLeo, K. Walsh, S. Velankar, Effect of compatibilizer concentration and weight fraction on model immiscible blends with interfacial crosslinking, Journal of Rheology 55(4) (2011) 713.

[17] S.M. George, D. Puglia, J.M. Kenny, V. Causin, J. Parameswaranpillai, S. Thomas, Morphological and Mechanical Characterization of Nanostructured Thermosets from Epoxy and Styrene-block-Butadiene-block-Styrene Triblock Copolymer, Industrial & Engineering Chemistry Research 52(26) (2013) 9121-9129.

[18] R. Jiang, R.P. Quirk, J.L. White, K. Min, Polycarbonate‐polystyrene block copolymers and their application as compatibilzing agents in polymer blends, Polymer Engineering & Science 31(21) (1991) 1545-1548.
[19] J.D. Martin, S.S. Velankar, Effects of compatibilizer on immiscible polymer blends near phase inversion, Journal of Rheology (1978-present) 51(4) (2007) 669-692.
[20] Y. Huo, G. Groeninckx, P. Moldenaers, Rheology and morphology of polystyrene/polypropylene blends with in situ compatibilization, Rheologica acta 46(4) (2007) 507-520.
[21] M. Moan, J. Huitric, P. Mederic, J. Jarrin, Rheological properties and reactive compatibilization of immiscible polymer blends, Journal of Rheology (1978-present) 44(6) (2000) 1227-1245.
[22] C.L. DeLeo, S.S. Velankar, Morphology and rheology of compatibilized polymer blends: Diblock compatibilizers vs crosslinked reactive compatibilizers, Journal of Rheology (1978-present) 52(6) (2008) 1385-1404.
[23] J. Oldroyd, The elastic and viscous properties of emulsions and suspensions, Proceedings of the Royal Society of London A: Mathematical, Physical and Engineering Sciences, The Royal Society, 1953, pp. 122-132.
[24] J. Palierne, Linear rheology of viscoelastic emulsions with interfacial tension, Rheologica acta 29(3) (1990) 204-214.
[25] J. Oldroyd, The effect of interfacial stabilizing films on the elastic and viscous properties of emulsions, Proceedings of the Royal Society of London A: Mathematical, Physical and Engineering Sciences, The Royal Society, 1955, pp. 567-577.
[26] R.-E. Riemann, H.-J. Cantow, C. Friedrich, Interpretation of a new interface-governed relaxation process in compatibilized polymer blends, Macromolecules 30(18) (1997) 5476-5484.
[27] R. Giri, K. Naskar, G.B. Nando, In-situ compatibilization of linear low-density polyethylene and Polydimethyl siloxane rubber through reactive blending, Materials Express 2(1) (2012) 37-50.
[28] Z. Guo, Z. Fang, L. Tong, Z. Xu, Degradation and thermal properties of in situ compatibilized PS/POE blends, Polymer Degradation and Stability 92(4) (2007) 545-551.
[29] N. Satyanarayana, H. Alper, Rhodium-catalyzed modification of poly (methylhydrosiloxane) into a highly cross-linked polysiloxane, Macromolecules 28(1) (1995) 281-283.
[30] Y. Zhang, J. Yang, T. Ellis, J. Shi, Crystal structures and their effects on the properties of polyamide 12/clay and polyamide 6–polyamide 66/clay nanocomposites, Journal of applied polymer science 100(6) (2006) 4782-4794.
[31] Y. Ma, X. Cao, X. Feng, Y. Ma, H. Zou, Fabrication of super-hydrophobic film from PMMA with intrinsic water contact angle below 90°, Polymer 48(26) (2007) 7455-7460.
[32] D. Zhang, D. Gracias, R. Ward, M. Gauckler, Y. Tian, Y. Shen, G. Somorjai, Surface studies of polymer blends by sum frequency vibrational spectroscopy, atomic force microscopy, and contact angle goniometry, The Journal of Physical Chemistry B 102(32) (1998) 6225-6230.
[33] C. Ozcan, N. Hasirci, Evaluation of surface free energy for PMMA films, Journal of applied polymer science 108(1) (2008) 438-446.
[34] R.N. Shimizu, N.R. Demarquette, Evaluation of surface energy of solid polymers using different models, Journal of Applied Polymer Science 76(12) (2000) 1831-1845.
[35] E. Chibowski, R. Perea-Carpio, Problems of contact angle and solid surface free energy determination, Advances in colloid and interface science 98(2) (2002) 245-264.
[36] C. Extrand, A thermodynamic model for wetting free energies from contact angles, Langmuir 19(3) (2003) 646-649.
[37] W.-H. Chen, P.-C. Chen, S.-C. Wang, J.-T. Yeh, C.-Y. Huang, K.-N. Chen, UV-curable PDMS-containing PU system for hydrophobic textile surface treatment, Journal of polymer research 16(5) (2009) 601-610.

[38] S. Stern, V. Shah, B. Hardy, Structure‐permeability relationships in silicone polymers, Journal of polymer science part B: Polymer physics 25(6) (1987) 1263-1298.
[39] V. Shah, B. Hardy, S. Stern, Solubility of carbon dioxide, methane, and propane in silicone polymers: effect of polymer side chains, Journal of Polymer Science Part B: Polymer Physics 24(9) (1986) 2033-2047.
[40] J.C. Maxwell, A Treatise on Electricity and Magnetism: By James Clerk Maxwell, Dover1954.
[41] S.A. Hashemifard, A.F. Ismail, T. Matsuura, A new theoretical gas permeability model using resistance modeling for mixed matrix membrane systems, Journal of Membrane Science 350(1-2) (2010) 259-268.
[42] O. Gain, E. Espuche, E. Pollet, M. Alexandre, P. Dubois, Gas barrier properties of poly(?-caprolactone)/clay nanocomposites: Influence of the morphology and polymer/clay interactions, Journal of Polymer Science Part B: Polymer Physics 43(2) (2005) 205-214.
[43] T. Merkel, V. Bondar, K. Nagai, B. Freeman, I. Pinnau, Gas sorption, diffusion, and permeation in poly (dimethylsiloxane), Journal of Polymer Science Part B: Polymer Physics 38(3) (2000) 415-434.
[44] M. Sadrzadeh, M. Amirilargani, K. Shahidi, T. Mohammadi, Gas permeation through a synthesized composite PDMS/PES membrane, Journal of Membrane Science 342(1) (2009) 236-250.
[45] K. Prakashan, A. Gupta, S. Maiti, Effect of compatibilizer on micromehanical deformations and morphology of dispersion in PP/PDMS blend, Journal of applied polymer science 105(5) (2007) 2858-2867.
[46] T. Bremner, D. Hill, M. Killeen, J. O'Donnell, P. Pomery, D.S. John, A. Whittaker, Development of wear‐resistant thermoplastic polyurethanes by blending with poly (dimethyl siloxane). II. A packing model, Journal of applied polymer science 65(5) (1997) 939-950.

Chapter IV: PBT reactive blending with polymethylhydrosiloxane (PMHS) by ruthenium-catalyzed carbonyl hydrosilylation reaction

Abstract

In this chapter, carbonyl hydrosilylation reaction was developed to prepare reactive blending between polybutylene terephthalate (PBT) and polymethylhydrosiloxane (PMHS). It focused on the addition reaction of Si-H groups from PMHS onto carbonyl groups from PBT catalyzed by triruthenium dodecacarbonyl [$Ru_3(CO)_{12}$]. An approach on PBT model compounds was carried out and investigated by NMR spectroscopy to evidence the potentiality and efficiency of carbonyl hydrosilylation reaction. At temperatures up to 100 °C, the hydrosilylation reaction could reach a conversion rate of 33 mol% in a few hours. Side reactions were also highlighted. Such side reactions could reach more than 23 mol% of the final products when the temperature increased to 180 °C.

Then hydrosilylation reaction was extended to PBT modification with a molar ratio of ester group/SiH=3.5 and viscosity ratio polysiloxane/PBT= 4 x 10^{-6}. The reaction was carried out in an internal mixer at 220°C and followed through the evolution of the torque of the reactional medium. Samples made by different processing times were investigated by SEM and rheology. From these analyses, the dispersion of PMHS was promoted and PMHS domains' diameters were reduced to few micrometers. The elastic behavior of the final material was characteristic of a solid or gel-like structure, suggesting a network structure formation consistent with the gel fraction increase from 0 to 0.55.

Keywords: *polymer blends, carbonyl hydrosilylation reaction, polybutylene terephthalate (PBT), polymethylhydrosiloxane (PMHS)*

Résumé

Dans ce chapitre, la réaction d'hydrosilylation a été développée pour préparer un mélange réactif entre le polybutylène téréphtalate (PBT) et le polyméthylhydrosiloxane (PMHS). Il se consacre à la réaction d'addition des groupes Si-H du PMHS sur les groupes carbonyle du PBT catalysée par le triruthénium dodecacarbonyle [$Ru_3(CO)_{12}$]. Une approche par un composé modèle de PBT a été choisie qui est analysé par spectroscopie RMN pour mettre en évidence le potentiel et l'efficacité de la réaction d'hydrosilylation des carbonyles. Lorsque réalisée à température inférieure à 100°C, la réaction d'hydrosilylation a pu atteindre un taux de conversion de 33mol% en quelques heures. Des réactions secondaires ont également été mises en évidence. De telles réactions secondaires ont pu atteindre plus de 23mol% du produit final lorsque la température a été augmentée à 180°C.

La réaction d'hydrosilylation a ensuite été étendue à la modification du PBT avec un ratio molaire entre les groupes ester et les SiH de 3,5 et un ratio de viscosité entre le polysiloxane et le PBT de $4*10^{-6}$. La réaction s'est déroulée en mélangeur interne à 220°C et suivie par l'évolution du couple de mélange du milieu réactionnel. Des échantillons réalisés pour différents temps de mise en forme ont été analysés par MEB et rhéologie. D'après ces échantillons, la dispersion du PMHS a été promue et la taille caractéristique des domaines a été réduite à quelques microns. Le comportement élastique du matériau final et caractéristique d'un solide ou d'un gel, suggérant la formation d'un réseau, en accord avec l'augmentation de la fraction de gel de 0 à 0.55.

Mots clés : *Mélanges polymères, réaction d'hydrosilylation carbonyle, polybutylène téréphthalate (PBT), polyméthylhydrosiloxane (PMHS)*

IV.1 Introduction

Polydimethylsiloxane (PDMS) exhibits excellent characteristics like thermal stabilities, UV resistance, oxidation resistance, low glass-transition temperature (-125 °C), gas barrier and electrical properties [1] *etc*. In order to combine the properties of PDMS with others materials different strategies were developed. First, synthesis of PDMS based copolymers is widely reported. For example, Takashi Miyata *et* al. [2] synthesized different kinds of membranes, consisting in ethanol-permselective PDMS and water-permselective poly(methylmethacrylate) (PMMA), using PDMS macro-azoinitiator initiating the addition reaction between vinyl-ester terminated PDMS and MMA in solution. The copolymers were prepared into membranes to investigate the relationship between their micro-phase separation and their permselectivity for aqueous ethanol solutions during pervaporation. They found PMMA-g-PDMS membranes changed from water- to ethanol-permselective at a DMS content of 35 mol %. In addition, Brown *et* al. [3] reported also the synthesis of a A-B-A block copolymers with B = PDMS and A = polystyrene (PS) or PMMA through atom transfer radical polymerization (ATRP) between hydride terminated PDMS and styrene or methyl methacrylate initiated by chloromethyl terminated polysiloxanes. Through characterizing their thermal properties by DSC, they found the short PDMS block seems to have a considerable plasticisation effect on the PMMA or PS blocks.

However, due to the cost and complex steps, the method of PDMS copolymer synthesis is not easy to be widely applied. Therefore the use of polymer blends seems to be the trend of application. Nevertheless, due to the low surface energy and relatively low viscosity of polysiloxane compared with most thermoplastics, dispersion of polysiloxane is difficult and always results in phase separation. In order to improve dispersion of polysiloxane and achieve compatibilized polymer blend, physical compatibilization [4-6] is usually performed. In practical applications, premade amphipathic copolymer was used to increase the interfacial tension between the immiscible phases. As reported, the addition of block copolymers for polyolefin/PDMS is widely reported [7-10]. For instance, Hu and Kobersteins [7] investigated the effects of diblock copolymer addition on the interfacial tension of immiscible homopolymer blends for the ternary system containing polystyrene (PS), (PDMS), and poly(styrene-*b*-dimethylsiloxane) [P(St-*b*-DMS)]. Interfacial tension is measured, as a

function of the diblock copolymer concentration and the molar mass of PDMS, using an automated pendant drop tensiometer. They found the interfacial tension of the blend initially decreases upon an increase in the copolymer concentration and then reaches a constant value above a certain critical concentration. A maximum interfacial tension reduction of 82% is achieved at a critical concentration of 0.002 wt% diblock copolymer. In another publication [11], PE-*b*-PDMS diblock copolymer was prepared through the esterification reactions between monohydroxy-terminated poly(dimethylsiloxane) (PDMS-OH) and the corresponding carboxyl terminated polyethylene (PE-COOH) in the presence of tetrabutyl titanate (TBT). Then the copolymer was used as a compatibilizer in the blends of high-density polyethylene (HDPE) and silicone oil. The copolymer (1wt%) promoted the dispersion of silicone oil in HDPE from more than 5μm (silicone oil) to no obvious phase segregation through SEM observation and improved the mechanical properties of HDPE/PDMS blends. These observations confirmed that amphipathic copolymers were efficient in modifying the interface of immiscible blends.

Even though the addition of premade copolymer is an efficient way to achieve compatibilization in polymer/PDMS blends, there are also some limits to use pre-made block or graft copolymers in melt blending. In order to find a more efficient method to improve the properties of polymer blend, efforts have been turned towards reactive compatibilization. Reactive blending is a very robust, low-cost way for material preparation. It is effective to control morphology and to design expected new materials. This is the case of the *in situ* compatibilization, in which copolymers are formed directly at the interface during polymers processing meaning that it can be achieved in one step. A few studies have demonstrated the reactive blending of PDMS with organic polymers. For instance, Marie *et* al. [9] used reactive compatibilization to control and stabilize 20-30wt% PDMS dispersion in polyamide 6 (PA6). Specifically, two kinds of anhydride (An) functional PDMS (one is An-difunctional and the other one contains 4 random An along PDMS chain) were used to react with amine (NH_2) end-groups of PA6. They found reactive blending of PA6 and difunctional PDMS-$(An)_2$ did not decrease PDMS particle size compared with non-reactive blend (~ 10 μm). However, particle size decreased significantly to about 0.5 μm when PA6 was blended with PDMS containing 4 random An. Similarly, Zhou and Osby [12] demonstrated the formation of

polycarbonate (PC)/PDMS compatibilized blends through the use of hydroxyl-terminated PDMS (PDMS-OH) reacted with PC by twin-screw extrusion at 280 °C. The new formed PC-PDMS copolymer provides a compatibilization effect for the stable sub-micron blend morphology in an otherwise immiscible PC/PDMS blend system, silicone material was found to be well dispersed in the polycarbonate major phase forming small spherical domains with the domain size of about 0.2-0.9 μm. In general, reactive blending between functional PDMS and thermoplastic provides a new and efficient way to promote the compatibility of such system, at the meantime it improves some properties of thermoplastic through the introduction of PDMS.

Very recently, Igarashi *et* al. found that ruthenium catalyst could be used for hydrosilylation between ester and SiH functional PDMS [13], it offers another route for *in-situ* reactive compatibilization among PDMS-SiH and polyester. For example, Bonnet *et* al. [14] developed a new and original reaction between PDMS and EVA based on EVA carbonyl hydrosilylation by Si-H groups of hydride terminated PDMS (PDMS-SiH). The occurrence of the hydrosilylation reaction at the EVA/polysiloxane interface promoted a homogenization of the blend depending on the molar ratio SiH/vinyl acetate groups, [SiH]/[VA], and the viscosity ratio of the blend. Two distinct behaviors were observed. The formation of a crosslinking network under shear was obtained for a low viscosity ratio between polysiloxane and EVA (polysiloxane/EVA = $4.0x10^{-6}$) with a high concentration of SiH groups ([SiH]/[VA] =0.5), while the formation of a compatibilized blend was observed for high molar mass polysiloxanes (Mn > 15,000 g mol^{-1}) with a low concentration of SiH ([SiH]/[VA] < $4.0x10^{-3}$).

In this study, we focus on the carbonyl hydrosilylation of polybutylene terephthalate (PBT) with PMHS. Since the previous work carried out by Bonnet *et* al. [14] about EVA was processed at relatively low temperature (115 °C) compared to most thermoplastics, so we choose PBT melted at 220 °C to investigate the reactive blending at higher temperature. First, a model-system was carried out to investigate the efficiency and selectivity of the reaction. Melt-reacted blends of PBT and PMHS were also prepared and their morphological and rheological properties were investigated. This work is aimed to find a viable way to achieve stable and homogeneous ester-polydimethylsiloxane blends at high processing temperature.

IV.2 Experimental part

IV.2.1 Materials and reagents

Butyl benzoate, hexafluoro-2-propanol (HFIP), acetone and chloroform were purchased from Aldrich. Anhydrous toluene was purchased from Acros. $Ru_3(CO)_{12}$ and polymethylhydrosiloxane (PMHS) were commercial products from ABCR. Viscosity of PMHS is $4x10^{-2}$ Pa.s) at room temperature. The average molar mass is 2100 g/mol. All the products were used without further purification. The chemical structures of the reactants used for hydrosilylation reaction are shown in Figure IV.1. Polybutylene terephthalate (PBT) was provided by Dupont (Crastin® PBT S600f10 NC010, density is 1.30 g/ml at 25 °C, *M*n=20400), the melting temperature is 225 °C.

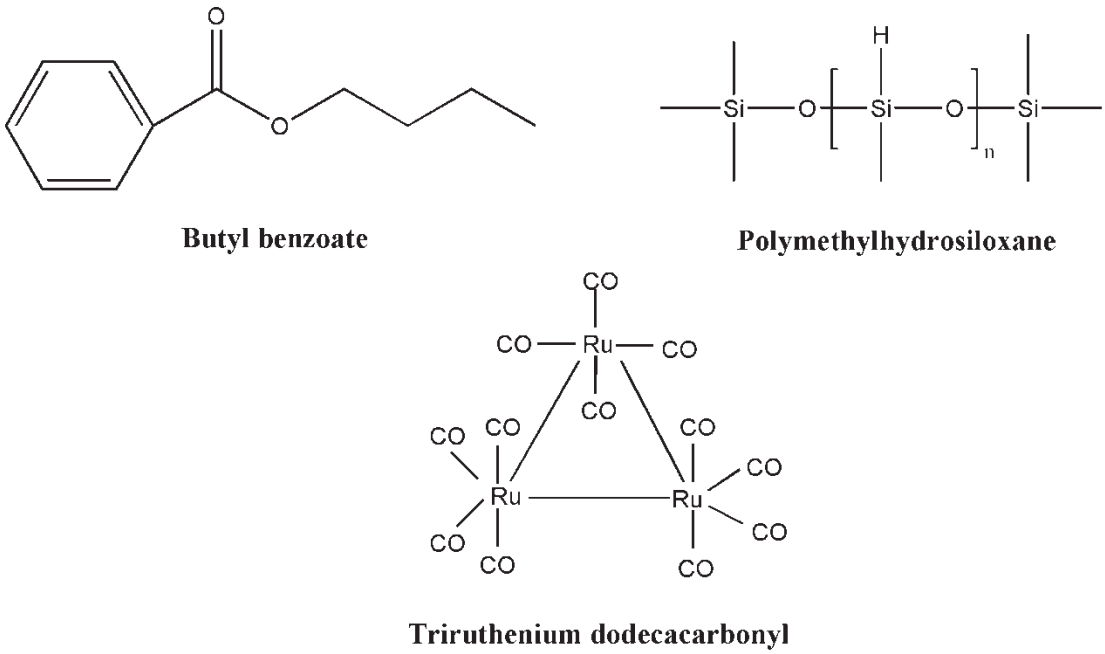

Figure IV.1: Chemical structure of reagents and catalyst used for the carbonyl hydrosilylation reaction.

IV.2.2 Carbonyl hydrosilylation reaction with butyl Benzoate

Butyl benzoate was chosen as model compound to assess the efficiency and selectivity of carbonyl hydrosilylation reaction between ester group and SiH functions of PMHS at high temperatures. Equimolar amounts of SiH and ester group (0.04 mol) were added in a schlenk, under argon atmosphere. The catalyst $Ru_3(CO)_{12}$ (0.03 mmol) was first dissolved in

anhydrous toluene (2 ml) and then the catalyst solution was added in the previous schlenk of butyl benzoate and PDMS mixture. The reactional medium was heated to 100 °C (or 180 °C) from 10 min up to 4 h. Aliquot parts were collected at different reaction time and analyzed by ^{1}H NMR.

IV.2.3 Carbonyl hydrosilylation reaction with ester group from PBT

PBT pellets were dried in vacuum at 80 °C for 24 h. Melt reactive processing between PBT and PMHS was carried out in a Haake Plasticorder intensive batch mixer equipped with a Rheomix 600 internal mixer. The mixer chamber temperature was set at 220 °C, the rotation speed was 50 rpm. The melt temperature and resistant torque were monitored during the experiments. Dried PBT (40 g) was first added in the chamber and mixed during 2 min until it was melted. Then, the mixture of PMHS and catalyst were added with a predetermined mass (PMHS (10wt%) and for $Ru_3(CO)_{12}$ (0.1wt%), ratio of ester group/SiH is 3.5). The extent of the reaction can be followed through the torque variation.

IV.2.4 Characterization

^{1}H and ^{13}C NMR spectroscopy was carried out with a 5-mm BBFO+ probe on a Bruker AVANCE III spectrometer working at 400 MHz for ^{1}H and 100.6 MHz for ^{13}C. ^{29}Si liquid-state NMR spectra were recorded on a Bruker AVANCE II spectrometer (79.5 MHz for ^{29}Si) with a 10 mm ^{29}Si selective probe with a z-gradient coil. Deuterated chloroform ($CDCl_3$, Aldrich), was used as solvent, tetramethylsilane was used as reference for ^{1}H chemical shifts. All the samples were analyzed at 25 °C. Chemical shift (δ) are given in parts per million (ppm). Chromium acetylacetonate [$Cr(acac)_3$] was added to shorten the ^{29}Si spin-lattice relaxation times. ^{29}Si solid-state NMR was carried out with a Bruker ADVANCE 500 spectrometer with a Bruker 4 mm CP-MAS (cross-polarization magnetic angle rotation) probe. The sample was analyzed as finely ground powder and the experiment was working at 5 kHz.

The morphology of the polymer blend was characterized by scanning electron microscopy (SEM), the samples were cryo-fractured in liquid nitrogen or by cryo-ultramicrotomy with a Leica EMFCS microtome device equipped with a diamond knife

(this technique was used to prepare planed surface). The sample surfaces were then sputter coated with gold/palladium. The morphology was analyzed using a QUANTA 250 microscope with an accelerating voltage of 10kV.

Rheological measurements were carried out using a Rheometer ARES. The samples were first molded as disk (d=25 mm, h=1mm). The samples were heated at 230°C for 6 min until equilibrium was reached and the gap between the two plates was adjusted to 1 mm, then the samples were equilibrated for 1 min before starting the test. Nitrogen gas was used to prevent thermal oxidation of the samples. The linear complex shear modulus ($G^*(\omega) = G'(\omega) + jG''(\omega)$, j^2=-1) was measured at 230 °C.

The crosslinking extent of the PBT network was measured from gel fraction. The PBT gel fraction (τ_i) was determined after immersion (48 h, 25 °C) of 200 mg PBT/PMHS samples in HFIP/chloroform (20 ml, 1:4 in volume) mixed solvent. The samples were then filtered and washed with acetone. After drying for 24 h at 80 °C under vacuum, the gel fraction was calculated from equation1

$$\boldsymbol{\tau_i = m_d/m_o} \quad \textbf{(1)}$$

m_o is the mass of the sample before dissolution and m_d is the mass of the insoluble fraction after filtering and drying.

The swelling ratio was calculated according to the following equation 2,

$$\boldsymbol{G_v = 1 + (G_P - 1)x(\rho_1/\rho_2)} \quad \textbf{(2)}$$

G_P is the mass ratio of swollen sample to dried sample, ρ_1 is density of the solvent, ρ_2 is density of the polymer.

Crosslinking density of the elastic strand (mol.m^{-3}) was based on the volume swelling degree ($v_2 = 1/G_v$). On the basis of the Flory–Rehner equation, Patel *et* al. [15-18] derived a relationship between the swelling degree and the number of elastic strand v for the networks.

$$\boldsymbol{v = -\left[\frac{(\ln(1-v_2)+v_2+\chi v_2^2)}{V_1 v_2^{1/3}}\right]} \quad \textbf{(3)}$$

V_1 is the molar volume of the solvent, and χ is the polymer-solvent interaction parameter, which is related to the solubility parameters via Equation(4)

$$\chi = 0.34 + \frac{V_1}{RT}(\delta_1 - \delta_2)^2 \quad (4)$$

Where R is the gas constant, T is the absolute temperature, V_1 is the molar volume of the solvent, and δ_1 and δ_2 are the solubility parameters of polymer and solvent, respectively. δ_1 was calculated by Van Krevelen model [19] equals to 10.8 $MPa^{1/2}$ and for solvent (HFIP/Chloroform=1/4 in volume $\delta_{HFIP} = 18.5$, $\delta_{CHCl3} = 9.3$), δ_2 is 11.1 $MPa^{1/2}$.

Surface wettability tests were carried out using an optical contact angle meter (DSA 100, Kruss, Germany) at room temperature, using the sessile drop technique. For this measurement, the samples were hot pressed to films between Teflon film and a piece of glass. Drops of purified water were gently deposited on the smooth surface (the one next to the glass) by the delivering syringe. Three water contact angle measurements on each mat surface were taken at different positions on the sample.

IV.3 Results and discussion

IV.3.1 Butyl benzoate/PMHS hydrosilylation reaction

The hydrosilylation reaction is an addition reaction of the SiH group from PMHS onto the carbonyl group of the ester function and it is expected to form a new SiOCH bond as shown in Figure IV.2.

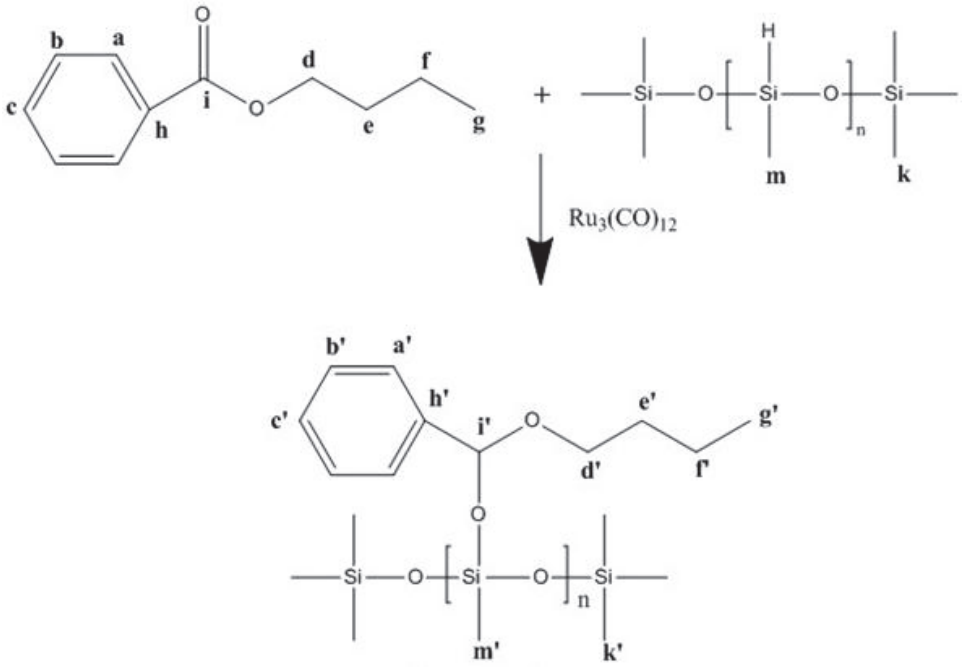

Figure IV.2: Scheme of expected hydrosilylation reaction between butyl benzoate and PMHS catalyzed by $Ru_3(CO)_{12}$.

Through comparing the ^{1}H NMR spectrum of the reactional medium before (Figure IV.3) and after 4 hours reaction (Figure IV.4) at 100 °C, we observe the formation of the expected addition product characterized by several broad signals at 5.87 ppm from SiOC<u>H</u> protons, at 3.3-3.7 ppm, 1.2-1.7 ppm and 0.85 ppm from -OC<u>H</u>$_2$- (d'), -C<u>H</u>$_2$C<u>H</u>$_2$- (e', f') and -C<u>H</u>$_3$ (g') protons of butyl group, respectively. Except the signal of –SiOCH, the others are complex to distinguish, because they overlap with several other peaks assigned to starting butyl benzoate and by-products (the side reactions were shown in Figure IV.5). In literature, it was reported that at high temperature in the presence of water or in acidic conditions, SiOCH bonds can be split into SiOH and CHOH end groups. In the reactional medium, the addition product is leading to form hemiacetal (P) and silanol by hydrolysis. Hemiacetals are also unstable compounds and can be split into butanol (Q) and benzaldehyde (O) [20, 21]. In this reaction, we also found the formation of butyl benzyl ether (R) and benzyl alcohol (S) coming from other kinds of side reaction. Therefore, the signals between 3.3 and 3.7 ppm can also be attributed to -OC<u>H</u>$_2$- protons from hemiacetal [d'(p)], butanol [d'(q)] and butyl benzyl ether [d'(r)]. The several signals near 0.85 ppm also come from -C<u>H</u>$_3$ belonging to the three by-products. In addition, the signal at 10.01 ppm is assigned to -C<u>H</u>O proton of benzaldehyde (O) and the one at 5.50 ppm belongs to <u>H</u>COH of hemiacetal [i'(p)]. There are also two

signals at 4.48 ppm and 4.61 ppm corresponding to proton of methylene coming from Ph-C<u>H</u>$_2$-OR [i'(r)] and Ph-C<u>H</u>$_2$-OH [i'(s)], respectively.

In the meantime, the signal of unreacted –SiH is no more a singlet compared with the initial one from PMHS, disclosing a composition effect due to the functionalization of SiH groups along the PMHS chains. As the functionalization is not total, the remaining SiH groups have different environments and their proton chemical shifts are depending on the nature of neighboring functions (SiH or SiOCH). In addition, a part of the signal coming from Ph-C<u>H</u>$_2$-OH [i'(s)] proton also overlapped with it.

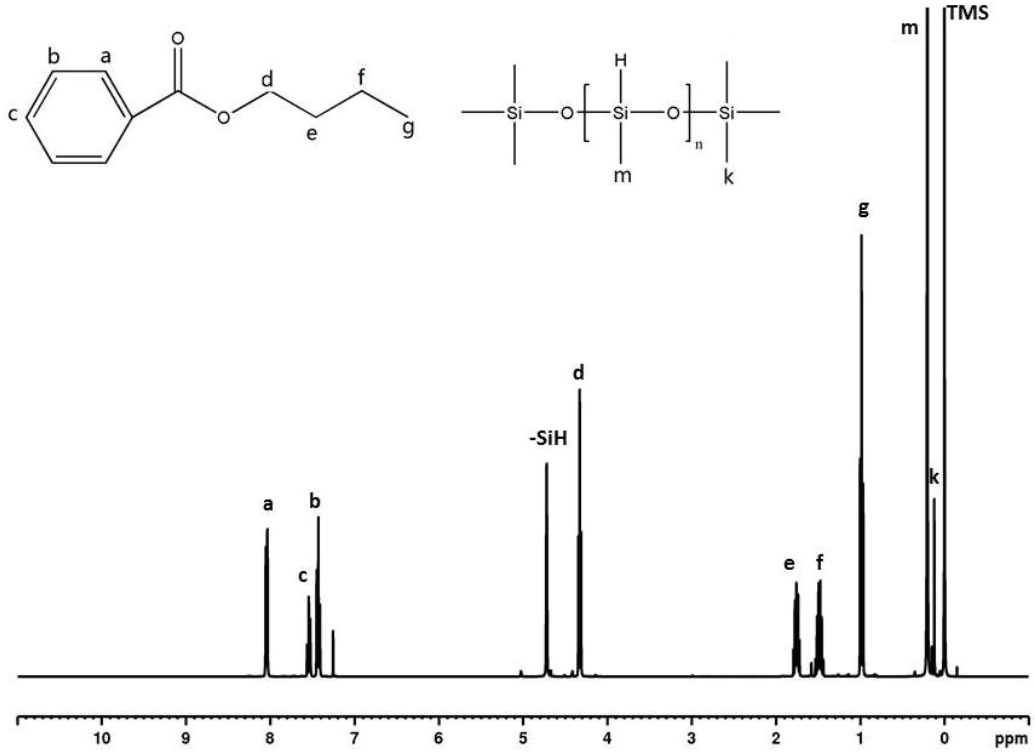

Figure IV.3: ^{1}H NMR spectrum of the initial mixture of butyl benzoate and PMHS ($CDCl_3$-25°C).

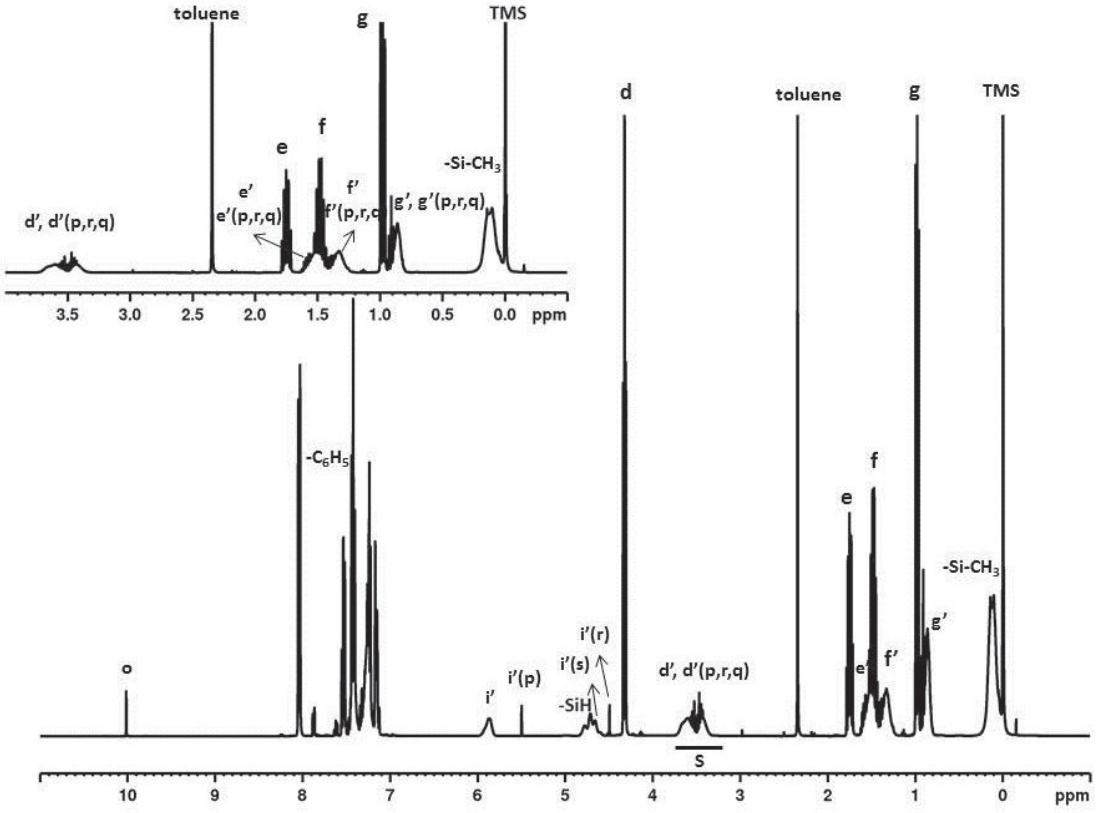

Figure IV.4: ^{1}H NMR spectrum of butyl benzoate/PMHS mixture after 4 h reaction time at 100 ° C and zoom 0-3.9ppm, ($CDCl_3$-25°C). * Toluene is observed due to its use to introduce the catalyst.

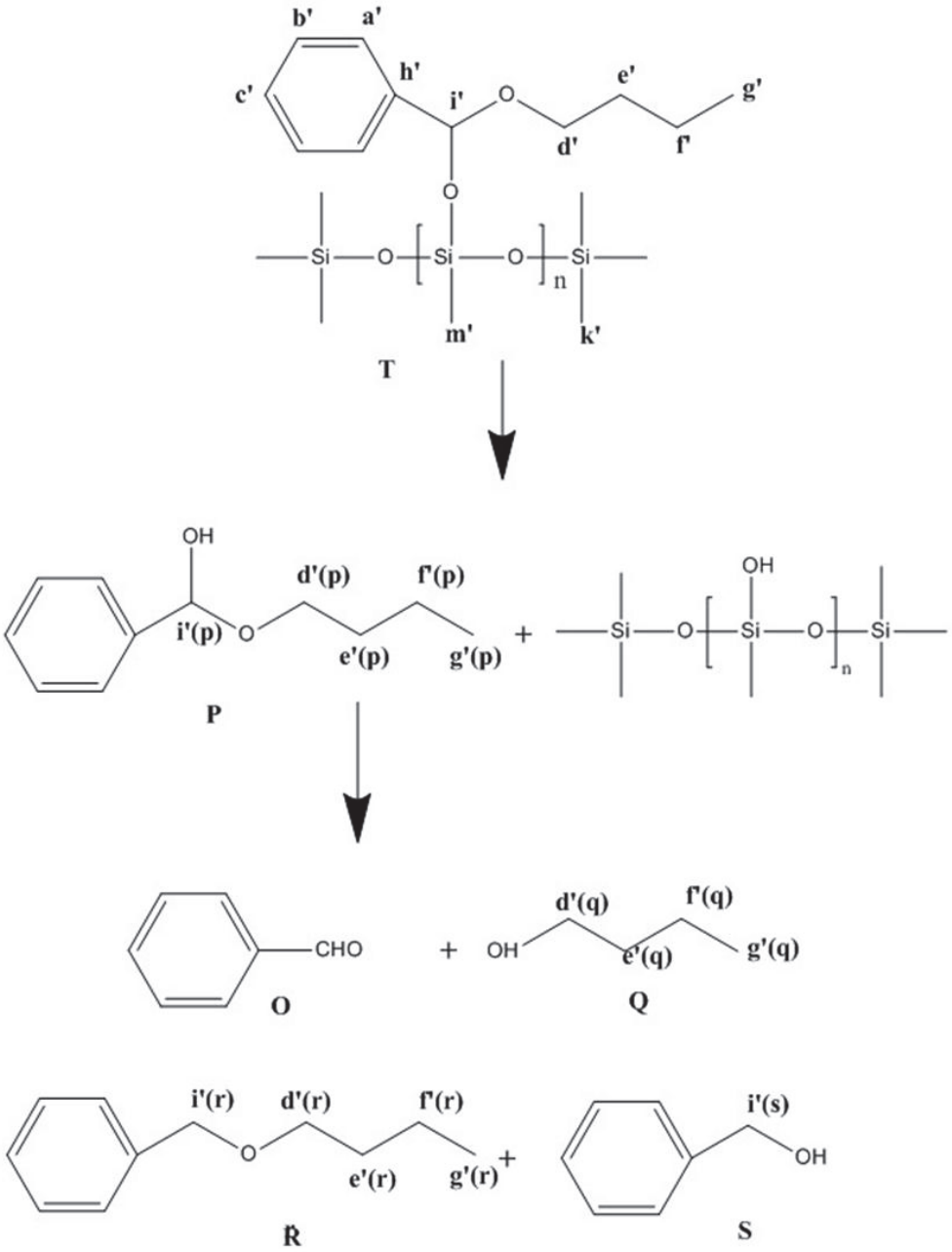

Figure IV.5: Scheme of side-reactions of butyl benzoate hydrosilylated products, mainly hydrolysis reaction.

These observations were also supported by ^{13}C NMR analysis of the previous reactional medium (Figure IV.7). On the ^{13}C NMR spectrum, the addition product is characterized by four main signals at 140.94, 96.81, 66.14 and -3.27 ppm from $C_6H_5\underline{C}CHOSi$ (h'), $-\underline{C}HOSi$ (i'), $-O\underline{C}H_2CH_2CH_2CH_3$ (d'), $-CHOSi(\underline{C}H_3)_3$ (m') carbons, respectively. Other phenyl carbons and $-\underline{C}H_2$ are compared to the initial butyl benzoate ones in Figure IV.6 and Figure IV.7. The by-products were confirmed by five signals at 192.12, 101.55, 72.88, 64.7 and 62.14 ppm corresponding to $C_6H_5\underline{C}HO$ (o), $-O\underline{C}H(OH)$ [i'(p)], $C_6H_5\underline{C}HOR$ [i'(r)], $C_6H_5\underline{C}HOH$ [i'(s)]

and $C_3H_{10}\underline{C}H_2OH$ [d'(q)] carbons, respectively.

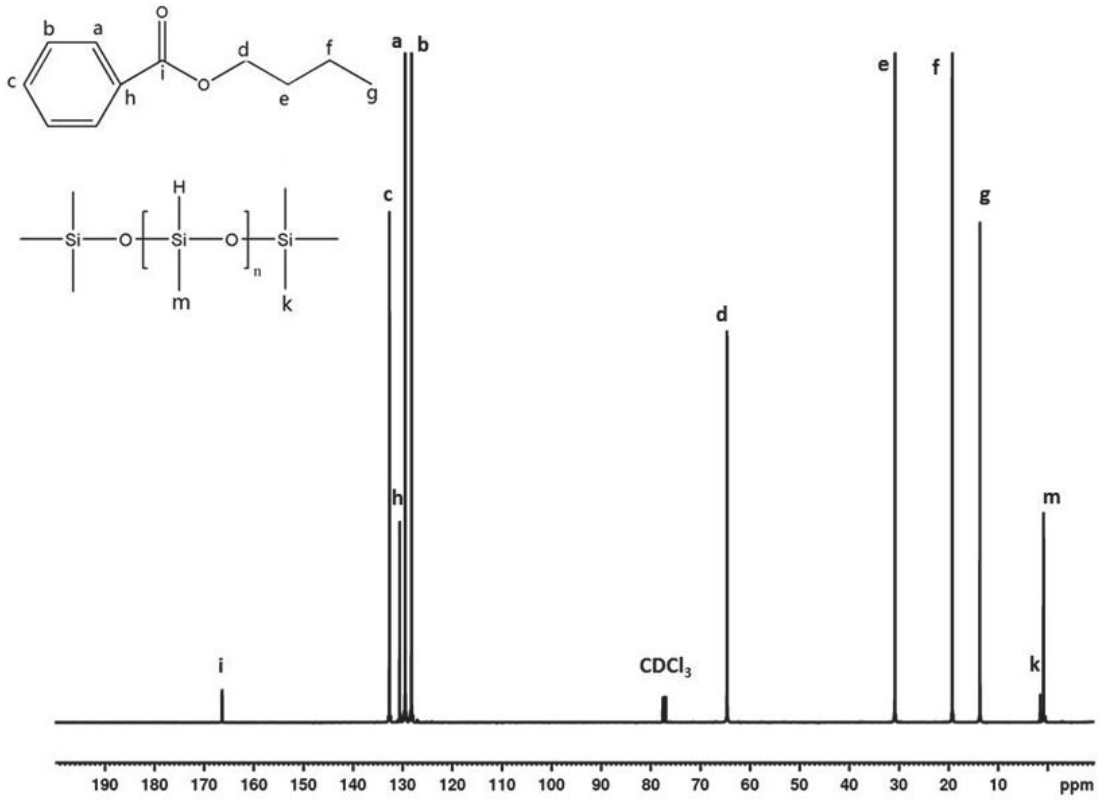

Figure IV.6: ^{13}C NMR spectrum of butyl benzoate and PMHS mixture before reaction (CDCl3-25°C).

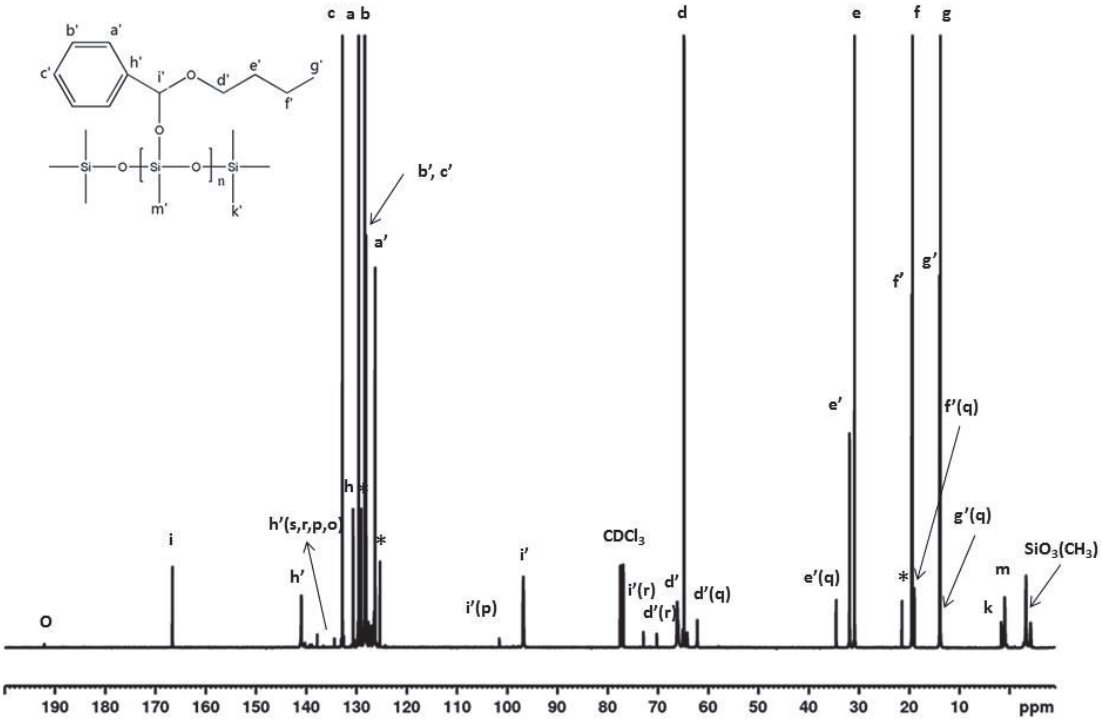

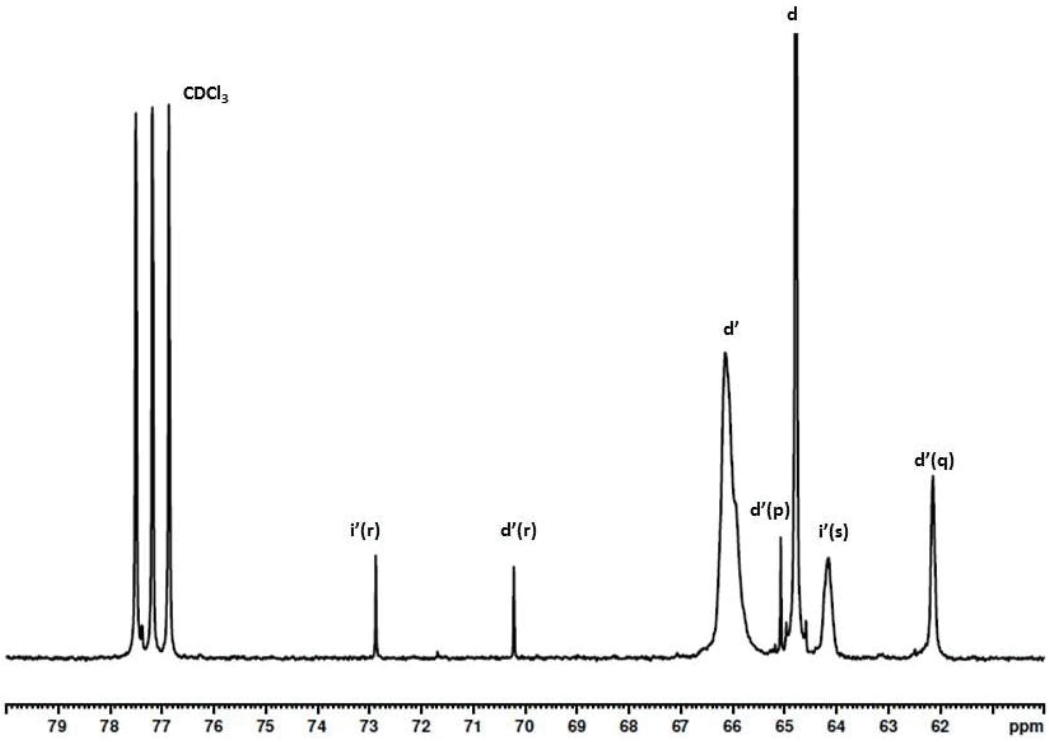

Figure IV.7: ^{13}C NMR spectrum of butyl benzoate/PMHS mixture after 4h reaction time at 100 ° C and zoom 60-80 ppm], (CDCl3-25°C). * Toluene is observed due to its use to introduce the catalyst.

Figure IV.8 and Figure IV.9 depicted the ^{29}Si NMR spectra of PMHS and of the reactional medium after 4 h reaction time at 100 °C, respectively. As shown in Figure4.8, PMHS exhibits two obvious signals at 10.07 and -34.71 ppm corresponding to $(CH_3)_3\underline{Si}O$- (a) and -$CH_3(H)\underline{Si}O$- (b), signal of b is divided into three signals at -34.71, -35.15 and -35.63 ppm owning to different neighboring functions of Si-H groups on the chains. After 4h reaction time at 100 °C (Figure IV.9), 5 main broad and split signals around 9.50, -35.80, -55.00, -59.70 and -65.60 ppm are observed. Signals at 9.50, -35.80 ppm are assigned to $(CH_3)_3\underline{Si}O$- (a) and unreacted -$CH_3(H)\underline{Si}O$- (b) units. As observed in the proton spectrum for SiH resonances, the signals of -$\underline{Si}$H are split to two peaks b and d, since neighboring groups are different on the PMHS molecular chains. In addition, as mentioned in the literature the chemical shift of ^{29}Si NMR at the arrange -55 to -68 ppm is assigned to Si-T (trifunctional) unit of siloxane, so the signals at -55.00, -59.70 and -65.60 ppm are assigned to trisiloxane cycle (e), expected product -$\underline{Si}$OCH(c) and -Me$\underline{Si}$(O-)$_3$ (f) respectively. For the expected product, after hydrosilylation Si-H disappeared and formed a new Si-O bond, the structure -$(CH_3)SiHO_2$- changed to -$(CH_3)SiO_3$-. Trisiloxane cycle (e) and -Me$\underline{Si}$(O-)$_3$ (f) comes from the silicone resin that PMHS formed itself when heated in presence of $Ru_3(CO)_{12}$ catalyst. Satyanarayana *et* al. [22] had actually demonstrated that in the presence of

transition-metal-catalyst, a part of PMHS can form cross-linked polysiloxane through oxidative reaction. $(CH_3)SiO_3$- (T_1) and cyclic trisiloxane (T_3) (silicon atom combined with 3 oxygen and 1 methyl) had been detected. The observation of Si-T units is also supported by ^{13}C NMR as signals of -CH_3 linked to Si (T) are around -3.27 ppm and -4.28 ppm as shown in Figure IV.7.

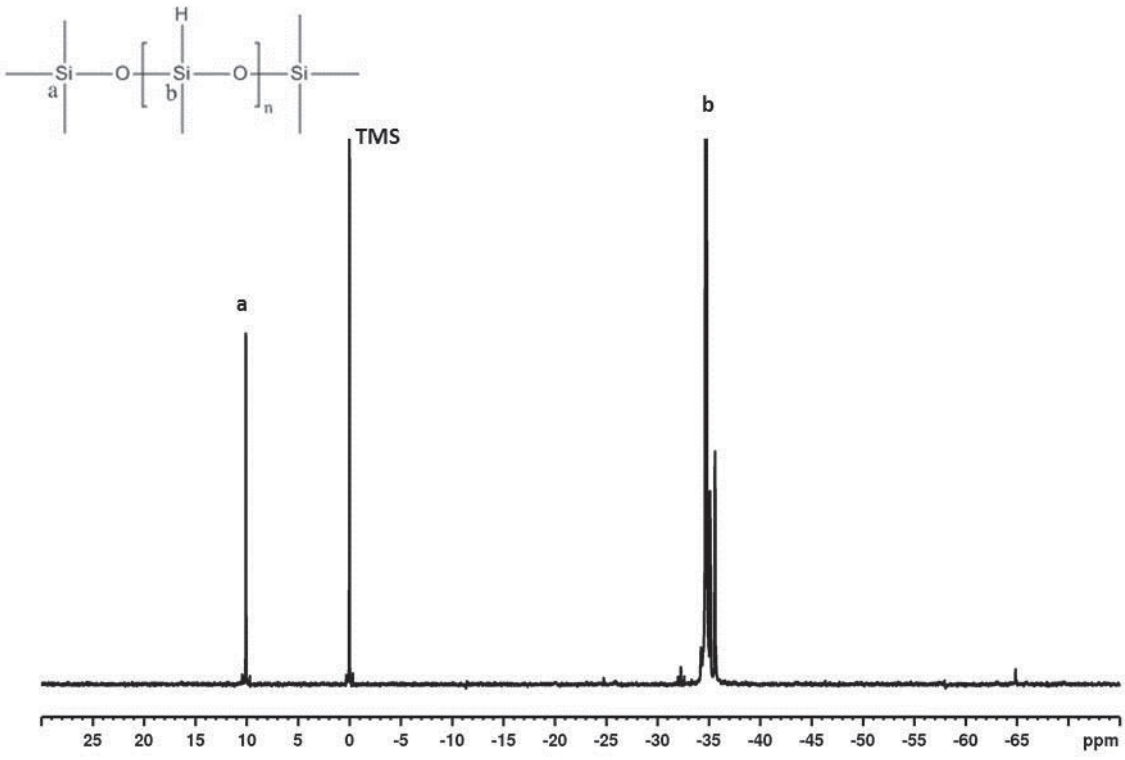

Figure IV.8: Liquid-state ^{29}Si NMR spectrum of polymethylhydrosiloxane (PMHS), ($CDCl_3$-25°C).

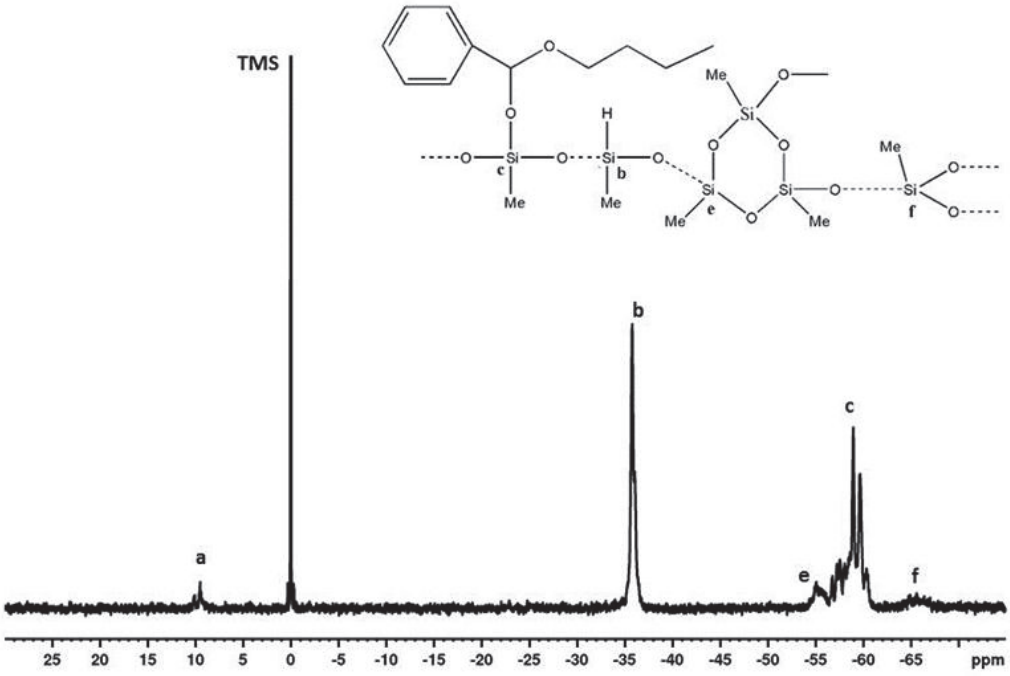

Figure IV.9: Liquid-state ^{29}Si NMR spectrum of butyl benzoate/PMHS mixture after 4 h reaction time at 100 ° C, ($CDCl_3$-25°C).

2D-NMR HMBC combined with ^{1}H and ^{29}Si NMR was used to analyze the reactional medium after 4 h to confirm the previous results. As shown in the 2D-NMR spectrum (Figure IV.10), silicon signals at -59.7 ppm has an obvious correlation with the signals of -CH- at 5.87 ppm, clearly indicating that SiH added on the C=O group and formed SiOCH. Information of residual SiH can also be found in the spectrum. However, there is another clear cross peak at (3.60, -59.65), which means there is another T structure Si correlated with -CH_2- of butanol, the product may come from the dehydration reaction between butanol and silanol formed $SiOCH_2$ groups.

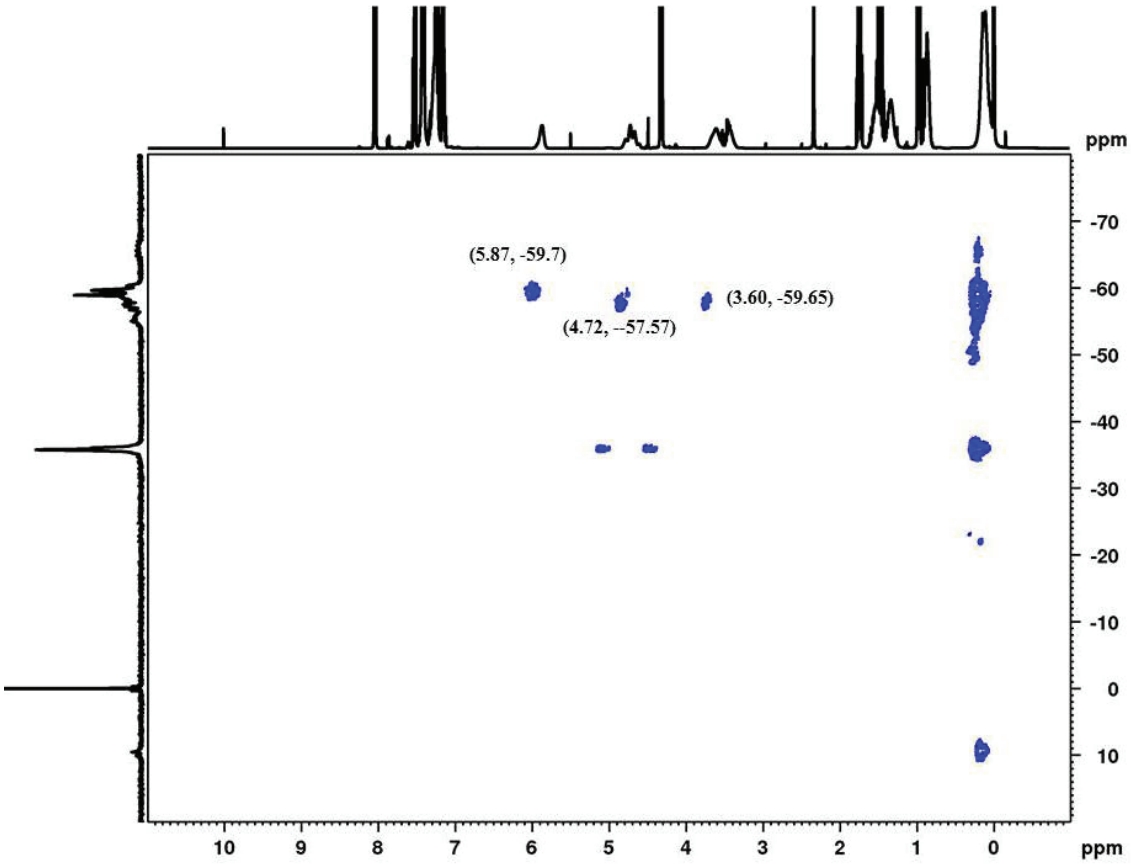

Figure IV.10: 2D-NMR HMBC (^{1}H-^{29}Si) of reactional medium after 4 h reaction, (CDCl3-25°C).

The NMR characterizations of the reactional medium at different reaction time and temperature respectively evidenced the occurrence of the expected carbonyl hydrosilylation reaction in these conditions. The main product of the reaction is a silyl acetal. However, in addition, we also observed side reactions due to hydrolysis especially at high temperature. The high reactive PMHS is also modified by the thermal treatment to some siloxane based compounds in the presence of ruthenium catalyst.

IV.3.2 Kinetics

The kinetics of hydrosilylation reaction between butyl benzoate and PMHS was analyzed by ^{1}H NMR from 0 min to 4h at 100 °C and 180 °C. To quantify the proportion of the main and side products of reaction all along the kinetics conducted at 100°C and 180°C, the integral of the signals from 0.8 to 1.0 corresponding to methyl end groups of butyl chain was calibrated to 3. Indeed, these signals belong to butyl groups of the expected addition units (T), hemiacetal (P), butanol (Q), butyl benzyl ether (R) and residual butyl benzoate. The amounts of addition units and hemiacetal are given by the integrals of signals at 5.87 ppm

and 5.50 ppm respectively. Integral of the new signals from 3.3 and 3.7 ppm (s) gives then the amount of butanol which should be the same as the one of benzaldehyde, theoretically. However, we found there was a small amount of butanol reacted with silanol and formed another acetal, so amount of butanol is not calculated here. The ratio of each structure and residual SiH units are shown in Table IV.1 and depicted in Figure IV.11 for the expected acetal product.

Table IV.2: Evolution of new species formed during hydrosilylation reaction.

Temperature(^{O}C)	Time of reaction (min)	^{T}Si-O-CH(mol%)	^{P} Hemiacetal (mol%)	^{O} Benzaldehyde (mol%)	^{R} Butylbenzylether(mol%)	PMHS (mol%)
100	10	4.8	3.3	3.2	1.5	71.1
	30	21.8	3.5	3.4	2.3	58.6
	60	27.4	3.3	3.1	2.5	51.5
	90	30.4	2.9	2.5	2.5	50.9
	120	32.6	1.7	1.6	2.7	49.6
	180	29.9	3.4	3.5	2.7	49.4
	240	32.8	2.1	2.4	2.9	49.4
180	10	15.1	5.5	6.5	2.8	56.1
	30	9.8	7.4	10.9	2.8	57.1
	60	5.7	6.4	15.2	2.9	56.2
	90	1.8	6.5	18.4	3.0	50.5
	120	0.1	1.4	23.3	3.0	53.9
	180	/	0.1	21.4	2.6	53.9

[T], [P], [O] and [R] were measured through integral of the signals i', i' (p), o and i'(r) directly.

Experiments were repeated 3 times, data in the table 1 is average value and the errors are shown in Figure Ⅳ. 11.

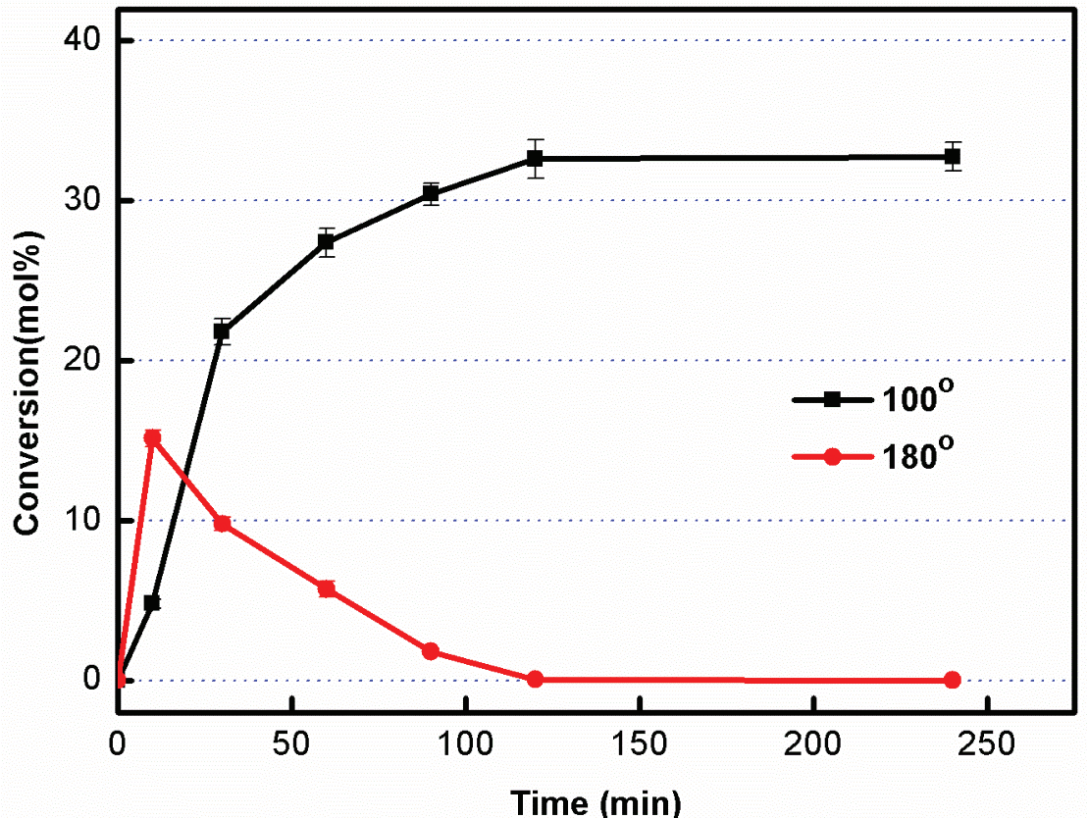

Figure IV.11: Proportion of hydrosilylation products (T) obtained from reaction between butyl benzoate and PMHS.

The NMR analyses have demonstrated that the hydrosilylation reaction between ester group and SiH is possible. In literature, Bonnet et al obtained a yield of 60 mol % of the expected products after 250 min at 100 °C, for octyl acetate, but they also demonstrated that the addition reaction rate depends on the nature of the each ester structure and on the reaction temperature [23, 24]. In the present case, at 100 °C, more than 30 mol% of the expected structure is reached after 250 min of reaction. It confirmed the role of the ester structure (aromatic compared to aliphatic for Bonnet et al. works). The situation is different for the reaction carried at 180 °C. The yield was 15mol % after 10 min and afterward decreased drastically down to almost no more expected adduct after 180 min of reaction. Actually the contributions of the side reactions due to mainly the hydrolysis reaction of alkyl silyl ester inhibited the increase of expected products. The situation is enhanced by the increase of the temperature up to 180 °C with a main contribution of the benzaldehyde for the longest reaction times.

In conclusion and according to the kinetics study, the hydrosilylation reaction between butyl benzoate and SiH is possible and occurs within few minutes, similar reaction products

are formed at 100 and 180 °C. Even though the yield of alkyl silyl ester is low caused by the appearance of side reactions, it is feasible for further reactive compatibilization between PBT and PMHS as it just cost a few minutes to obtain the highest quantity of copolymer. Besides, as a large number of publications reported that a few percent of copolymer is enough to change completely the interface in a polymer blend, we can evaluate the efficiency of this reaction in the PBT processing conditions [25, 26].

IV.3.3 PBT/PMHS hydrosilylation reaction

Hydrosilylation reaction between PBT and PMHS was carried out under shear at 220 °C, in molten conditions. The expected reaction is shown in Figure IV.12. In addition, at this temperature as shown previously by ^{29}Si liquid NMR, PMHS could react on itself in presence of ruthenium catalyst to form T structure [–O[(CH_3)-O-SiO]- and a trisiloxane cycle [22].

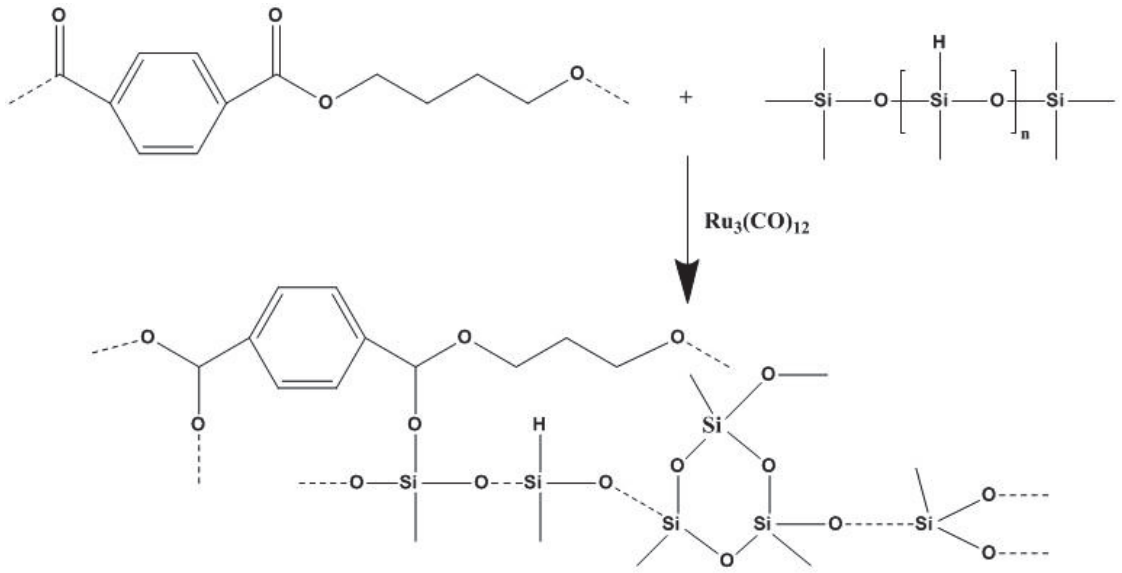

Figure IV.12: Scheme of hydrosilylation reaction between PBT and PMHS.

The torque variation was monitored to evidence the reaction occurrence (Figure IV.13). At the beginning of the experiment, PBT was introduced and melted. Two minutes later, the addition of the blend PMHS/$Ru_3(CO)_{12}$ into molten PBT caused a rapid decrease of the torque. This phenomenon is related to the lubricant effect of PMHS [27]. Actually the viscosity of PMHS (η=4x10^{-2} Pa.s) is quite lower compared to the viscosity (1x10^3 Pa.s) of the molten PBT at 220 °C. Under shear and mixing, this decrease is followed by a rapid

increase of the torque as the crosslinking reaction takes place. Then, the torque decreases strongly as the crosslinking network of PBT became a solid which under shear changed into a powder. Qualitatively, the variation of the torque is a signature of the hydrosilylation reaction catalyzed by $Ru_3(CO)_{12}$. Besides, such phenomenon has not been observed without catalyst.

In Figure IV.13, the gel fraction (τ_i) and swelling ratio (G_v) of PBT/PMHS blend during reaction were also shown. The gel fraction increased from 0.13 to 0.55 from the beginning of the torque increase to the end of network powder formation. The result is related to the formation of crosslinking network between PBT and PMHS. Conversely, the swelling ratio decreases to 3.2 due to the densification of network.

On the other hand, through swelling test and based on the Flory–Rehner theory, we found the molar concentration of elastic strands increased from 13 to 40 $mol.m^{-3}$ according to the torque increase. These results are qualitatively in agreement with the literature. For example, Bonnet *et* al. [14] reported a molar concentration of elastic strand to be 62 $mol.m^{-3}$ for a EVA/PMHS (90/10wt%) blend with a molar ratio [SiH]/[VA]=0.5 obtained at 115°C. In our case, the concentration of elastic strands is lower possibly due to a lower molar ratio [SiH]/[-COO]=0.3 and higher processing temperature 220° which may cause by self-crosslinking of PMHS a consumption of some SiH groups. Hence, the occurrence of side-reactions as shown previously through model compounds approach may also contribute to the lower value of crossliking density. However, not only the self-crosslinking of PMHS can explain this value as only 10 wt% of PMHS was introduced.

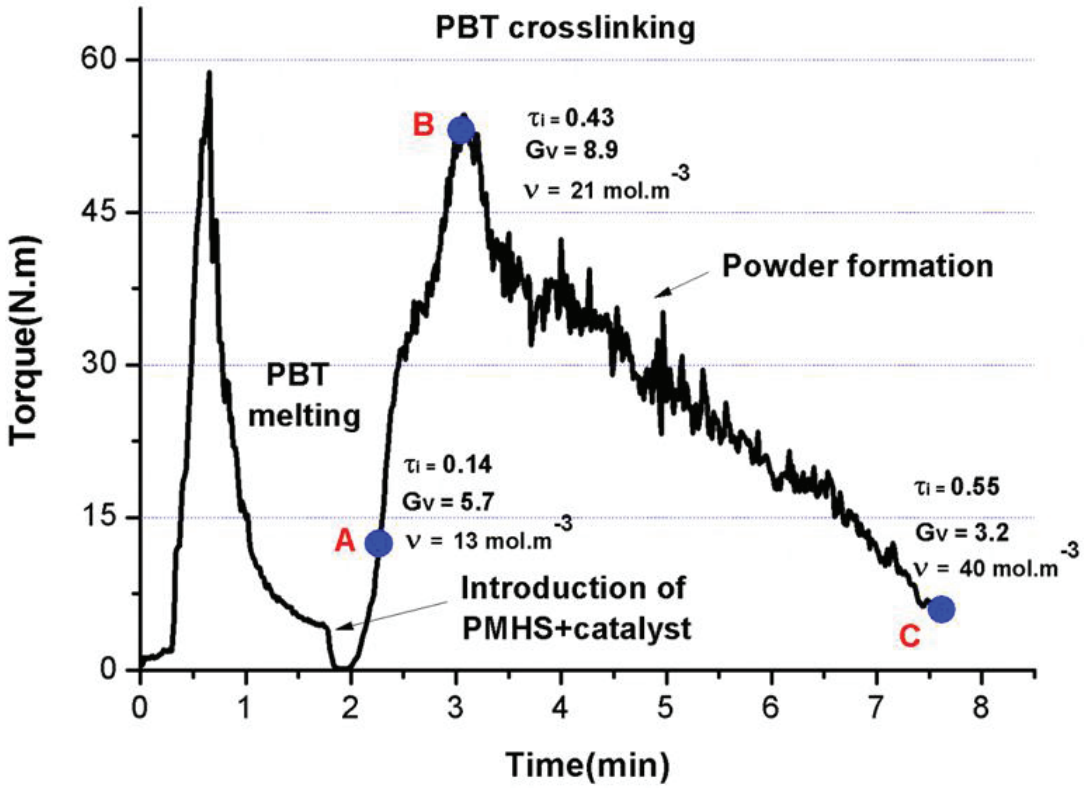

Figure IV.13: Torque variation during bulk hydrosilylation reaction of PBT with PMHS (90/10 wt%) at 220 °C in presence of catalyst.

To confirm the hypothesis, Sample C was also grinded into powder for solid-state ^{29}Si NMR analyzing. Through the spectrum (Figure IV.14-a), we found that there are several peaks from -50 to -90 ppm. As mentioned before, the peaks around -55 to -68 ppm are assigned to Si-T (trifunctional) units of siloxane from the expected product -SiOCH(c) and from the PMHS crosslinking network. In addition, there is another peak at -86 ppm, which was not observed in the case of model compound study (Figure IV.9). This signal is similar to the Si-Q units (SiO_4- at -95 ppm on solid-state ^{29}Si MAS NMR spectrum) reported by Camino *et* al. [28] when PDMS and Pt-based catalyst reacted at high temperature.by flash pyrolysis. So in the present case, the peak at -86 ppm is possible assigned to Si-Q units which are formed by crosslinking at high temperature of PMHS catalyzed by $Ru_3(CO)_{12}$.

To demonstrate such phenomenon, 4 g PMHS is mixed with a solution containing 50 mg $Ru_3(CO)_{12}$ and heated in a schlenk at 220 °C with stirring. After 10 min, the solution changed to a gel. The solid-state ^{29} Si NMR analysis of the grinded gel (Figure IV.14-b) depicted the signals of Si-T_1, Si-T_3 and Si-Q units coming from PMHS self-crosslinking. The main difference between the both zoom is the observation of a signal at -62 ppm on the solid-state 29Si NMR spectrum for PBT/PMHS reactive blend (sample C) assigned to the silicon from

the expected hydrosilylated product SiOCH-(c).

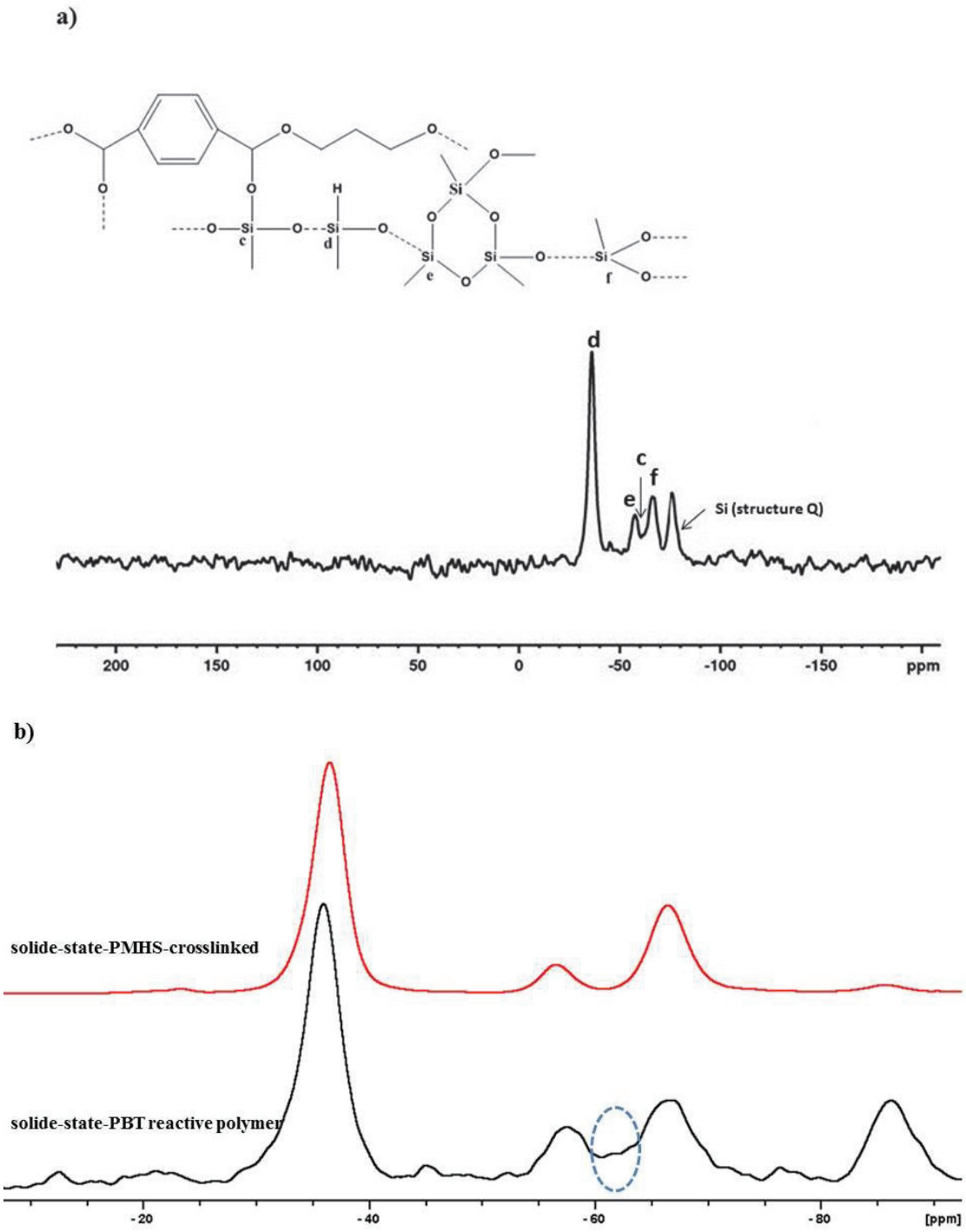

Figure IV.14: Solid-state ^{29}Si NMR spectra of a) PBT/PMHS reactive blend (sample C, full scale) and b) comparison of ^{29}Si NMR spectra between PMHS self-crosslinking sample and PBT/PMHS reactive blend (sample C), zoom -94_ -7 ppm.

Through the investigation of NMR, torque variation and swelling measurements, we can confirm the occurrence of hydrosilylation in ruthenium-catalyzed PBT/PMHS blend in molten conditions and the formation of a crosslinking network between the two compounds.

In addition under such processing conditions, we also found that the PMHS self-crosslinking.

To complete the crosslinking study, the rheological and morphological properties of the blend were carried out on the different samples A, B and C removed from the mixing chamber at different processing stages (Figure IV.13). The rheological behavior for the three samples was compared to the one corresponding to a non-reactive PBT/PMHS blend, used as reference (the process was the same without catalyst and no increase of torque was observed in that case). First the rheology behavior of sample A, compared with sample PBT/PMHS, shows an increase of the elasticity. The gel fraction was around 0.14, G' changed to be equal to G'', according to Mours *and* Winter, this means that the sol-gel transition had happened during PBT crosslinking process [29]. However, the sol-gel transition cannot be precisely determined from these experiments. For samples B and C, an obvious increase was observed corresponding to the drastic torque rise. The rheological behavior of sample B and C were similar, storage modulus at low frequency ($1.3x10^4$ and $5.7x10^4$ Pa, respectively) were higher than loss ones ($8.3x10^3$ and $2.4x10^4$ Pa, respectively). Especially for sample C, the storage modulus tends to a secondary plateau at lower frequency, corresponding to the equilibrium elastic modulus. This elastic behavior is characteristic of solid or gel-like structure meaning a network formation [14, 29]. These results are similar to the work on EVA/PMHS crosslinking network carried out by Bonnet *et* al. [14]. He found that after the hydrosilylation reaction, the storage modulus of EVA and PMHS blend is around $2x10^4$ Pa and tend to be plateau at low frequency, suggesting a network of EVA chains.

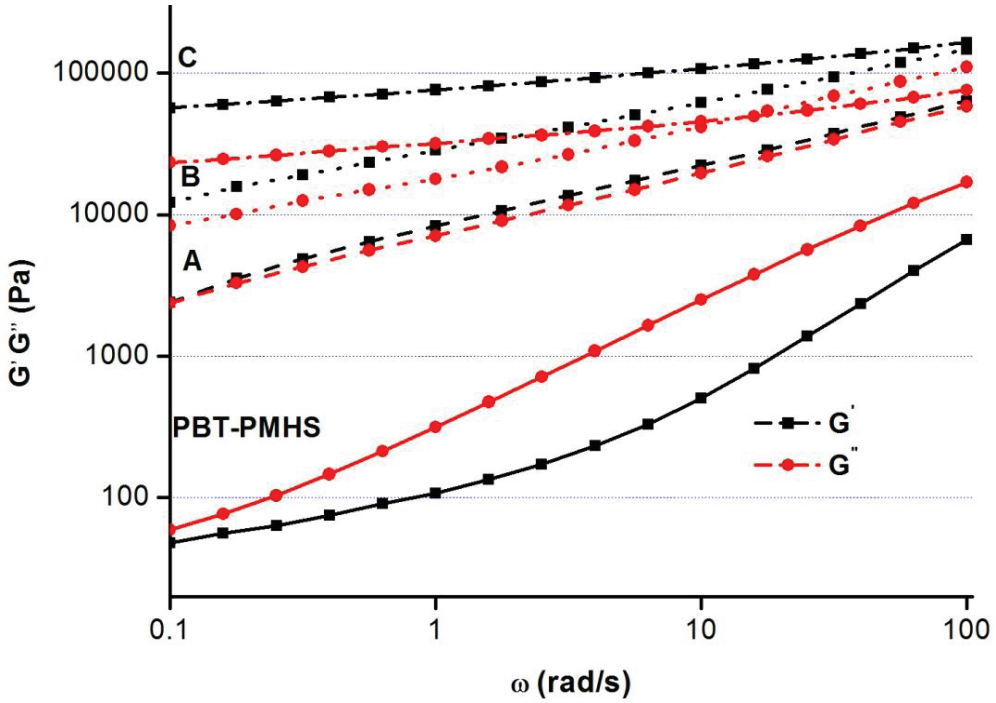

Figure IV.15: Variation of the loss (G'') and storage (G') modulus of PBT samples reacted by PMHS in the internal mixer being measured at 230 °C.

From the SEM analysis (in Figure IV.16) of sample A, the dispersion of PMHS was around 10 µm and not with a spherical forma as observed for the non-reactive blend. It means that the hydrosilylation reaction occurred in non-homogeneous conditions at least at the early stages of crosslinking reaction. The initial nodular morphology is explained by non-miscibility between PBT and PMHS. Nonetheless, the hydrosilylation reaction took place under mixing and shear, the dispersion of PMHS became a little finer from the sample A to sample C, the size of PMHS decreased from 10 µm to 2-3µm. The improvement of compatibilization between PBT and PMHS is possible because of the PBT/PMHS copolymer produced by hydrosilylation. This point is also demonstrated by Zhang *et* al. [30]. They added from 4% to 12% PMHS/butylene terephthalate (SLCI) into PP/PBT blend and they found that the domain size of the PBT phase decreased significantly, the diameter of the largest particle of PBT changed from10 µm to almost disappearance. Through FTIR and SEM, they identified the intermolecular interaction between sulfonate acid groups of SLCI and PBT phase since they both contain aromatic ring and ester groups.

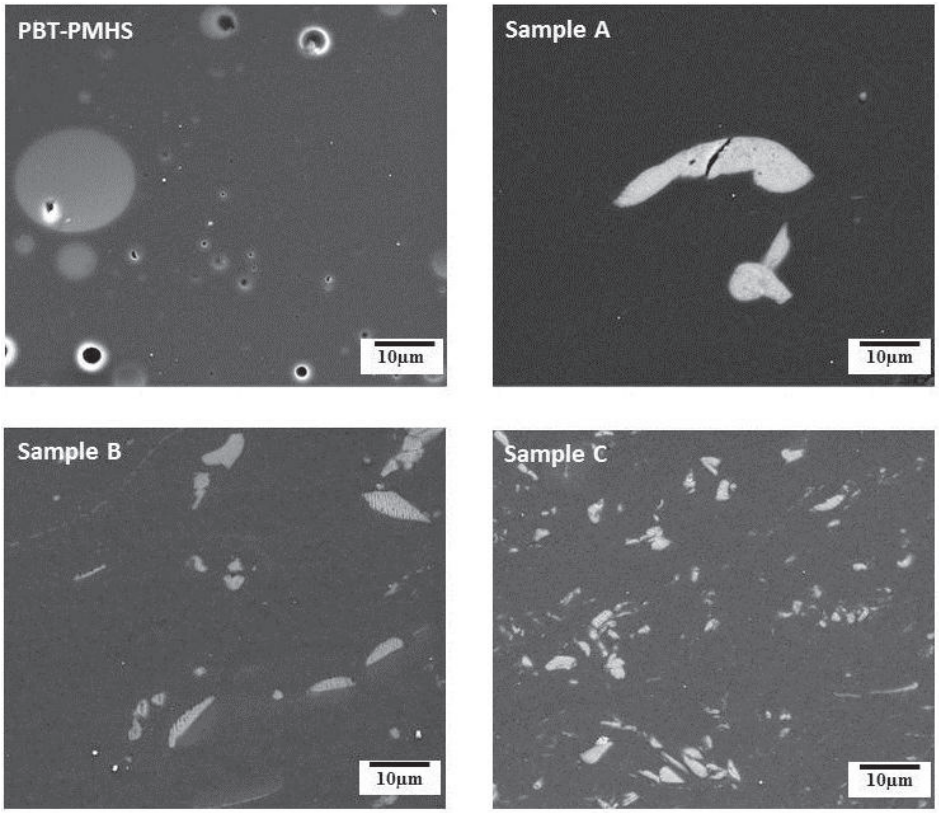

Figure IV.16: Representative SEM morphology of pure PBT-PMHS and PBT/PMHS/$Ru_3(CO)_{12}$ reactive blends at different stage: sample A, sample B, sample C.

However, as demonstrated previously, another reaction occurred during the reactive process. Actually, there is not only the crosslinking caused by hydrosilylation reaction between PBT and PMHS but also the reaction of PMHS self-crosslinking in presence of $Ru_3(CO)_{12}$ at such high process temperature. Therefore, after the whole process, the dispersion of PMHS is better than non-reactive system but part of the PMHS changed to gel also.

Such thermoplastic/polysiloxane crosslinking materials have many potential applications like biocompatibility, chemical resistance or work as matrix of electronic device. As reported in literature, Kalfat *et* al. [31] found membranes of polysiloxane-based gel can be used as host matrices for three different ionophores (2,9-(*o*-methoxy)-phenox-ydecane dicarboxylic acid (AE), α- and β-cyclodextrin). Pekala e*t* al. [32] also prepared polyether/polysiloxane network named PGPMS which was produced via the platinum-catalyzed addition of allyl glycidyl ether (AGE) to polymethylhydrosiloxane (PMHS) for blood-interfacing applications. The most well know application of PDMS is the modification of surface tension to some commercial thermoplastic based blends. To illustrate such potentiality, we measured the water

contact angle of PBT/PMHS blend for some preliminary research.

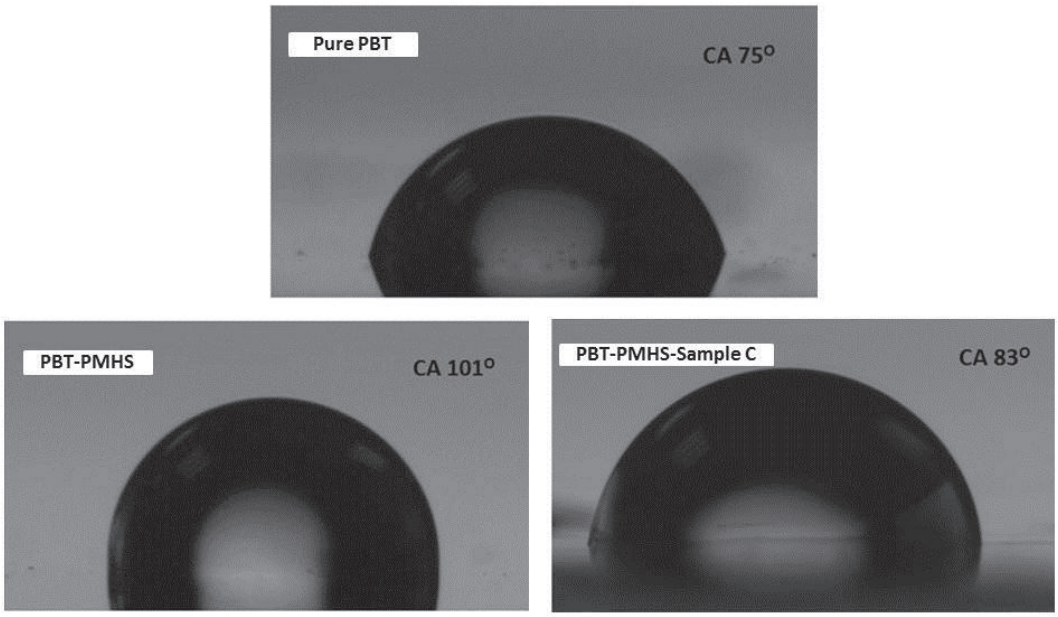

Figure IV.17: Water contact angles of pressed films, Pure PBT, PBT-PMHS10 wt % (PBT-PMHS) and PBT-PMHS10 wt % -$Ru_3(CO)_{12}$-sample C (PBT-PMHS-Sample C).

As known, the low surface energy and relatively low viscosity of PMHS compared to most thermoplastics, lead to a difficulty to reach fine dispersion. As mentioned in some research publications, the surface energy of methyl polysiloxane is 21 mJ/m^2 while that of PBT is 46 mJ/m^2, it is easy to foresee that if we introduce and stabilized a proportion of PDMS into the PBT, the hydrophobicity of the blend can be increased [33]. As already mentioned, the addition of compatibilizer or *in-situ* compatibilization can achieve interfacial modification, inhibit the surface segregation of silicone oil and then reduce the interfacial tension between silicone oil and thermoplastics. Therefore water contact angle tests were carried out to measure the change of surface energy of the samples. As shown in Figure IV.17, water contact angle (θ) of pure PBT is 75^o. In the meantime, after the addition of 10 wt% of PMHS, without any compatibilization, PMHS migrated and enriched on the surface formed a silicone oil film, so the water contact angle increased to 101^o. Besides, the water contact angle of sample C compared with non-reactive PBT/PMHS blend, decreased to 83^o but still higher than pure PBT. The tendency is in agreement with others systems such as the polyester/PDMS blend prepared by Xiong *et* al [33]. They modified the hydrophobicity of poly(ethylene terephthalate) (PET) with 3wt% polysiloxane (multifunctional, viscosity: 4 Pa.s) by reactive extrusion. The water contact angle can increased of around 40 ^{o} compared with pure PET. So

the increase of hydrophobic ability of our blend is not significant and high enough yet, possible caused by lower viscosity of PMHS ($4x10^{-2}$ Pa.s) *and* its self-crosslinking, but this method is quite encouraging for future investigations.

IV.4 Conclusion

Ester carbonyl hydrosilylation by ruthenium-catalyzed PMHS was evidenced at high temperature, 15 mol% at 180 °C versus 5% at 100 °C in 10 min for the butyl benzoate. However, through extending the reaction time, the side-reaction contribution increased and was worse with higher temperature.

From carbonyl hydrosilylation reaction of ester groups, a new method for PBT crosslinking was proposed. By this method, high crosslinking density may be reached in polymer processing conditions that means at high temperature and under shear. In a few minutes a crosslinking density of elastic strands of 40 $mol.m^{-3}$ was obtained. Besides the expected carbonyl hydrosilylation reaction, the self-crosslinking of PMHS caused by high temperature and the presence of ruthenium catalyst was also observed. A final insoluble fraction of 55% was reached, which results in the reduction of the polysiloxane phase size from 10µm to 2-3µm. Finally, the one-step compatibilization opens a new way to crosslinking polyester based on ruthenium-catalyzed hydrosilylation.

IV.5 References

[1] M. Pradeep, N. Vasudev, P. Reddy, D. Khastgir, Journal of applied polymer science, 104 (2007) 3505.

[2] T. Uragami, E. Fukuyama, T. Miyata, Journal of Membrane Science, 510 (2016) 131.

[3] D.A. Brown, G.J. Price, Polymer, 42 (2001) 4767.

[4] Y. Lee, I. Akiba, S. Akiyama, Journal of applied polymer science, 87 (2003) 375.

[5] T. Chang, C. Liao, K. Wu, G. Wang, Y. Chiu, Journal of Polymer Science Part A: Polymer Chemistry, 36 (1998) 2521.

[6] M. Gorelova, A. Pertsin, A. Muzafarov, O. Gritsenok, N. Vasilenko, Journal of applied polymer science, 55 (1995) 1131.

[7] W. Hu, J.T. Koberstein, J. Lingelser, Y. Gallot, Macromolecules, 28 (1995) 5209.

[8] U. Sundararaj, C. Macosko, Macromolecules, 28 (1995) 2647.

[9] M. Marić, N. Ashurov, C. Macosko, Polymer Engineering & Science, 41 (2001) 631.

[10] K. Prakashan, A. Gupta, S. Maiti, Journal of applied polymer science, 105 (2007) 2858.

[11] Z. Xu, S. Jie, B.G. Li, Journal of Polymer Science Part A: Polymer Chemistry, 52 (2014) 3205.

[12] W. Zhou, J. Osby, Polymer, 51 (2010) 1990.

[13] M. Igarashi, R. Mizuno, T. Fuchikami, Tetrahedron Letters, 42 (2001) 2149.

[14] J. Bonnet, V. Bounor-Legaré, P. Alcouffe, P. Cassagnau, Materials Chemistry and Physics, 136 (2012) 954.

[15] S.K. Patel, S. Malone, C. Cohen, J.R. Gillmor, R.H. Colby, Macromolecules, 25 (1992) 5241.

[16] T. Caykara, Journal of Macromolecular Science, Part A, 41 (2004) 971.

[17] J.-S. Chen, C.K. Ober, M.D. Poliks, Y. Zhang, U. Wiesner, C. Cohen, Polymer, 45 (2004) 1939.

[18] P.L. Jackson, M.B. Huglin, A. Cervenka, Polymer international, 35 (1994) 135.

[19] A.F. Barton, CRC handbook of solubility parameters and other cohesion parameters, CRC press1991.

[20] B.-H. Phe, V. Bounor-Legare, L. David, A. Michel, Journal of sol-gel science and technology, 31 (2004) 47.

[21] J.G. Clayden, Organic Chemistry, (2001).

[22] N. Satyanarayana, H. Alper, Macromolecules, 28 (1995) 281.

[23] J. Bonnet, V. Bounor-Legaré, F. Boisson, F. Mélis, P. Cassagnau, Journal of Polymer Science Part A: Polymer Chemistry, 49 (2011) 2899.

[24] C. Eaborn, K. Odell, A. Pidcock, Journal of Organometallic Chemistry, 63 (1973) 93.

[25] P. Guégan, C. Macosko, T. Ishizone, A. Hirao, S. Nakahama, Macromolecules, 27 (1994) 4993.

[26] F. Ide, A. Hasegawa, Journal of applied polymer science, 18 (1974) 963.

[27] P. Cassagnau, F. Fenouillot, Polymer, 45 (2004) 8031.

[28] G. Camino, S. Lomakin, M. Lazzari, Polymer, 42 (2001) 2395.

[29] H.H. Winter, M. Mours, Rheology of polymers near liquid-solid transitions, Neutron spin echo spectroscopy viscoelasticity rheology, Springer1997, pp. 165.

[30] B.Y. Zhang, Q.J. Sun, Q.Y. Li, Y. Wang, Journal of applied polymer science, 102 (2006) 4712.

[31] R. Kalfat, M.B. Ali, R. Mlika, F. Fekih-Romdhane, N. Jaffrezic-Renault, International Journal of Inorganic Materials, 2 (2000) 225.

[32] R.W. Pekala, M. Rudoltz, E. Lang, E. Merrill, J. Lindon, L. Kushner, G. McManama, E. Salzman, Biomaterials, 7 (1986) 372.

[33] B. Xiong, S. Zhu, Y. Fan, H. Li, M. Shi, Y. Cao, Journal of Macromolecular Science, Part B, 51 (2012) 630.

Chapter V: Conclusion

This PhD work is mainly dedicated the *in situ* reactive compatibilization between PA12 and hydride PDMS through $Ru_3(CO)_{12}$ catalyzed hydrosilylation reaction, and the modification of blend properties such as surface free energy, gas separation, thermal stability and mechanical. An extension to polybutylene terephatalate was proposed to evaluate such approach in a higher range of polymers processing range of temperature.

In this context, the study of the literature describes carbonyl hydrosilylation based on different kinds of catalyst especially transition metal complex which form a very important class of catalyst for this reaction. As reported both ruthenium and rhodium complexes show effectively catalytic efficiency in hydrosilylation reaction for carbonyl from ester or amide. Especially for amide it can be reduced and finally achieve amine or silyl amine after this addition reaction. But almost all these studies are carried out under mild conditions: temperature below 90 °C, low molar mass organic compounds, atmospheric pressure, in solution, *etc.* Except our work dedicating to ethylene-vinyl acetate copolymer modified by PDMS-SiH through such hydrolsilylation reaction at 120°C, no study dealt with this polymer modification.

For the PA12 study, the first step of the experiment is the model approach based on the reaction between the *N*-methylpropionamide and 1-PDMS-SiH (726 $g.mol^{-1}$). It was carried out in schlenk at 100 °C. The mechanism and kinetics were investigated with multinuclear NMR (^{1}H, ^{13}C and ^{29}Si). We confirmed that the main products are *N*-siloxane-*N*-methylpropionamide and *N*-siloxane-*N*-methylpropionamine with a total yield of 70 mol% after 2 hours of reaction. These *N*-silylated products were achieved through the initial addition reaction of SiH to carbonyl group, and then others rearrangement or additional SiH addition reactions.

The extension of the ruthenium catalyzed hydrosilylation between PA12 and hydride terminated PDMS was carried out in mixer chamber at 170 °C. We first studied 1-PDMS-SiH/ PA12 system, since it has low viscosity ratio ($3x10^{-7}$) and high ratio of functional groups ($6.7x10^{-2}$). The first evidence of the hydrosilylation reaction was through the evolution of torque value versus time of blending (increase from 18-50 N.m after the introduction of PDMS and $Ru_3(CO)_{12}$ mixture in 6 min). Then, we investigated the morphology of these blends at different process stages through SEM and found that the size

of the 1-PDMS-SiH domains decrease from 3-4 μm to finally 800 nm with the reaction time. The dispersion of PDMS was significantly improved with the *in situ* formation of *N*-silylated copolymers which worked as a compatibilizer. Besides, we also found another nanostructuration of the blend by TEM with a dispersion of PDMS domains with a diameter around 20-30 nm. Actually, we demonstrated that they are silicone gel-like due to partial PDMS-SiH oxidation reaction. Such reaction of hydride PDMS can take place at high temperature in the presence of ruthenium or rhodium complexes.

2-PDMS-SiH, another kind of hydride terminated PDMS with higher viscosity and lower reactivity was also used in such reactive blending with PA12 under the same conditions as 1-PDMS-SiH to evaluate the impact of PDMS characteristics on the final morphology. The compatibilization was observed and the dispersion of 2-PDMS-SiH was also promoted (2-PDMS-SiH domain size decreased from around 50 μm to 3-4 μm). Therefore, it is clear that through changing physico-chemical parameters like viscosity, reactivity, it is possible to control the final morphology of the blend.

About the properties, we mainly investigated the PA12/1-PDMS-SiH blends. The initial degradation temperature evaluated by TGA increased from 419 to 430 °C after reactive compatibilization. This increase indicated the improvement of PDMS phase stability in the blend, because of the *in situ* formed PA12-PDMS copolymer by hydrosilylation reaction enhanced the interaction between polymers. For crystalline behavior, the introduction of PDMS did not have influence on the crystalline degree kept at 61%.

The significant modification of PA12 after reactive compatibilization with PDMS is the decrease of surface free energy. PA12 with an initial hydrophilic character with a water contact angle $80^{o}\pm4.5^{o}$ changed to a slight hydrophobic behavior after 10 wt% introduction of PDMS, with a water contact angle increased to $100^{o}\pm2.1^{o}$. The surface free energy also decreased from 38.0 to 24.2 mN/m. If the PDMS concentration increased to 20 wt%, the improvement of hydrophobicity is more obvious. In addition, the introduction of PDMS also promoted the CO_2 permeability of PA12 from 1.42-2.24 barrer after reactive blending with 20 wt% PDMS due to the high gas permeability of PDMS itself.

Mechanical property of PA12/PDMS was studied by uniaxial tension experiment. We

found that the introduction of PDMS without compatibilization had negative influence on mechanical property as there were significant decreases of Young's modulus and elongation. Specifically, PA12/PDMS (10 wt%) non-reactive blend had 5% loss of Young's modulus and 50% decrease of elongation. After compatibilization, the Young's modulus is increased by 19% compared with pure PA12, due to a better dispersion and enhancement of the interfacial adhesion but also to the *in situ* creation of a silicone gel-like phase.

In a second part, we extended this hydrosilylation reaction at higher processing temperature with the study of PBT/ PMHS reactive blending at 220 °C. The model study between butyl benzoate and PMHS was carried out at 100 and 180 °C, respectively. The model hydrosilylation reaction was evidenced at high temperature, the yields were 15 mol% at 180 °C versus 5% at 100 °C in 10 min for the butyl benzoate. However, through extending the reaction time or reacting at higher temperature, the side-reaction contributions. Besides, the oxidation reaction of PMHS is also observed as in the case of PA12/1-PDMS-SiH system and formed $(CH_3)SiO_3$- (T_1) and cyclic trisiloxane (T_3) structures. To the extension to PBT molten conditions lead to a PBT-PMHS crosslinking network creation evidenced by solid-state NMR, increase of torque value and gel fraction, powder formation and morphology study. Concomitantly the self-crosslinking of PMHS lead to dispersed phase modification from liquid to gel.

Generally, the ruthenium catalyzed hydrosilylation is an original and efficient way to achieve reactive compatibilization between PA12 and hydride PDMS. The new formed *N*-silylated copolymers at the interface can promote the dispersion of PDMS in the matrix and improve interfacial adhesion between them. Some excellent properties of PDMS such as hydrophobicity, gas permeability or gas separation can be combined with PA12 after such reactive blending. It could be potentially applied to others polyamides. The application of such reaction at higher temperature is also efficient but a judicious choice of the PDMS physico-chemical parameters has to be take into account to limit the self-crosslinking of hydride PDMS.

Appendix: Hydrosilylation reaction in polymer blending between PA12 and PMHS

A.1 Introduction

This hydrosilylation reaction was extended to the reactive blending of PA12 with polymethylhydrosiloxane (PMHS) under molten processing conditions. Comparing with PDMS-SiH, PMHS has higher reactivity and the molar ratio ([SiH]/[CONH]) with PA12 is 0.38. The structure of the blend was investigated by rheology and electronic microscopy. As a result, self-crosslinking of PMHS causing by oxidation in the presence of $Ru_3(CO)_{12}$ was more obvious and almost all of the PMHS changed from liquid to gel-like phase.

A.2 Experiment

A.2.1 Materials and reagents

PA12 was supplied by Arkema (AESNO TL RILSAN®). PMHS (molar mass: 2100 $g.mol^{-1}$, viscosity: $40x10^{-3}$ Pa.s) and triruthenium dodecacarbonyl ［Ru3(CO)12］were commercial products from ABCR, number average molar mass *Mn* is 26000 $g.mol^{-1}$, weight average molar mass *Mw* is 47000 $g.mol^{-1}$ and the density is 1.01 $g.cm^{-3}$ at room temperature. Hexafluoro-2-propanol (HFIP), acetone and chloroform were purchased from Aldrich and used without further purification.

A.2.2 Hydrosilylation reaction in polymer blending

PA12 pellets were dried in vacuum at 80 °C for 24 h. Melt reactive processing of PA12 and PMHS was carried out in a Haake Plasticorder intensive batch mixer equipped with a Rheomix 600 internal mixer. The temperature of the mixer chamber was set at 170 °C and the rotation speed was 50 rpm. The resistant torque and temperature were monitored during whole process. In a typical experiment, dried PA12 (40g) was added in the mixer chamber to melt the polymer until the torque curve reached a plateau. Then, the catalyst and PMHS mixture with a predetermined composition (4 g PMHS and 50 mg $Ru_3(CO)_{12}$) was added in the molten PA12 with a syringe. The extent of the reaction was then qualitatively followed (tracked) from the torque variation and the samples were characterized by SEM.

A.2.3 Characterization

The morphology of the polymer blend was characterized by scanning electron

microscopy (SEM). The samples were prepared by cryo-ultramicrotomy with a Leica EMFCS microtome device equipped with a diamond knife (this technique was used to prepare planed surface). Then the fractures were sputter coated with gold/palladium. The morphology was analyzed using a QUANTA 250 microscope with an accelerating voltage of 10kV.

The PA12/PDMS reactive blend solubility was determined after immersion (48 h, 25 °C) of 200 mg blend in HFIP/chloroform (20 ml, 1:4 in volume) mixed solvent and then observe whether there is insoluble matter.

A.3 Results and discussion

We carried out PA12/PMHS reactive blend with a molar ratio $\lambda_{PMHS/PA12}$ = 0.38 and viscosity ratio $\lambda_{PMHS/PA12} = 4.0x10^{-6}$. Torque variation of reactive blend (Figure A.1) shows that after the introduction of PMHS and $Ru_3(CO)_{12}$ the value of torque increased first at 2 min until reached around 18 N.m at 2.3 min, then the speed of increase slowed down a little bit since the slope of the curve decreased. This means during this process mixing defeated lubrication, PMHS flowed into PA12 melt. Then the torque increased rapidly to the top before decreasing, as confirmed before, increase of torque due to the change of viscosity and caused by reaction.

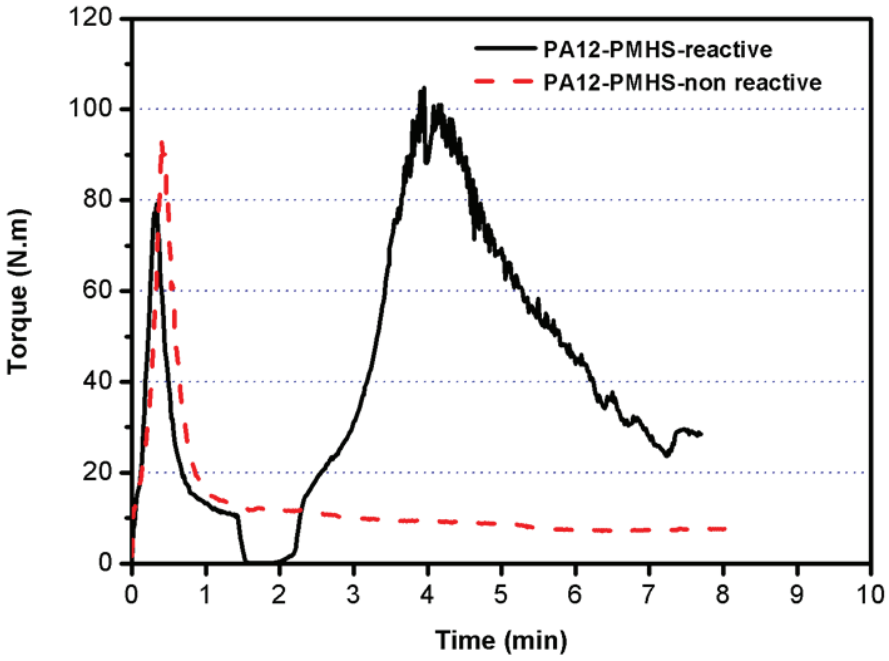

Figure A.1: Variation of the mixing torque between PA12 and PMHS under shear in the internal mixer at 170 °C: reactive blending (solid line) and non-reactive blend (dotted line).

In order to better understand the effect of the chemical modification to PA12/PMHS blend, SEM analysis was carried out. Through comparing the morphologies of non-reactive and reactive blends (Figure A.2), we found the size of PMHS did not decrease obviously (from 10μm to 7μm) means improvement of dispersion was not obvious as PA12/PDMS-SiH, even though the reactivity of PMHS is better and viscosity is similar compared with 1-PDMS-SiH. The reason of such phenomenon is complex, crosslinking between PA12/PMHS took place since we measured the gel fraction of 25% over the amount of PMHS introduction. But PMHS changed to silicone particles (Figure A.2) as mentioned in the previous work during the hydrosilylation the oxidation of PMHS also occurred [1, 2]. Specially for PMHS with such high concentration of SiH groups. The crosslinking of PMHS formed at the same time and changed to gel fast. Crosslinking of PMHS inhibited the flow itself and encapsulated the catalyst inside. So it is difficult to form enough copolymer to promote the dispersion and achieve crosslinking materials of PA12/PMHS.

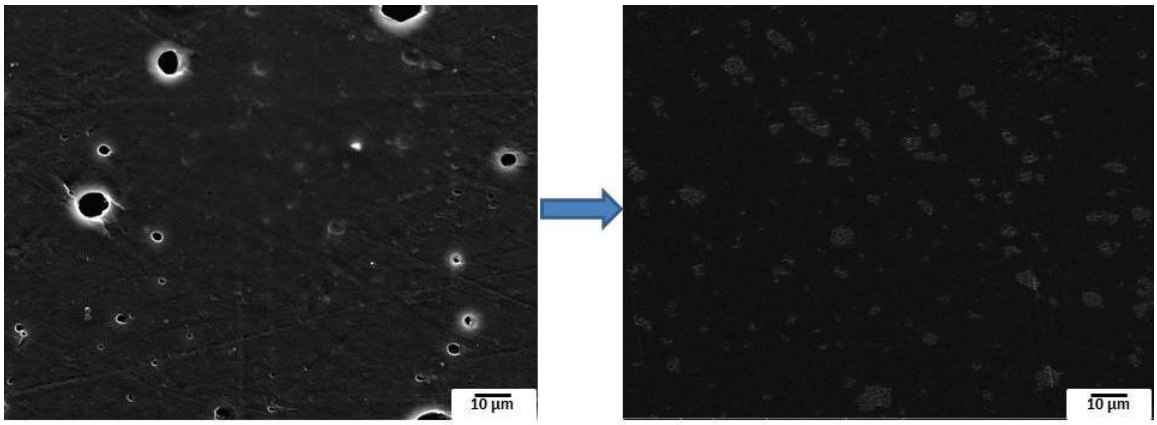

Figure A.2: Representative SEM morphologies of PA12/PMHS blends: left) PA12/PMHS non-reactive blend, right) PA12/PMHS reactive blend.

A.4 Conclusion

Ruthenium-catalyzed hydrosilylation also works between PA12 and PMHS, due to the obvious increase of torque during process. However, PMHS comparing with hydrosilyl terminated PDMS (PDMS-SiH) has higher reactivity and the functional groups are attached on the backbone. Therefore, the self-crosslinking of PMHS is more significant and almost all of them changed from liquid to gel-like phase except the part reacted with PA12 (gel fraction is 25%). The oxidation reaction of hydrosilane in the presence of ruthenium catalyst was enhanced with the increase of reactivity at high temperature.

A.5 References

[1] Stiubianu, G., et al., Silicone-modified cellulose. Crosslinking of cellulose acetate with poly[dimethyl(methyl-H)siloxane] by Pt-catalyzed dehydrogenative coupling. Journal of Materials Science, 2010. **45**(15): p. 4141-4150.

[2] Motoyama, Y., et al., Self-encapsulation of homogeneous catalyst species into polymer gel leading to a facile and efficient separation system of amine products in the Ru-catalyzed reduction of carboxamides with polymethylhydrosiloxane (PMHS). Journal of the American Chemical Society, 2005. **127**(38): p. 13150-13151.

List of Figures

List of Tables